2022 Biennial Report on Seismic Monitoring and Research in Texas

December 31, 2022

The University of Texas at Austin

Bureau of Economic Geology

Scott W. Tinker, Director

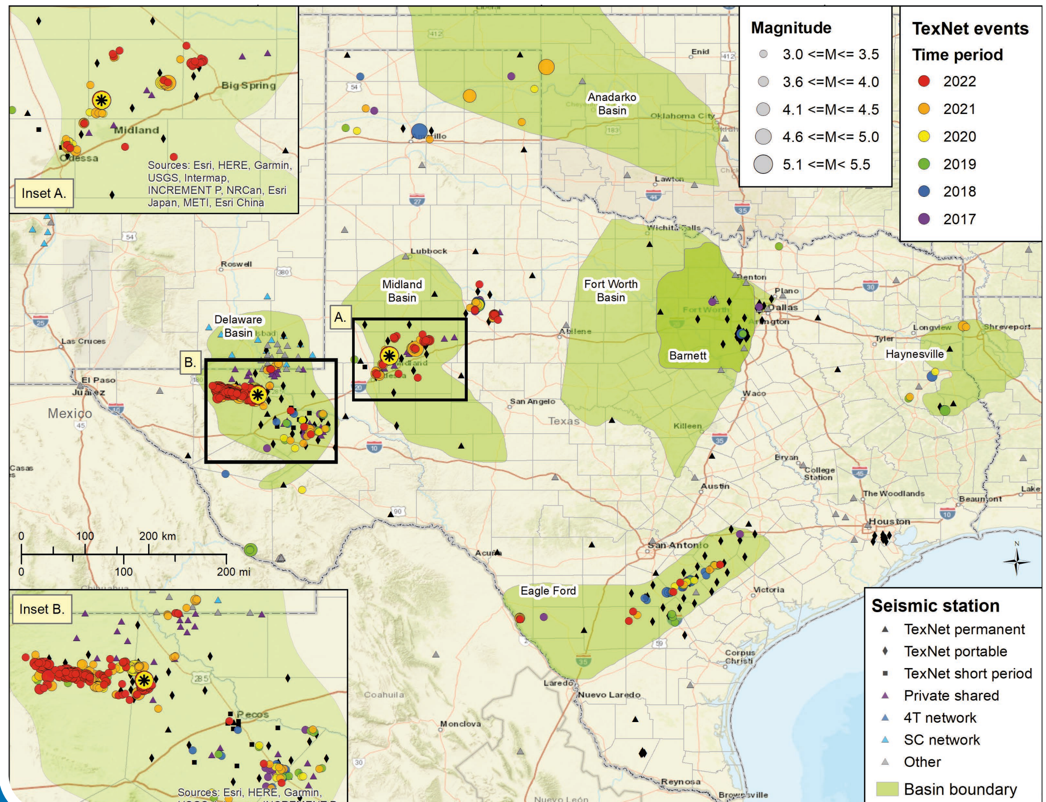

by

Alexandros Savvaidis

with contributions from:

P. Hennings, E. Rathje, K. Smye, A. Averett, A. Banerji, P. Bazzurro, G. Beroza, L. Binneti, C. Breton, M.R. Brudzinski, C. Bolton, A. Calle, J. Chen, P. Chen, Y. Chen, Y.F. Chen, H. DeShon, R. Dommisse, D. Doser, N. Dvory, R. Eastwood, W. Ellsworth, J. Faith, Z. Fan, P. Fleck, S. Fomel, R. Gao, J. Ge, I. Grigoratos, V. Guzman, C. Hayward, E. Horne, D. Huang, N. Igonin, S.J. Jeong, M. Karplus, F. Kavoura, P. La Pointe, H. Lee, A. Li, M. Li, P. Martone, C. McCabe, G. McDaid, C. McKeighan, A.P. Morris, S.M. Mousavi, Z. Nagy, P. Newell, J.-P. Nicot, V. O'Sullivan, V. Ozuna, N. Pham, L. Quinones, R. Reedy, J. Rosenblit, O. Saad, L. Samy, B. Scanlon, M. Shirley, D. Siervo, J-E Lund Snee, S. Staniewicz, B. Stump, C. Templeton, D. Trugman, B. Uku, S. Veitch, X. Wang, K. Wisian, B. Young, C. Zahm, A. Zanjani, X. Zhang, W. Zhu, and M. Zoback

TexNet

Bureau of Economic Geology

TexNet Mission Statement and Objectives

Provided by the Technical Advisory Committee, July 28, 2020.

Mission Statement

Serve as an independent scientific body that measures and analyzes earthquakes and associated data, and distributes and communicates these data and related products to government, industry, and the public for their benefit and the benefit of the State of Texas.

Objectives

- Maintain a network of seismometers capable of accurately recording earthquake data across Texas.
- Exceed the network technical performance metrics established in consultation with the TexNet Technical Advisory Committee (TAC), USGS, and other authoritative bodies.
- Continuously strive to increase the accuracy of hypocenter location analyses and report with uncertainties.
- Maintain high-quality electronic databases of all event catalogs and products and make them available as appropriate.
- Seek to understand causes of seismic activity in Texas.
- Seek to understand and quantify the impact and risk to public safety and infrastructure.
- Distribute data and analyses to stakeholders effectively and in a timely fashion, recognizing their different needs. Stakeholders include:
    - Railroad Commission of Texas (timely, mission-critical supporting information)
    - Texas Division of Emergency Management, Texas Department of Transportation, Texas Commission on Environmental Quality, University Lands (rapidly for large events)
    - Local Communities
    - Oil and Gas Industry
    - Academic Research Community
    - General Public
    - Media
- Receive and utilize input from the stakeholders.

TexNet Technical Advisory Committee Members

Brian Stump, Committee Chair – SMU (Southern Methodist University)
Mark Boyd, Committee Member – ConocoPhillips
David Cannon, Committee Member – Diamondback Energy
Chris Hillman, Committee Member – City of Irving
Jeff Nunn, Committee Member – Chevron
Kris Nygaard, Committee Member – ExxonMobil (retired)
Scott Mitchell, Committee Member – Deep Blue Water
Aaron Velasco, Committee Member – Texas Railroad Commission
Scott Tinker, *ex officio*

Table of Contents

1.0 Executive Summary

Seismicity in Texas has rapidly increased. There were more M_L2.5 or higher earthquakes in Texas than in California in 2022. The TexNet network now exceeds 200 stations versus the original plan for a total of 60 new stations. In spite of this rapid growth, TexNet funding has decreased by 27% since 2016. As a result, TexNet has been unable to meet its primary goal of prompt publication of all earthquakes down to M_L1.5, a metric which has been designed to support stakeholders including Railroad Commission of Texas (TRRC) and industry partners. As a temporary solution, $500,000 was moved from the TexNet research budget to help meet operational requirements in 2022. However, reducing research funding, in turn, negatively impacts delivery of new data analysis tools used by TRRC and industry. The proper long-term solution for all stakeholders is to increase funding to $6.1 million, which would provide the necessary resources to meet TexNet's growing needs. Without this influx of resources, the productive research program and the TexNet earthquake catalog which is the basis for risk mitigation by both industry and TRRC would be further negatively impacted.

Seismic activity in Texas is occurring in six main areas: the Delaware Basin and Midland-Odessa area in West Texas, the Panhandle, East Texas, the Eagle Ford area of South Texas, and the Cogdell Field near Snyder. All areas have had at least one felt earthquake with magnitude higher than 3.0 since January 2020. In the area of North Culberson and Reeves Counties, TexNet cataloged thirty-seven earthquakes with $M_L \geq 4.0$ from January 2020 through December 2022, compared to zero earthquakes with $M_L \geq 4.0$ prior to that period, since 1975. Although the seismicity in Dallas-Fort Worth urban area has decreased, there is an increase in seismicity in the Odessa Midland region (Midland Basin). A magnitude M_L5.4 Coalson earthquake and a M_L5.4 North of Midland, Range Hill earthquake were reported on November 16, and December 16, 2022, respectively, and are the highest magnitude earthquake since the M5.7 event in 1995 (Brewster County). The Coalson earthquake was felt as far as San Antonio and Dallas-Fort Worth, and the Range Hill earthquake as far as Dallas-Fort Worth. The TexNet network has been invaluable in providing precise epicenter location to enable rapid stakeholder response to examine possible local impacts.

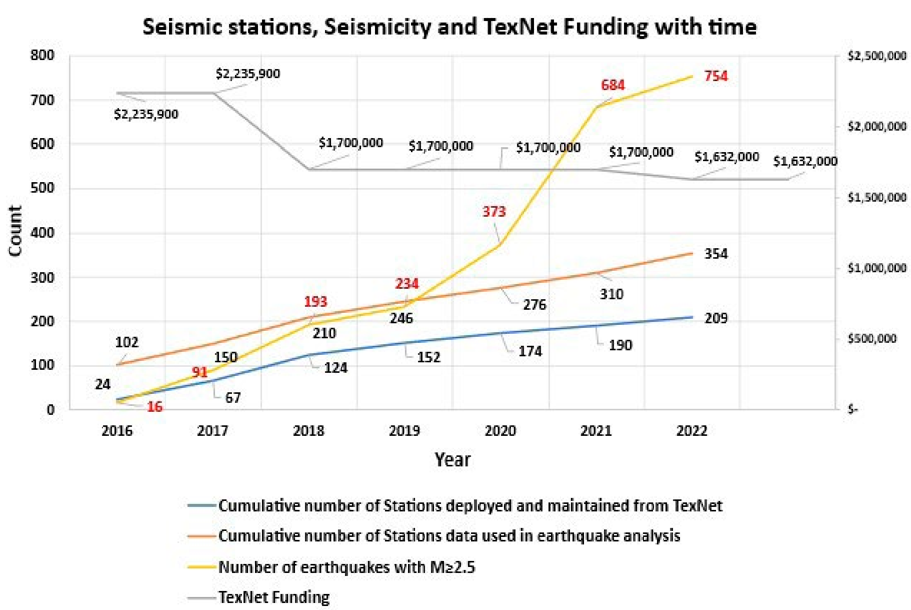

Figure 1. Cumulative number of seismic stations deployed and maintained by TexNet, and number of stations used in earthquake analysis. Numbers of earthquakes of $M_L \geq 2.5$ and amounts of the TexNet funding are also show for the time period 2016-November 2022.

The TexNet mission statement says that the highest priority objectives are to maintain a network of seismometers capable of accurate and timely recording and reporting of earthquake data across Texas. Currently, due to the increased number of seismic stations and the increase of seismicity, earthquakes below M_L2 are not being catalogued and there can be a delay of few weeks in cataloging earthquakes of $2.0 \leq M_L < 2.5$. A timely (within hours) updated earthquake catalog is essential to meet the needs of industry and TRRC in well permitting and mitigation of induced seismicity. In order to achieve our primary goals, TexNet needs to expand the operational staff to: 1) maintain the equipment of the seismic network that is now 3.5 times larger than initially envisioned; and 2) analyze an increasing number of events more timely providing better earthquake depth estimation. The additional staff will require funding to increase to $6.1 million for the 2023–24 legislative cycle. maintain **This funding will allow the State of Texas to ensure timely and accurate reporting of all earthquakes to M_L1.5 in order to enable stakeholder response and risk mitigation. However, without this expanded funding TexNet will not be able to provide timely and comprehensive earthquake data and catalogs to the industry and the Railroad Commission in order to properly mitigate the risk.** Ongoing research focused on development of tools and techniques that inform approaches for stakeholder risk mitigation would also be compromised and delayed should funding levels not be increased. These shortcomings would, in turn, lead to suboptimal decisions for industry and the TRRC.

2.0 Impact of TexNet Program on the State of Texas

TexNet provides essential applied research and educational products to the State of Texas, which:

- Enable risk mitigation in areas of increased seismicity or in areas of expected increases in oil and gas operations.
- Minimize earthquake activity associated with human activities.
- Reduce the impact of possible future earthquakes on the people and infrastructure of Texas.
- Provide information and outreach to improve understanding of seismicity risk and its avoidance to Texans.

These deliverables are generated through the TexNet process illustrated in **Figure 2**. From start to finish the process consists of 1) monitoring and timely and accurate analysis of earthquake activity, 2) understanding causes of seismicity, and 3) providing information to enable mitigation for the socioeconomic risks to the State. Research takes advantage of state resources at UT Austin, Southern Methodist University (SMU), and the University of Houston (UH) in order to improve monitoring. This collaboration increases the linkage between these different research groups and the operational task.

Seismicity monitoring across the State of Texas is designed to provide earthquake source information, 24/7, about events with magnitude greater than or equal to 3.0 in less than 20 minutes. This is our number one goal. A secondary goal is continuous monitoring and evaluation of events, at least down to magnitude 1.5 (with appropriate error quantification), within the next business day. These analyses are captured in an earthquake catalog which is the primary source for subsequent operational decisions made by both the Railroad Commission of Texas (TRRC) and industry operators and also provides primary data for several of our research initiatives. Research is designed to reduce bias and modelling errors necessary to improve earthquake locations, including the critical assessment of earthquake depth which is essential to our mission. As a result, another goal of operations is to continuously decrease uncertainty estimates in order to improve the quality of locations used for assessment as well as distinguish the impact of shallow versus deep disposal in order provide assurance in ruling judgments.

This compilation, maintenance, and quality control of available earthquake catalogs, supporting geophysical information as well as operational factors provide stakeholders material to assess the causality of all seismicity across the State of Texas. Recent development and distribution of an expanding set of publicly available web tools (https://www.texnet.beg.utexas.edu/) makes this data easily available. These tools are part of the TexNet dashboard that provides information to the industry and TRRC to track the seismic monitoring expansion in the State, understand seismicity, monitor produced water injection and enable risk mitigation in areas of increased seismicity or in areas of expected increases in oil and gas operations.

Statewide seismicity online catalog to identify seismicity and support migration efforts:
https://catalog.texnet.beg.utexas.edu/

High resolution online catalog to identify and document faults zones:
https://injection.texnet.beg.utexas.edu/

Water injection volumes within SRAs to understand produced water injection:
https://hirescatalog.texnet.beg.utexas.edu/

Status of all seismic stations used in monitoring:
https://monitor.texnet.beg.utexas.edu/

Areas prone to seismicity are quantified and factors that might impact future earthquakes are identified using TexNet operational data combined with statistical and physics-based earthquake models which contribute to risk mitigation. Complementary to an understanding of the causes of seismicity, parameters important in assessing surface hazards and impacts of seismicity are provided.

TexNet provides essential applied research and products to:

- Enable risk mitigation in areas of increased seismicity or in areas of expected increases in oil and gas operations.
- Minimize earthquake activity associated with human activities.
- Reduce the impact of possible future earthquakes on the people and infrastructure of Texas.

Finally, by conducting an education program, and providing information and outreach TexNet facilitates, an understanding of seismicity risk and its avoidance is communicated to Texans.

During the current biennium (2021-23) and following the recommendations of the TexNet Technical Advisory Committee (TAC), we pursued research and delivered products that have significantly improved our understanding of induced earthquakes in Texas. Appendix A provides a list of these contributions with brief descriptions of the publications stemming from our work in order to demonstrate the breadth and depth of this progress. A full list of publications can be accessed at https://utexas.app.box.com/s/ifgbsi1m6shfg060j2xttjsvq56ezmqb.

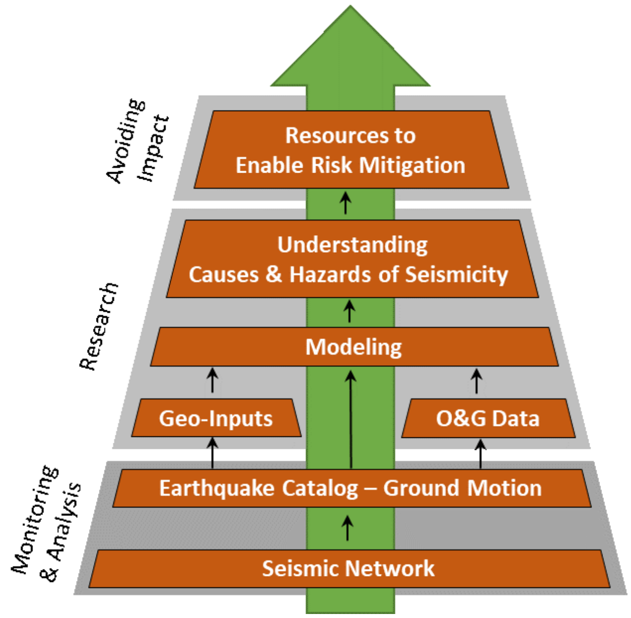

Figure 2. TexNet processes, products, and resources to the State.

Several of our research projects and related publications document how TexNet has improved our ability to detect, locate, and analyze earthquakes statewide. We have developed and deployed new techniques to further improve location accuracy and provide information in a timely manner. Ground motion data are denoised and automatic earthquake location accuracy has been enhanced, when compared to manual earthquake location. **Figure 3**, presents a comparison of manually assessed (ground truth) earthquake magnitudes with the automatic calculated (predicted) ones using Machine Learning (ML). The Mean Average Error (MAE) in magnitude is 0.12 showing that TexNet can reliably use ML methods and provide information through its operations to its stakeholders on a timely basis.

We have developed high precision and high-resolution earthquake relocation approaches using complex earth models in order to improve location accuracy and subsequent fault identification. This high-resolution earthquake location work has significant impact to our stakeholders (e.g., the petroleum industry and its regulators) supporting their investment and subsequent regulatory decisions that rely on identifying spatiotemporal seismicity trends.

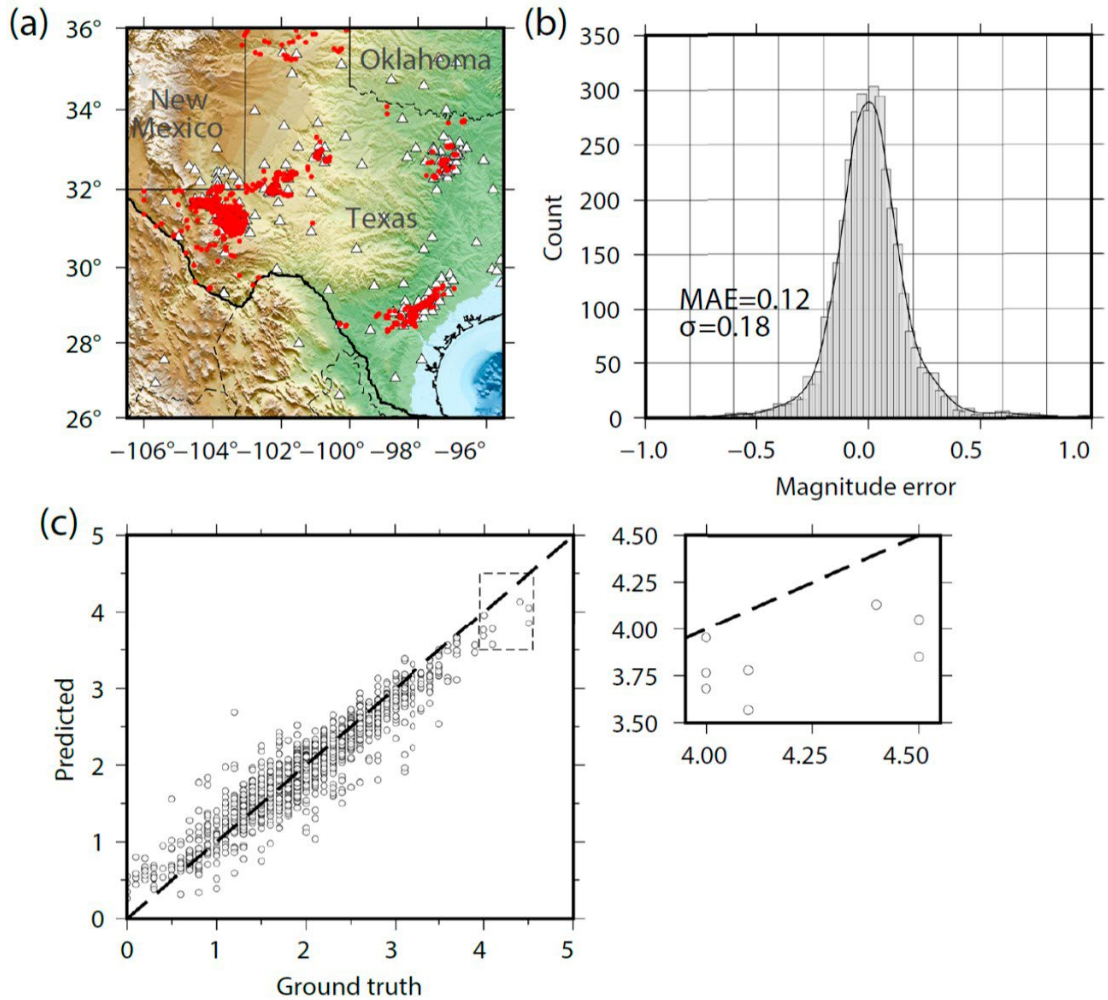

Figure 3. Figure 3. (a) Earthquakes from Texas were used as a test set for a machine learning (ML) magnitude determination. The white triangles indicate seismic stations, and the red circles indicate earthquakes. (b) The earthquake magnitude error (i.e., predicted vs ground truth (manually reviewed)) distribution is presented for the testing set of the TexNet data. (c) The predicted magnitude corresponding to the applied Vision Transformer (ML) network versus the ground truth is presented. (Saad et. al., 2022; https://doi.org/10.1029/2021JB023657) This result illustrates that a ML magnitude tool can provide effective and timely magnitude estimates thus streamlining operations.

Research designed to quantify attenuation characteristics of the ground motion in Texas (Kavoura et al., 2020; https://doi.org/10.1785/0220190366) has provided improved earthquake magnitude estimates while minimizing the discrepancy between magnitudes provided by U. S. Geological Survey (USGS) and TexNet operations (**Figure 4**).

Additionally, the characterization and understanding of the seismicity across the State has improved significantly, including the seismicity near highly populated areas such as the Midland - Odessa metropolitan area and other areas of increased oil and gas operations (e.g., Permian Basin, Eagle Ford play). This work has identified patterns and rates of seismicity, active faults, and local characteristics of ground motion. These results are being used to understand both the natural factors and the human influences that cause the seismicity. This work quantifies the changing seismic hazard across Texas and thus informs leaders in the State of Texas in mitigating the associated risk. Previously unknown fault zones have been mapped (Appendix A: Seismogenic Characteristics of the Midland Basin as Constrained by Earthquake Source Mechanisms; p.41) whereas others are now more fully characterized and are constantly updated in a publicly available fault database that captures the susceptibility of each fault to rupture.

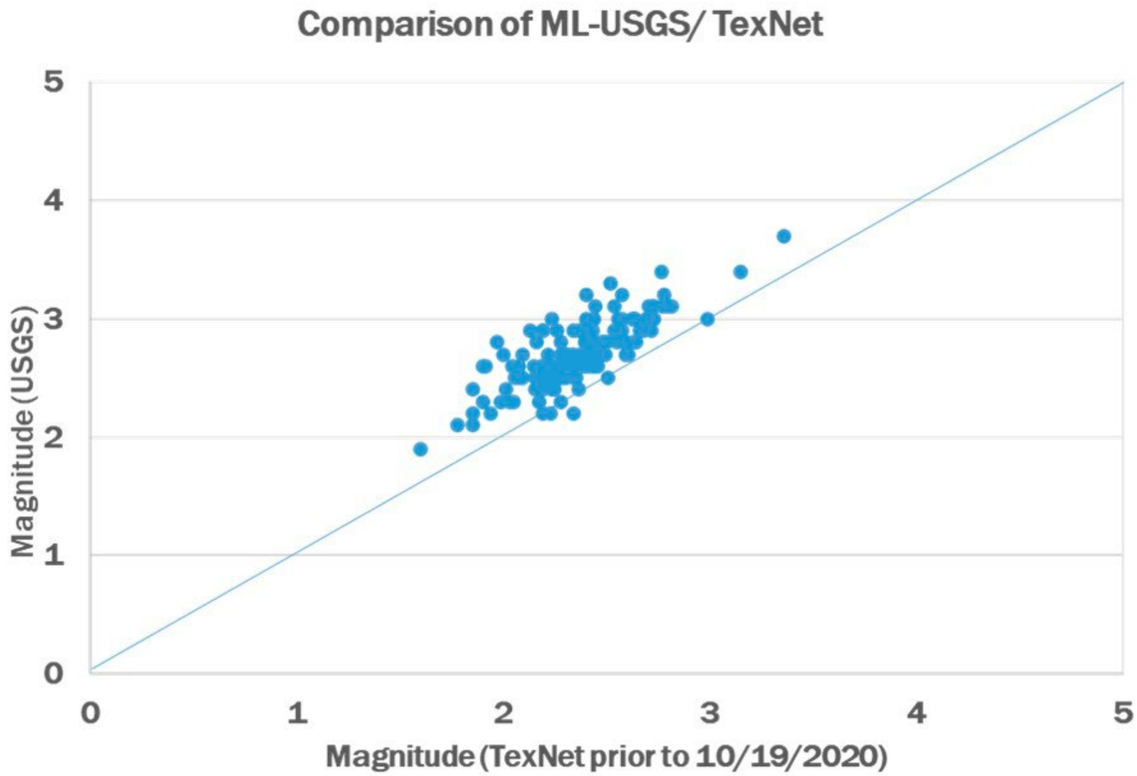

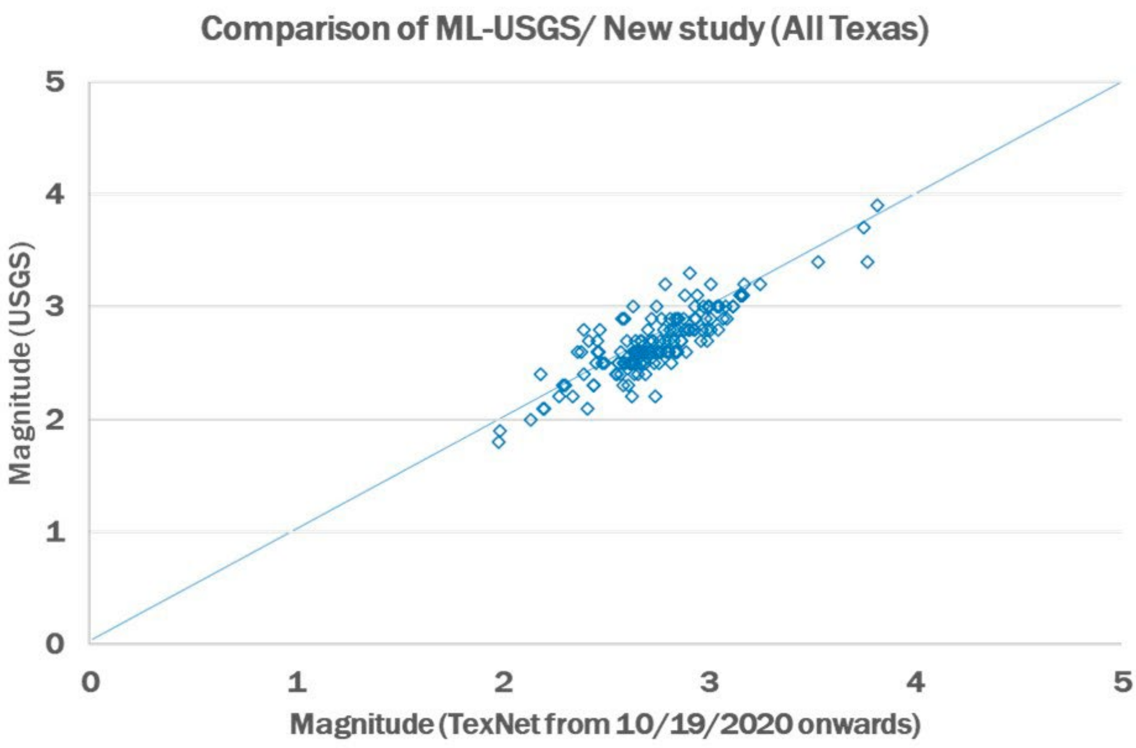

Figure 4. Comparison of magnitude calculated by the USGS and TexNet for the same dataset prior to 10/19/2020 (top) using the initial TexNet ground motion attenuation relations. Comparison of magnitude calculated from USGS and TexNet for the same dataset from 10/19/2020 onward using the revised TexNet ground motion attenuation relations developed by the research program.

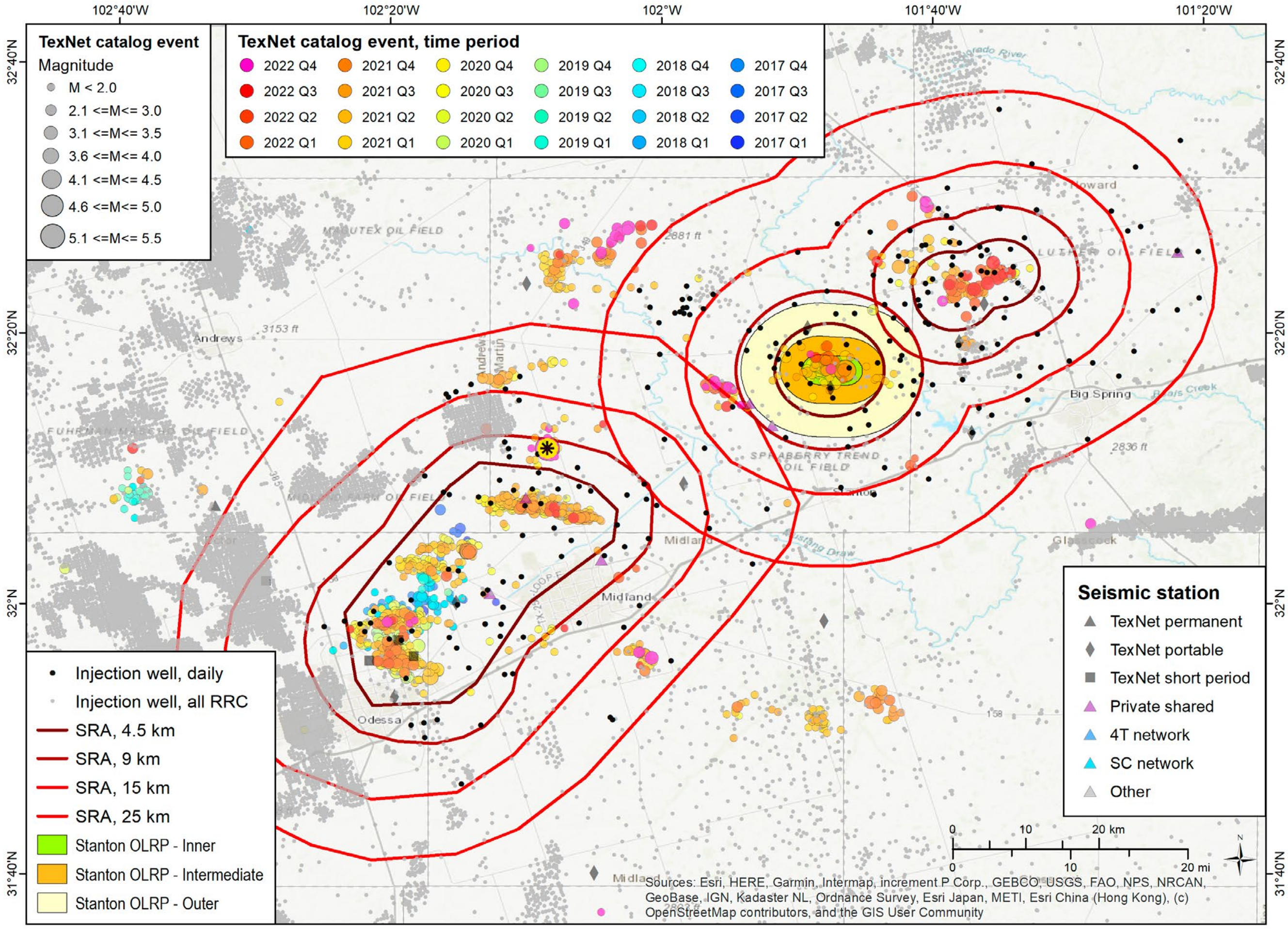

Figure 5. Spatiotemporal distribution of seismicity in the Midland Basin. The Seismic Response Areas (Gardendale to the southwest and Stanton to the northeast) defined by the Railroad Commission using TexNet data are denoted by colored isolines. Different guidelines are assigned based on the SRA isoline and for each SRA. Produced water injection wells are denoted with a dot (black dots denote the location of a well for which daily injection volume and pressure data are provided from the operator using the TexNet web tool https://injection.texnet.beg.utexas.edu). Asterisk denotes the M5.4 earthquake of December 16, 2022.

In areas of increasing petroleum industry activities, quality-controlled databases of hydraulic fracturing and wastewater injection data are being developed and used to identify either the lack of associated seismicity or to assess possible association of these operations with the seismicity. Our statistical or physics-based models are available to assess and understand possible cases where seismicity is related to human activities. These tools include a hindcast capability for assessing earthquake hazard to prior industrial activity. Finally, detailed geological and wastewater injection information are combined into comprehensive models that simulate how subsurface pore pressure can change as a function of time as a result of fluid extraction and injection, possibly altering the earthquake hazard (Savvaidis et al., 2020; BSSA https://doi.org/10.1785/0120200087 and Grigoratos et al., 2022; SRL https://doi.org/10.1785/0220210320). Through our analysis we managed to create a workflow (Appendix A: Workflow of Seismicity Causal Analysis; p. 59) to assess causality of seismicity.

Finally, the ground motion attenuation models of earthquakes in Texas and neighboring states provides a framework to better assess the regional seismic risk and validate new Shakemap models that are routinely used by emergency management authorities (e.g., Texas Division of Emergency Management). These ground motion models combined with assessments of the fragility of different critical infrastructure components (e.g., bridges) have improved the evaluation of seismic risk across the State (Appendix: A Regional Ground Motion Model for Earthquake Shaking in Texas; p.60).

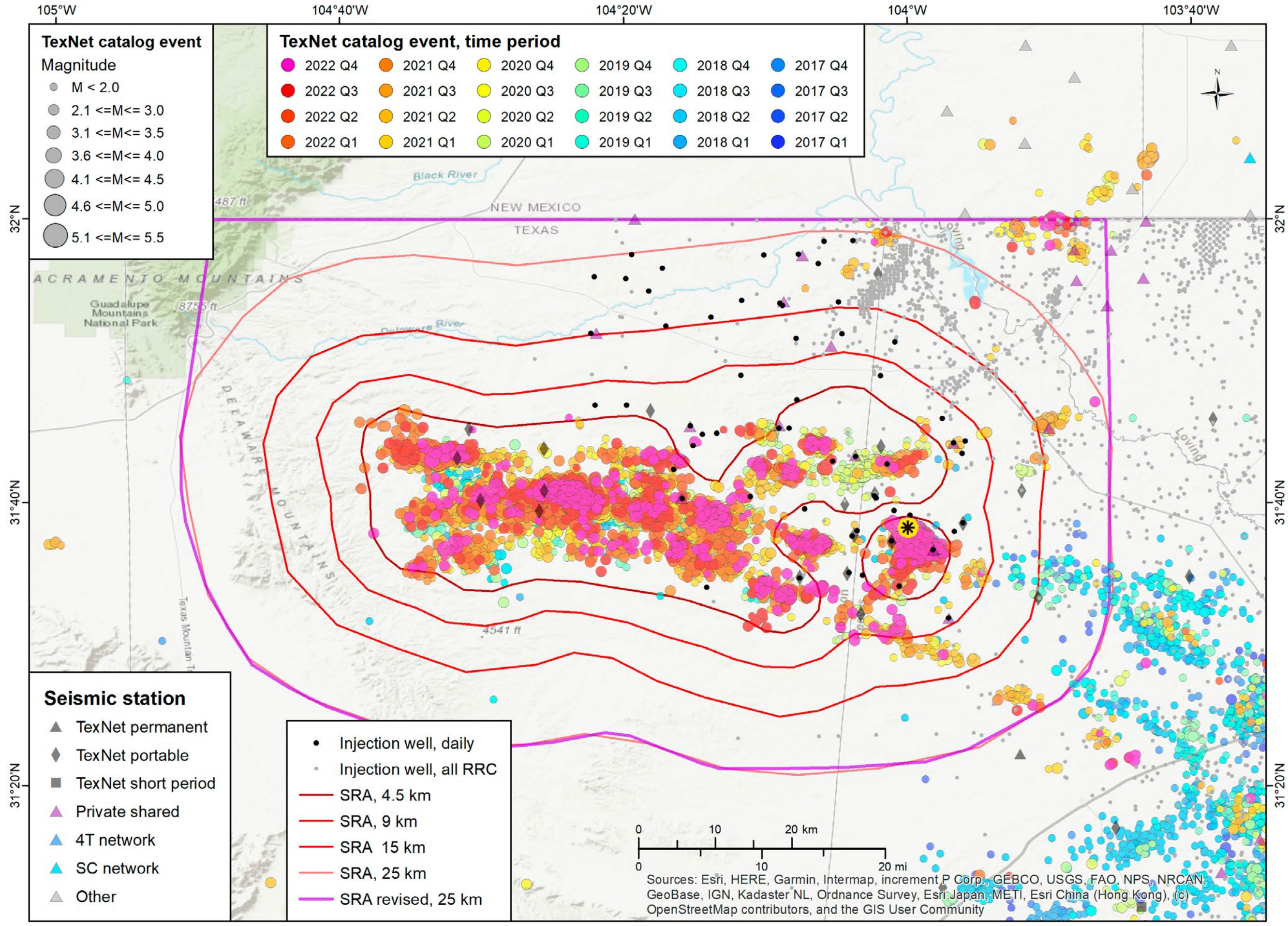

Figure 6. Spatiotemporal distribution of seismicity in North Culberson and Reeves Counties. The Seismic Response Area defined by the Railroad Commission using TexNet data is denoted with colored isolines. Different guidelines are assigned based on the SRA isoline. Produced water injection wells are denoted with a dot (black dots denote the location of a well for which daily injection volume and pressure data are provided from the operator using the TexNet web tool https://injection.texnet.beg.utexas.edu/). Asterisk denotes the M5.4 earthquake of November 16, 2022.

On September 2021, TRRC established the Gardendale Seismic Response Area (SRA) in the Midland Basin (**Figure 5**), a first such highlighted seismic area in State history. This action was in response to increasing seismic activity in the area, based on the TexNet catalog of earthquakes as of September 7, 2021. On October 22, 2021, TTRC established in the Delaware Basin, the North Culberson–Reeves (NCR) Seismic Response Area (SRA) (**Figure 6**). The high resolution TexNet catalog identified earthquake clusters (https://hirescatalog.texnet.beg.utexas.edu) that indicated know or unknown faults in the area (https://doi.org/10.18738/T8/UHOUX8; https://doi.org/10.18738/T8/UHWLDR). This designation of faults provided data that motivated TRRC and industry leaders to work together to establish a set of next steps to mitigate the hazard. In a similar manner as seismicity increased in the Stanton area, the TRRC created an additional SRA's using TexNet data (**Figure 5**).

Savvaidis et al. (2022) (SEG; https://doi.org/10.1190/image2022-3751081.1) documents improved focal depth accuracy that supports the causality of seismicity with industry operations in the South Delaware Basin.

3.0 TexNet Budget Utilization: Spending and Next Biennial Request

Summary: The biennium 2021-22 TexNet budget included $1.4 million to operate and maintain the seismic monitoring network and $1.9 million to support earthquake analysis and research for a total of $3.3 million. These operational funds support the deployment, maintenance, and running the network, as well as the reporting of earthquakes. Research funding supports conducting seismicity analysis, new tools for rapid earthquake assessment, improved location and depth estimates and development of tools and models that improve the understanding of the causes of earthquakes in Texas and their potential impact on the people and infrastructure.

Due to the increase in both the number of monitoring stations and number of earthquakes, TexNet cannot currently analyze earthquakes below magnitude 2.5 by the next business day and cannot analyze events down to magnitude 1.5. This recent change diverges from established TexNet goals and is below the performance standards initially requested by our stakeholders.

For the 2023-24 biennium, we request total funding of $6.1 million to increase staffing for earthquake analyses, improve network operations and continue TexNet research at the current level.

This increased funding will enable improved reporting of events down to magnitude 1.5, communicating agreed upon earthquake information and returning to compliance with the original TexNet goals. This funding increase will provide our community more timely and better spatial locations and depth estimations. Also, we will be able to return real-time data accessibility to at least 95% for TexNet stations.

Texas Seismic Network Operations includes deployment and maintenance of sensors; telecommunications; purchase and operation of TexNet Hub Servers; detection of seismicity and 24/7 operations of analyzing seismicity higher than M3.

Table 3.1 shows a breakdown of current expenses for specific TexNet elements. Operations costs are primarily used to support personnel, materials, services, equipment (seismic and IT) and travel. These costs include salaries of personnel who operate and maintain existing seismometer stations and, redeploy portable seismometer stations to detect, locate and report earthquakes of higher than M2.5 in the state. The majority of spending in research has been on personnel, services and sub-contracts to Southern Methodist University (SMU), The University of Texas Department of Geoscience (UT-DGS) and the University of Houston (UH).

Table 3.1. TexNet Expenses during the 2021-22 Biennium.

Theme	Project Title	Institution/ Unit	Personnel	Materials, Services, Equipment	Sub-Contracts	Computer Charges	Tuition	Travel	Fiscal Yr 21/22 Project Total
Seismology	T1.Texas Seismic Network Operations (Operations)	UT-BEG	$ 766,239	$ 563,645		$ 35,380		$53,265	$ 1,418,529
	T2. Seismicity Characterization in Texas (Operations and Research)	UT-BEG	$ 500,761	$ 74,616		$ 26,511		$15,132	$ 617,020
	T3. Ft. Worth Basin and Permian Basin Seismicity Studies (Research)	SMU			$ 230,516				$ 230,516
	T4. Relative Relocation (Research)	UT-DGS			$ 61,456				$ 61,456
	T5. Shear Wave Splitting Analysis (Research)	UH			$ 58,137				$ 58,137
	T6. Machine Learning in Seismology (Research)	UT-BEG	$ 192,387	$ 38,438		$ 6,151			$ 236,976
	T7. Seismicity Trends and Industry Impact (Operations and Research)	UT-BEG	$ 78,559	$ 119,320		$ 2,263			$ 200,142
Geology	Geologic Characterization and Analysis (Research)	UT-BEG	$ 155,784	$ 340		$ 6,365		$ 2,500	$ 164,989
Seismic Hazard and Risk Assessment	Seismic Risk Assesment (Research)	UT-BEG	$ 74,584	$ 300			$19,172		$ 94,056
Databases and Info Distribution	Geodatabases and Web Developments (Research and Outreach)	UT-BEG	$ 151,107	$ 43,649		$ 5,952			$ 200,708
Total:									$ 3,282,529

Due to the increase in recent seismicity coupled with requests from our stakeholders to improve the seismic network geometry (increasing number of seismometers) during the current biennium, an additional $500,000 from the TexNet research fund (T2 and T7) was moved to TexNet Operations in order to provide additional station maintenance, analysis of increasing seismicity and information distribution and public outreach. However, given the substantial increase in seismicity in the Permian Basin from 2020 to 2022 coupled with insufficient funding to hire five additional seismologists needed to process the substantial increase in seismic data, TexNet is currently unable to meet the operational performance metrics established in consultation with the TexNet Technical Advisory Committee (TAC) and stakeholder groups.

Despite these short comings and considering resource constraints, TexNet has continued to generate valuable products. The high-quality data continues to be recorded, earthquakes cataloged, and applied research completed that has had an increasing impact for various groups. For example, the U.S. Geological Survey (USGS) is now using the waveform data in real time for earthquake detection, location, and further research. In addition, IRIS (Incorporated Research Institutions for Seismology), CISR (Center of Integrated Seismicity Research), SCITS (Stanford Center for Induced and Triggered Seismicity) along with other research community participants have leveraged and some cases further distributed data, and products from TexNet. Finally, the Railroad Commission of Texas, Texas Department of Emergency Management, and other stakeholder groups (Industry, United States Army Corp of Engineers; USACE, etc) are utilizing the TexNet catalogue on a daily basis for decision making.

Details Accompanying Biennium 2023-24 Funding Request

On November 16, and December 16, 2022, there were two M5.4 earthquakes in the Permian basin. These recent events have the highest magnitude in the State of Texas since 1995. During 2022, Texas has experienced the highest rate of seismicity (number of earthquakes) at M2.5 and above in the continental United States including the active tectonic boundary spanning California (**Figure 7**). This illustrates the rapid increase is Texas seismicity and workload for TexNet. The largest 36 magnitude earthquakes in Texas from January 2017 until December 2022 are plotted in **Figure 8** illustrating the preponderance of earthquake activity in far West Texas.

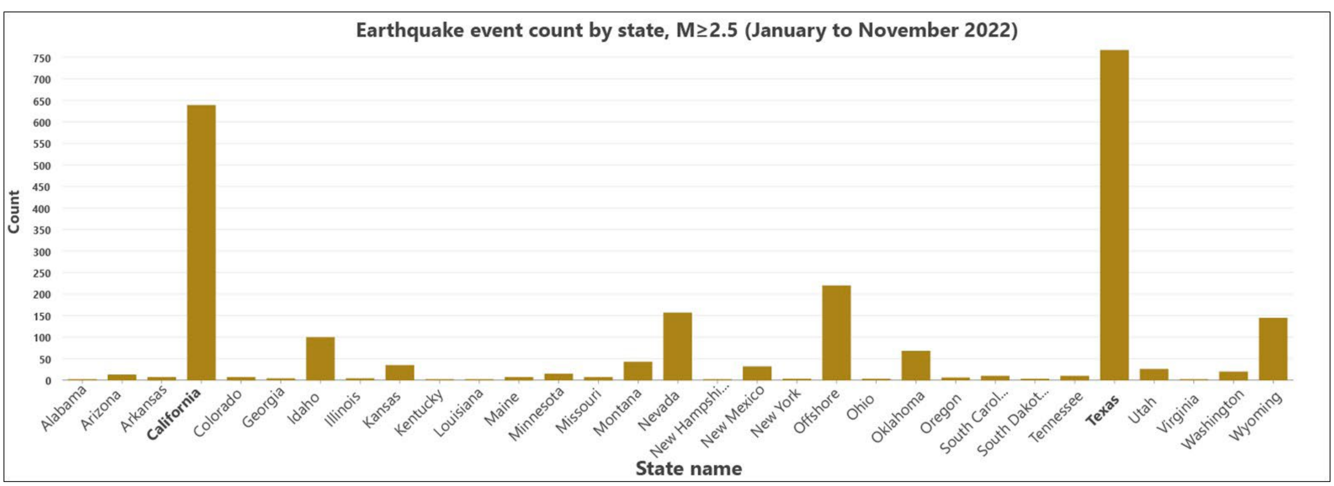

Figure 7. Earthquake count for M≥2.5 events per state in the continental U.S from January to November 2022 (source USGS).

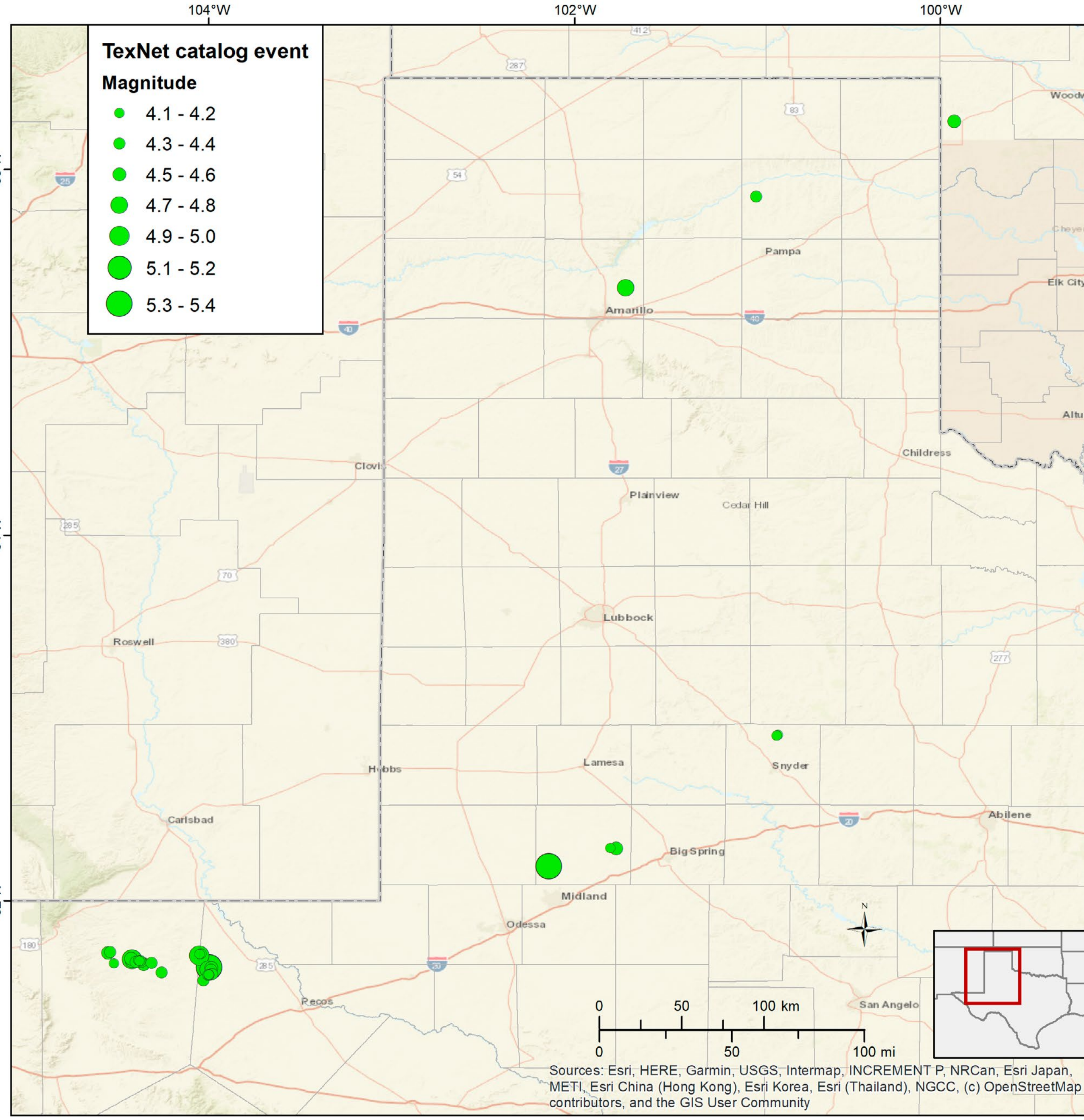

Figure 8. Map showing the 36 highest magnitude earthquakes in Texas from January 2017 to December 2022. Dots are sized by magnitude.

As a result of the increasing seismicity across Texas and the needs of stakeholders to understand, quantify, and mitigate seismic risk, TexNet's reduced funding and an expanding number of seismic stations, has caused increasing strains. To address these immediate needs while trying to maintain a research budget designed to improve products and operations, approximately 27% of the research budget has been re-directed to analyze the increasing seismicity in a timelier manner. It is critical to extend earthquake analysis to M1.5 or below and provide these enhanced products to TexNet clients in a timely manner. This work will allow us to better understand the developing seismicity, better map faults and understand their relationship to disposal of wastewater in order to mitigate their effects. Each order of magnitude reduction in the magnitude threshold is accompanied by about a ten-fold increase in the number of earthquakes that must be analyzed across the state making this goal difficult for TexNet to achieve under current funding.

For TexNet to fulfill these requirements, i.e., analyze seismicity down to M1.5 quickly and effectively and deliver data with availability above 95%, corresponding to the needs of its stakeholders we believe an increase in the budget to $6.1 million for 2023-24 biennium (Table 3.2) is necessary. This new level of funding will allow the increased operational load to be met while maintaining a research budget sufficient to improve the analysis and tools TexNet provides to the user community.

Table 3.2. Anticipated TexNet Expenses during the 2023-24 Biennium.

Theme	Project Title	Personnel	Materials, Services, Equipment	Sub-Contracts	Computer Charges	Tuition	Travel	Fiscal Yr 23/24 Project Total
Operations (Seismology)	Texas Seismic Network Operations and Earthquake Analysis (Operations)	$ 3,420,000	$ 520,000		$ 80,000		$ 80,000	$ 4,100,000
Research (Seismology, Geology, Hazard, Databases and Web Developments)	Seismicity & Geologic Characterization, Earthquake Trends and Industry Impacts, Risk Assessment, Geodatabases and Web Developments (Research)							$ 2,000,000
Total:								$ 6,100,000

4.0 TexNet Seismic Monitoring: Increasing Numbers of Seismic Stations

In 2016, TexNet's initial plan and proposed budget was based on the deployment and subsequent data analysis using 60 additional seismic stations across Texas in addition to the existing 17 stations at the time. That goal was achieved by the end of 2017. With increasing seismicity, much in West Texas, and increased regulatory requirements, stakeholders have argued for increasing the number seismic stations to improve the precision of earthquake locations including depth estimates necessary for regulatory decisions. As result, with industry support, TexNet has deployed and now operates 209 stations as of 2022 (Figure 9). In addition to providing enhanced characterization of the seismicity in the State, TexNet analyzes seismic data from stations deployed and maintained by other groups (e.g., USGS, industry stations deployed through the TRRC incentive to license higher volumes of injecting produced water, seismometers in neighboring States, instruments deployed by a variety of research groups). The total number of seismic stations that TexNet is now archiving and routinely uses in both seismicity analysis and research has increased from 102 stations in 2016 to 354 stations in November 2022. Out of the 354 stations 34 are deployed and maintained by the industry providing data to TexNet. Also, 11 stations have been donated to TexNet. The associated analyst workload has dramatically increased consistent with the expanding number of stations. Experience has illustrated that this level of stations and data are necessary to extend the monitoring threshold to M1.5 as requested by operators and regulators.

From its inception, TexNet with the help of the TAC established standards[1] for seismic monitoring stations that ensures a real-time, high-quality network to provide the necessary ground motion data for daily earthquake analysis. To meet these goals, TexNet deployed an additional 35 stations during 2021–2022 (**Figure 9**). The strategy TexNet has used in deploying additional resources is driven by increased seismicity in key areas of the State and the locations of industrial operations and/or spatiotemporal seismicity patterns. Critical to these deployments is the location of one or more seismic stations directly above the earthquake activity to improve depth estimates, a critical parameter for mitigation strategies associated with industry activities. Specifically, TexNet deployed 15 stations in South Texas, 7 stations in Midland Basin, and 13 stations in the Delaware Basin all locations with ongoing and increasing seismicity. Twelve of the 13 new stations in the Delaware Basin are in North Culberson and Reeves Counties reflecting the recent increase in seismicity in this area including the recent M5.4 earthquake on November 16, 2022.

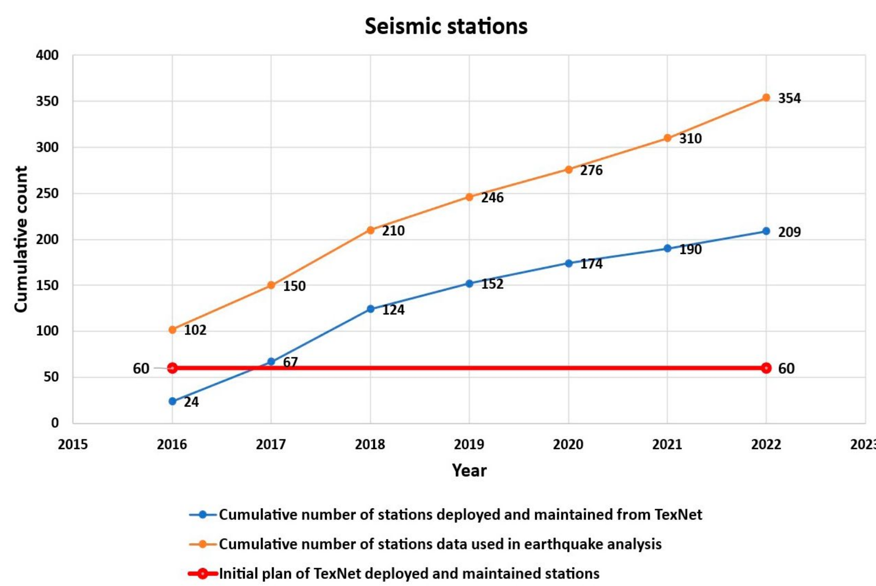

Figure 9. Cumulative number of seismic stations deployed and maintained by TexNet as a function of time (blue line) and seismic stations from which real-time data are archived and used by TexNet earthquake analysis and research (orange line). Red line denotes the number of seismic stations initially planned for TexNet to deploy and maintain was used to produce initial budget estimates for 2016-2017.

To support real-time data acquisition and long-term archival and distribution for more than 200 TexNet stations, additional IT hardware systems were recently purchased, and need to be operated and maintained. To properly support the real-time earthquake monitoring requirements of TexNet,

[1] https://www.beg.utexas.edu/texnet-cisr/seismic-station-requirements

a full backup system for the TexNet Hub was also purchased and installed in order to handle possible disruption of services at the primary site. This equipment is critical to reliably maintaining TexNet's 24/7 operations.

TexNet, continues its operations with on-call staffing based on USGS standards in order to provide earthquake source information to its stakeholders in a time sensitive manner. As an example of this near, real-time monitoring, we use our online catalog[2], to publish earthquake information for all events of $M_L \geq 3.0$ in less than 20 minutes of their occurrence. Earthquakes with $2.0 \leq M_L < 3.0$ are catalogued in the following weeks. Additional USGS performance standards include a magnitude of completeness for the catalog to M2 which based on our stakeholders needs to be lowered to M1.5. Since October 2021, our goal to provide timely reporting, in the next business day, of events down to M1.5, has not been achieved as a result of the increasing seismicity and number of stations while staffing levels have been stagnant. In addition, the USGS requests to post review all moment tensor solutions for events of M≥4.5 in 30 min. This metric is also not currently being met. During 2022Q3, due to increase in the cumulative number of stations maintained by TexNet the network stations uptime has also suffered dropping below the 90% threshold as defined by the USGS. If TexNet continues to miss USGS benchmarks, it may lose it designation as the authoritative source for earthquake information in Texas.

Although, our standard products continue to be used daily by our stakeholders, the lack of resources necessary to analyze seismicity to the levels identified by our oversite Technical Advisory Committee, USGS, industry the Railroad Commission (TRRC) has significantly impacted our daily and long-term operations. Delays in providing reviewed earthquake information down to M1.5 and information on earthquakes down to M2.0 by the next business day impedes the ability of the industry to make decisions necessary to protect their investment while meeting TRRC guidance to enable risk mitigation.

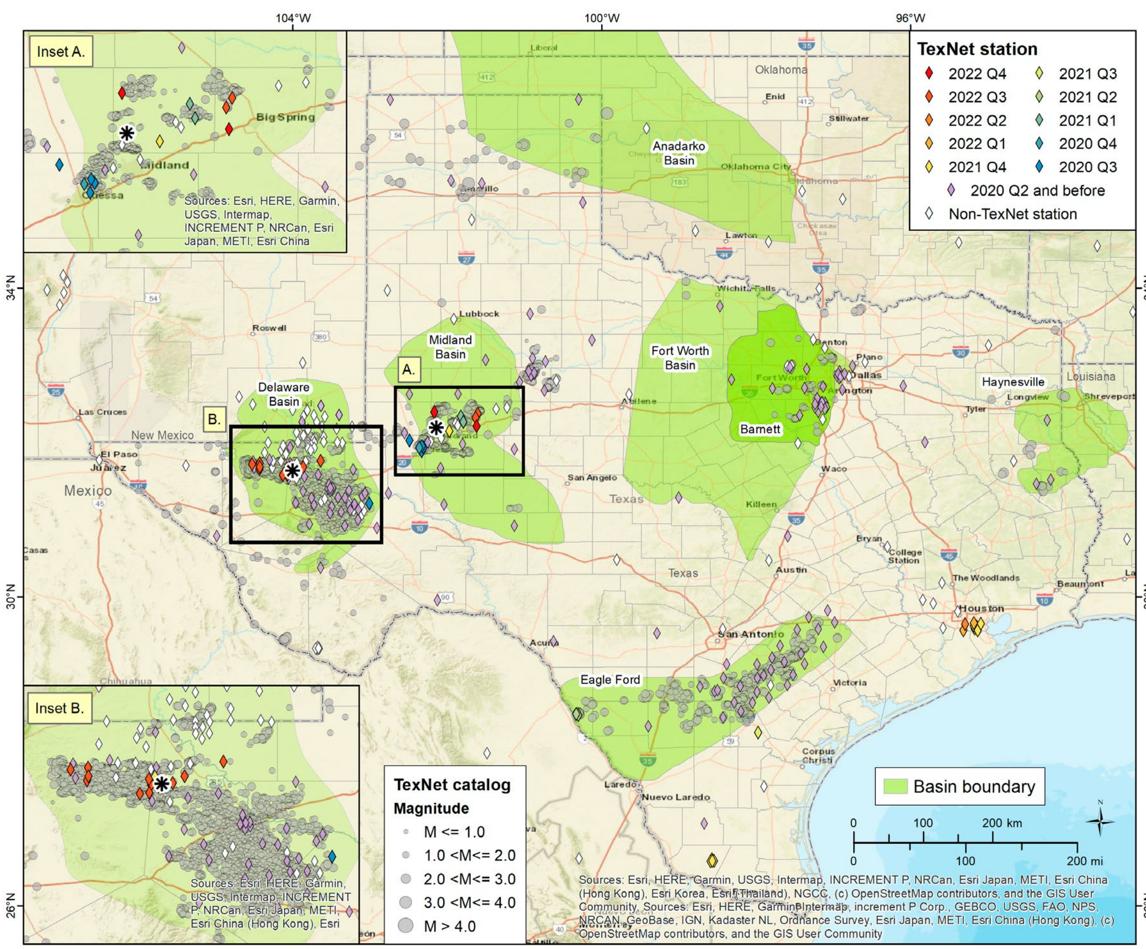

Figure 10. Seismic stations providing real time waveform data to the TexNet hub for seismicity monitoring. Stations deployed/maintained from TexNet are colored. Asterisks denote the M5.4 earthquakes of November 16, and December 16, 2022, in the Delaware and Midland Basins, respectively.

[2]https://catalog.texnet.beg.utexas.edu/

5.0 Seismicity in Texas: Increasing Number of Earthquakes

In **Figure 11** we present the number of earthquakes of M≥2.5 across the State illustrating the different key oil and gas production areas. TexNet, using observed ground motion data from our seismic stations and following a peer reviewed publication[3] TexNet staff have calibrated the local magnitude (M_L) calculation. After this update, which occurred on October 19, 2020, TexNet magnitude estimates became consistent with those produced by USGS for other regions of the United States. Most of the recent seismicity is in the Delaware Basin, which includes many of the highest magnitude earthquakes since 2017 (**Figure 12**). Within the Delaware Basin (West Texas), TexNet has cataloged 535 and 634 events with M_L≥2.5, for 2021 and 2022, respectively, compared to 288 events in 2020. These numbers illustrate the rapid increase in earthquake rate across this area over the last 2 years. The second highest rate of seismicity is in the Midland Basin where 72 and 89 events with M_L≥2.5 cataloged for 2021 and 2022, respectively, compared to 54 in 2020. This increase corresponds to approximately 250 events increase of events with 1.5≤M_L>25. In the Eagle Ford area, the seismicity rate has increased to levels similar to those in the pre-COVID-19 period (40-50 events with M_L≥2.5 annually).

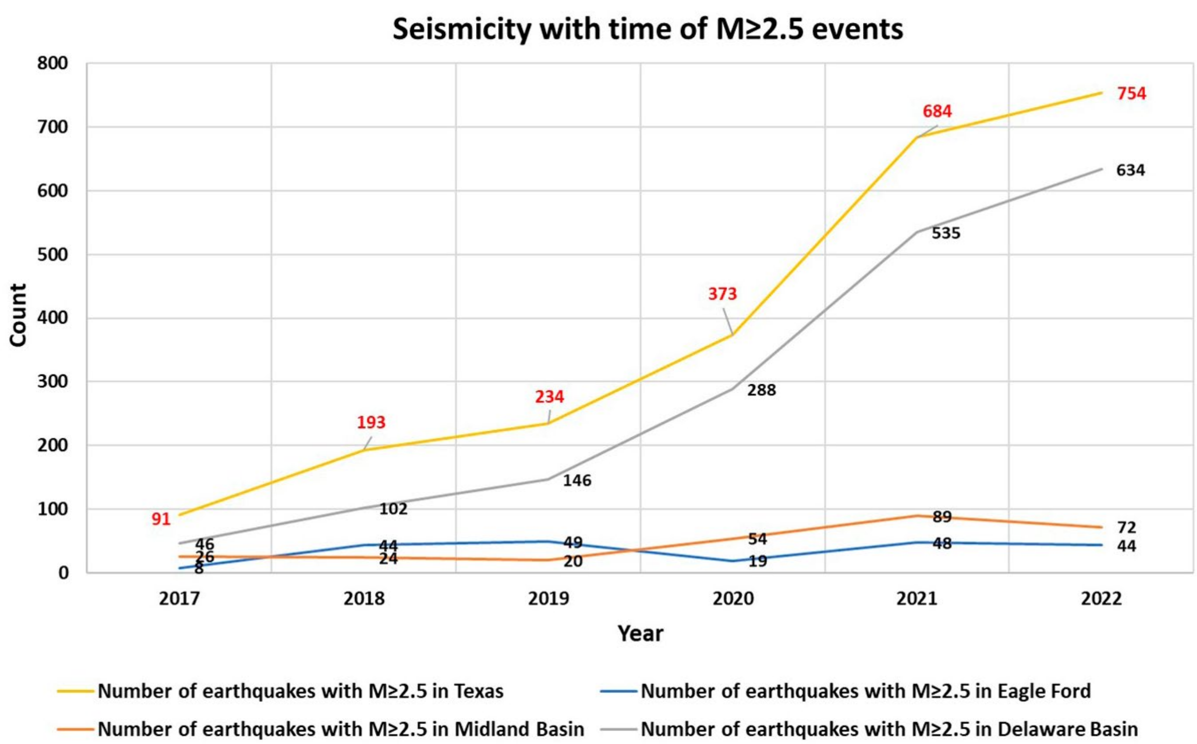

Figure 11. Number of earthquakes of M≥2.5 in Texas (yellow line) and in key oil and gas production areas, i.e., Eagle Ford (blue line), Midland Basin (red line), and Delaware Basin (gray line), 2017–November 2022.

[3]https://doi.org/10.1785/0220190366

In North Culberson and Reeves Counties there are thirty-seven earthquakes in the TexNet catalog with $M_L \geq 4.0$ from January 2020 to November 2022, compared to no earthquakes with $M_L \geq 4.0$ prior to this time extending back to Q1 of 2017. The highest magnitude ($M_L 5.4$) earthquake was reported on November 16, 2022, 3.5 miles east of the county line (**Figure 12**; **Inset B**). In **Figure 13** we present the spatial distribution of felt reports based on 2291 "Did You Feel It" (DYFI) reports from as far as San Antonio and Dallas, submitted to USGS and the ground motion data provided by TexNet stations, due to the Coalson M5.4 earthquake in the Delaware Basin.

In the Midland Basin (Martin County), the TexNet catalog has three events with $M_L \geq 4.0$. The highest magnitude ($M_L 5.4$) earthquake was reported on December 16, 2022, 13 miles north of the city of Midland (**Figure 12**; **Inset A**). The intensity distribution based on 2382 "Did You Feel It" (DYFI) reports from as far away as El Paso and Dalla-Fort Worth, submitted to USGS and the ground motion data provided by TexNet stations is shown in **Figure 14**.

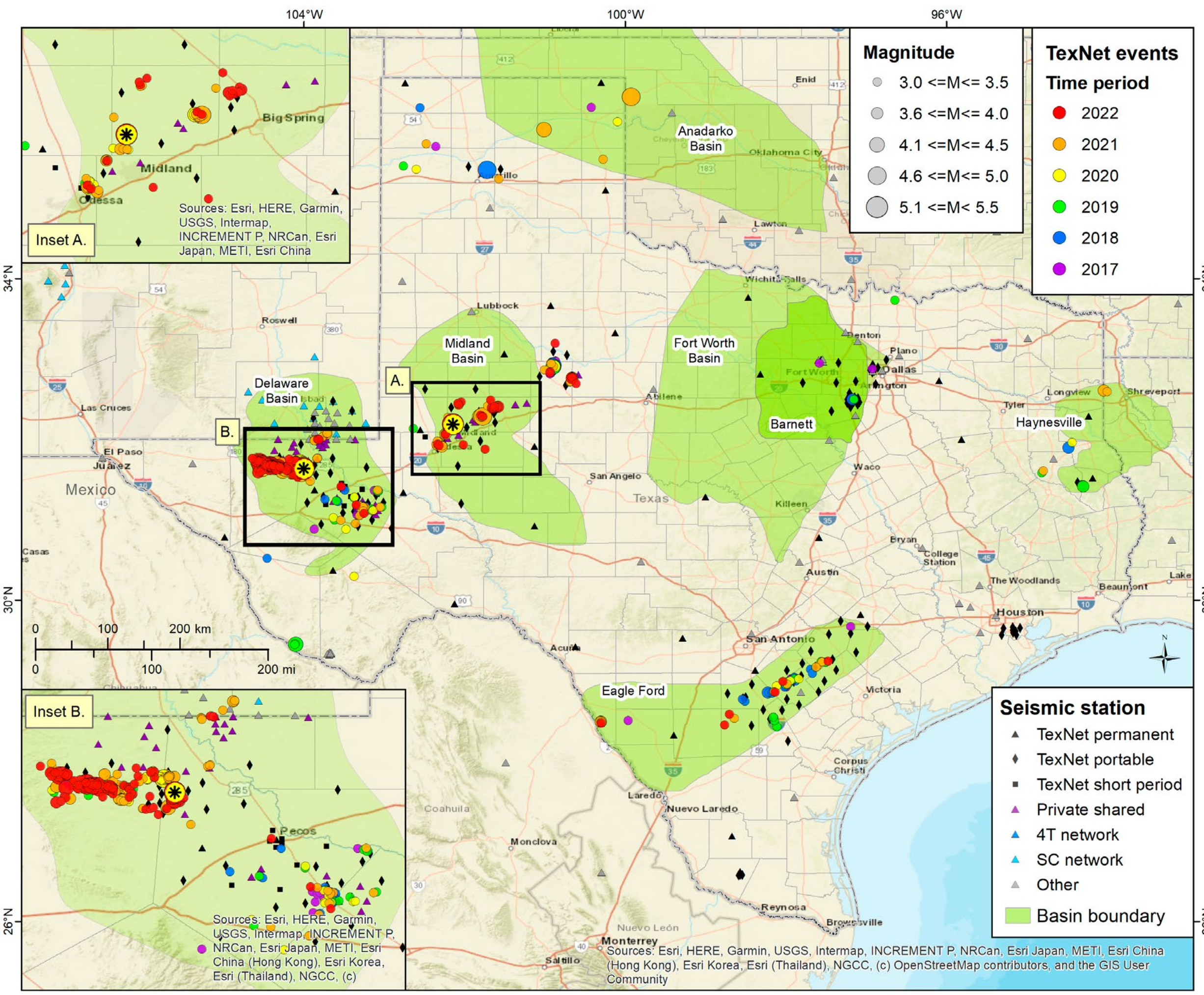

Figure 12. Earthquakes of M≥3.0 since 2017, reported by TexNet until December 2022. Highest magnitude events ($M_L 5.4$) are denoted by an asterisk in a yellow circle. Inset maps A and B indicate earthquake locations and sources of data from each area.

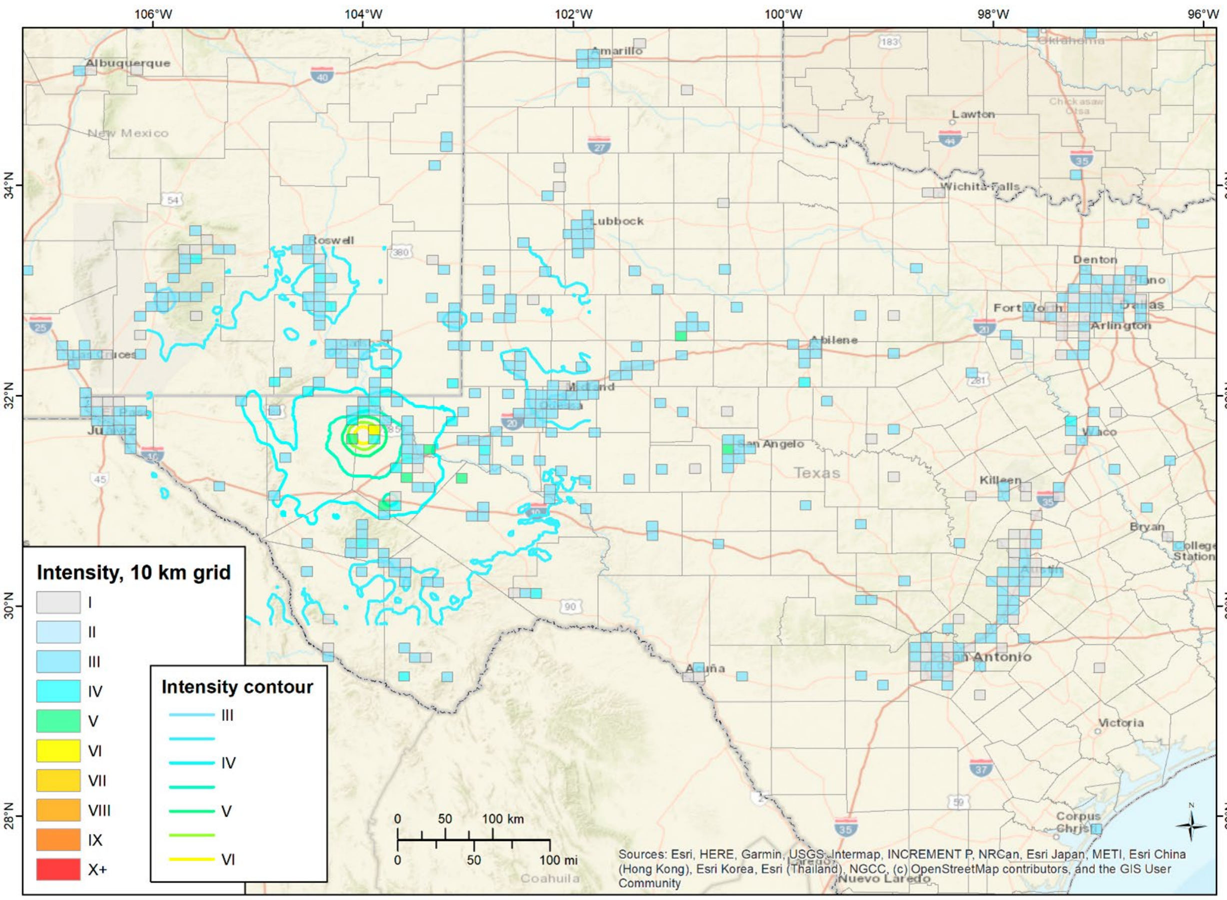

Figure 13. Intensity[4] spatial distribution for the M5.4 Coalson earthquake in West Texas on November 16, 2022. Intensity is provided at 10 km grid cells based on the Did You Feel It (DYFI) reports provided to USGS and as contour lines, based on ground motion data provided from TexNet stations.

[4] https://www.usgs.gov/programs/earthquake-hazards/modified-mercalli-intensity-scale

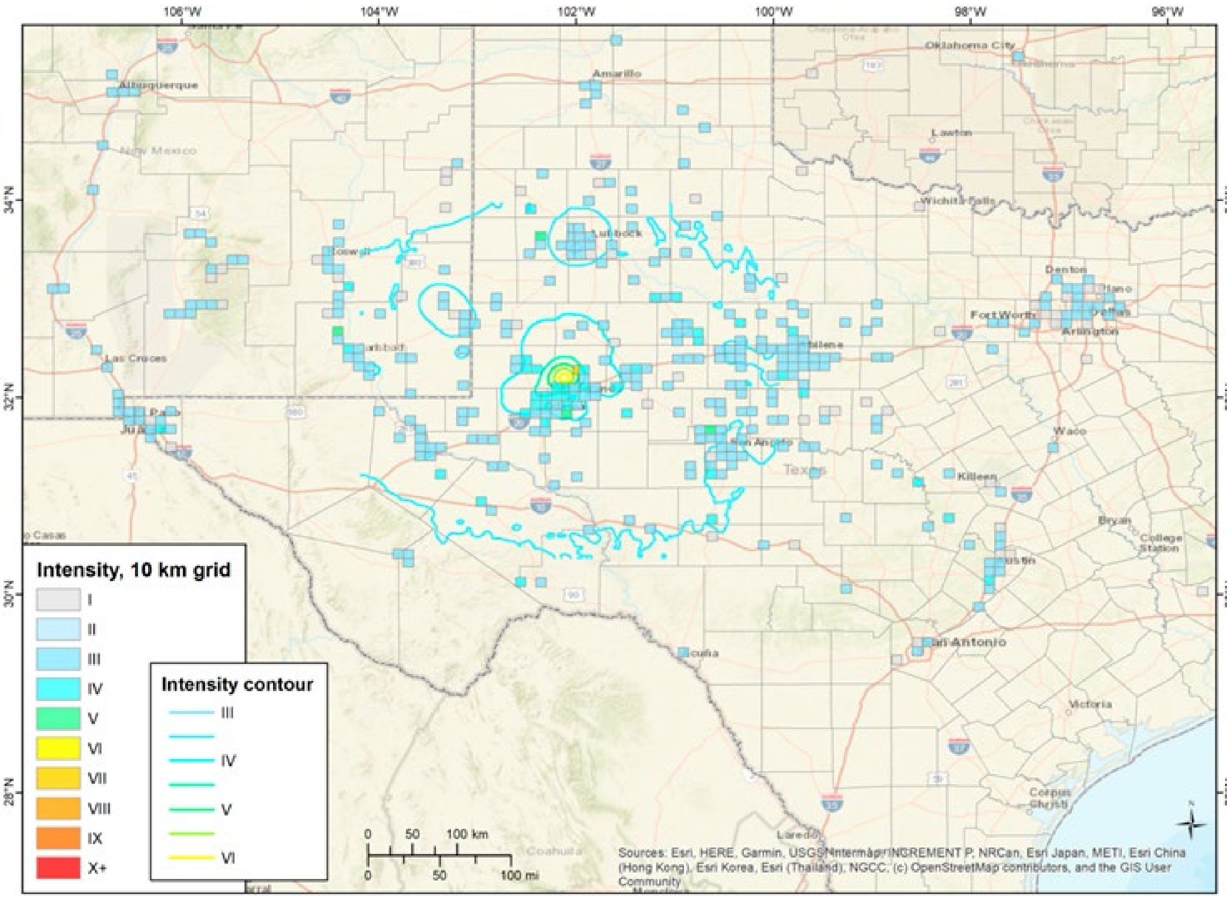

Figure 14. Distribution of ground motion intensity[5] for the M5.4 North of Midland earthquake in West Texas on December 16, 2022. Intensity is provided at 10 km grid cells based on the Did You Feel It (DYFI) reports provided to USGS and as contour lines, based on ground motion data provided from TexNet stations.

[5] https://www.usgs.gov/programs/earthquake-hazards/modified-mercalli-intensity-scale

6.0 Web Tools for Stakeholders

During the current biennium (2021-23), in response to the needs of TexNet stakeholders (e.g., petroleum industry and its regulators) new online tools have been developed and published (https://www.texnet.beg.utexas.edu/). These tools provide users analyses that can enhance the understanding the seismicity in order to mitigate earthquake hazards. Following high magnitude earthquakes (e.g., November 16, 2022), these Web tools experience their highest usage. from November 1 to 21, 2022, a record 973 new users visited TexNet's catalog (https://catalog.texnet.beg.utexas.edu/); of these users, almost 500 were online after the M5.4 earthquake in the Delaware Basin (**Figure 15**).

Along with the online catalog of seismicity we now provide a high-resolution catalog, updated semi-annually, (https://hirescatalog.texnet.beg.utexas.edu/). Based on this catalog, and using available focal mechanisms, we update our fault maps and assess fault reactivation, characterizing seismicity and earthquake triggering in space and time.

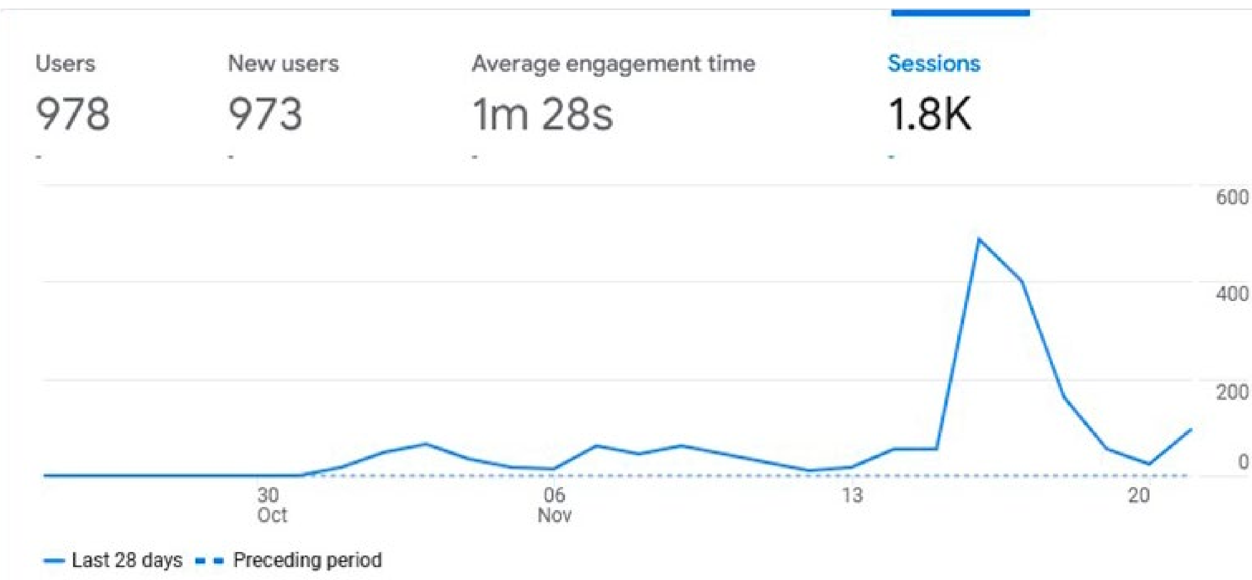

Figure 15. Number of visits to the TexNet web catalog (https://catalog.texnet.beg.utexas.edu/), showing total numbers of users, new users, viewing time, and number of visits in November 2022, relative to prior days

In collaboration with the Railroad Commission of Texas (TRRC) we have developed the TexNet Injection Volume Reporting Tool (https://injection.texnet.beg.utexas.edu/) to receive, store, and make accessible to stakeholders and the public daily injection volume and pressure information. TexNet's injection tool (**Figure 16**) as of November 2022, includes 280 wells registered to the system by 108 users, incorporating more than 251,000 injection records.

We have developed a web-based tool to monitor the lag time (i.e., current delay time to receive real time data) of ground motion data sourced from the seismic instruments deployed in the field (https://monitor.texnet.beg.utexas.edu/) in order to enhance operations by alerting needed maintenance.

In allocating a small portion of TexNet funding to developing and maintaining these web tools we are providing critical information, which is used daily, thus improving transparency and helping the industry and its regulators to mitigate seismic risk.

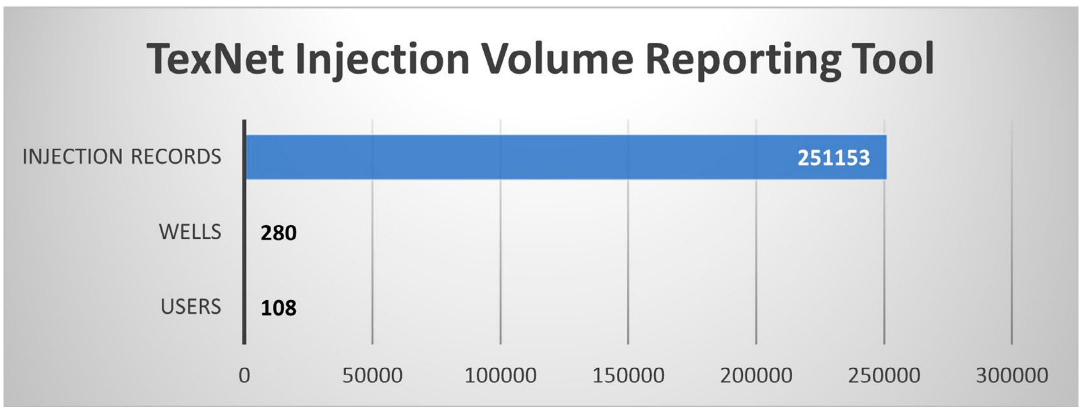

Figure 16. TexNet Injection Volume Reporting Tool (https://injection.texnet.beg.utexas.edu/) statistics showing numbers of records, wells, and users as of November 2022.

Appendices: Abstracts

TexNet: A Statewide Seismological Network in Texas

A. Savvaidis, V. O'Sullivan, D. Siervo, M. Shirley, B. Uku, C. McCabe, P. Fleck, C. Bretton and P. Chen

Induced seismic events have been recorded recently in the southern midcontinent of the United States, including Texas. These events, associated with hydrocarbon exploration and subsequent disposal of wastewater byproduct, have led to substantial public discussions regarding cause, public safety, and potential risks of damage to infrastructure. To better understand these events and to monitor earthquake activity in general, the 84th Texas Legislature funded creation of a statewide, seismic-monitoring program known as the Texas Seismological Network (TexNet). Since then, the goal of TexNet has been to provide authenticated data to evaluate the location, frequency, and likely causes of natural and induced earthquakes. TexNet, through November 2022, deployed more than 160 new seismic stations in the state of Texas (**Figure 1**), 32 of which were deployed between September 2020 and November 2022, to better monitor seismicity in key areas on the basis of industrial operations or spatiotemporal seismicity patterns. Specifically, TexNet deployed 12 stations in Eagle Ford, 5 stations in the Midland basin, and 15 stations in the Delaware basin. Thirteen out of the fifteen new deployments in the Delaware basin are in North Culberson–Reeves Counties, responding to a recent high-magnitude increase in seismicity in this area.

TexNet makes use of a cost-efficient network geometry—a hybrid set of instruments, including (1) broadband borehole installations (long interstation distance); (2) broadband, shallow-depth posthole deployments (mid-interstation distance); and (3) short-period installations (short-interstation distance). In this way the number of stations on top of an earthquake cluster increases.

An earthquake-management system (SeisComp3) is being used to detect, locate, and analyze earthquake events (**Figure 2**) and is available through various dissemination tools (https://catalog.texnet.beg.utexas.edu). Initial implementation of TexNet has reduced the magnitude of completeness (Mc) across Texas from 2.7 to less than 2.0 in specific areas and has played a role in a large decrease in uncertainties about earthquake-source parameters.

TexNet operations include on-call staffing who follow USGS standards and provide earthquake-source information to stakeholders in an increasingly timely manner. Toward this objective, the catalog website publishes earthquake information on events with ML ≥3.0 in less than 20 minutes from time of occurrence.

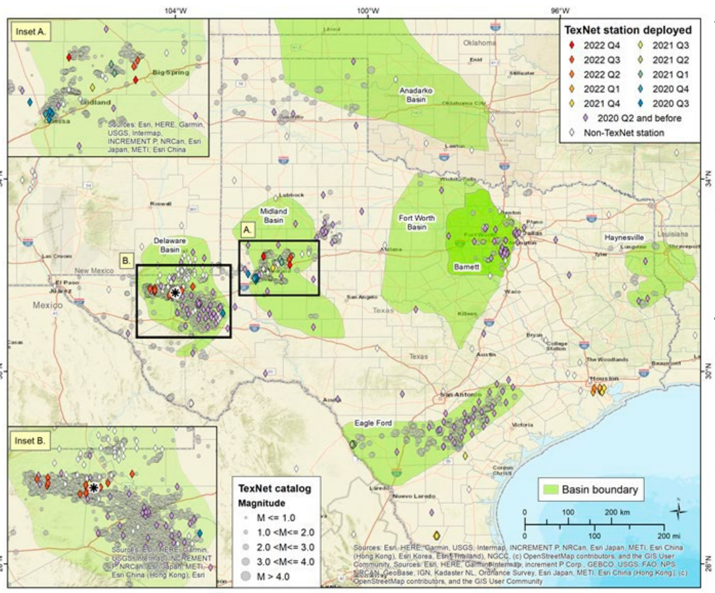

Figure 1. Seismic stations providing real-time waveform data to TexNet hub for seismicity monitoring. Asterisk = M5.4 earthquake of November 16, 2022.

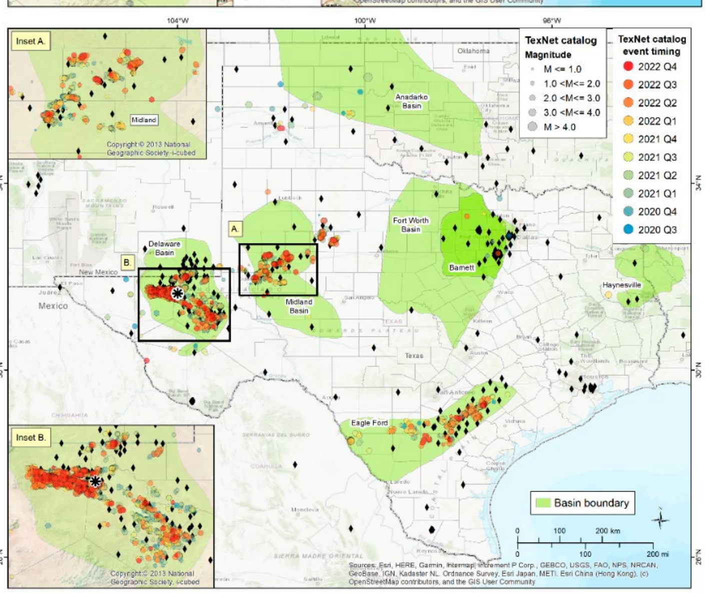

Figure 2. Earthquakes reported by TexNet between July 2020 and November 18, 2022. Star = highest magnitude event (ML5.4). Also shown, deployed seismic stations providing real-time data for earthquake cataloging as of July 2020.

Enhancing the TexNet Web Presence with New Applications, Simpler URLs, and Asynchronous Execution of Modeling Tools

A. Averett, C. Templeton, and A. Savvaidis

Since its inception, TexNet's website has been an important means of communicating the results of TexNet's efforts with its stakeholders, with the TexNet Earthquake Catalog being the primary feature. During the 2021 to 2023 biennium, we undertook significant efforts to enhance that web presence for supporting seismicity research in Texas, accelerating the pace of data delivery to stakeholders, and improving network functionality.

Among the completed enhancements are two totally new applications: (1) the TexNet Injection Reporting Tool (fig.1), which allows operators of injection wells to report their injection volume data directly on a daily basis, improving the temporal resolution of data available to researchers and regulators, and (2) the TexNet System Status Monitor, which allows near-real-time monitoring of the operating status of individual TexNet stations at a glance (fig. 2). A rearrangement of the URLs for each TexNet application, accompanied the release of these tools, provided users an easier to remember address for each tool. For example, the TexNet Earthquake Catalog can now be reached at https://catalog.texnet.beg.utexas.edu.

Planned additions in the coming year include creation of multiple features that allow the user to execute complex software tools developed by or in cooperation with TexNet within the web application. These applications will provide the public with access to TexNet's novel science logic without burdening the user with the complex setup required to run experimental software in a repeatable way. A key challenge presented by this task is the need to handle long-running code within a browser session, wherein users cannot necessarily be relied upon to keep the browser open, and they may need to notified afterward that the process has completed. Reusable software tools for addressing this challenge will be built and deployed for this purpose.

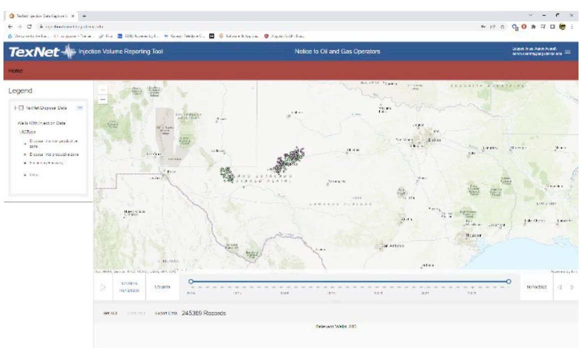

Figure 1. The TexNet Injection Reporting Tool.

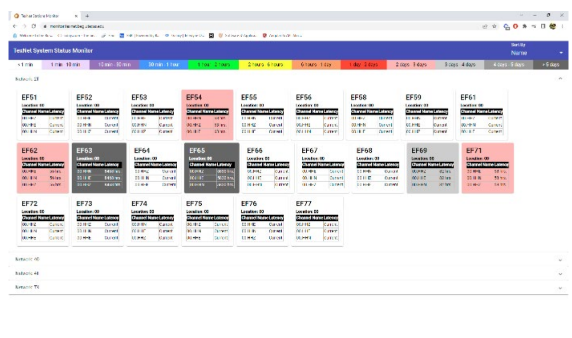

Figure 2. The TexNet System Status Monitor.

Induced-Seismicity Hypocentral-Depth Stability and Sensitivity to Vp/Vs in the South Delaware Basin, West Texas

A. Savvaidis, A. Lomax, R. Dommisse, C. Breton, M. Shirley, and V. O'Sullivan

Modified from Second International Meeting for Applied Geoscience & Energy (SEG-AAPG) https://doi.org10.1190/image2022-3751081.1

Understanding the causative activity and host formation of induced seismicity requires accurate hypocentral-depth determinations. However, depth determination is greatly complicated in the Delaware Basin by the presence of a shallow, high-seismic-velocity, Ochoan salt-evaporite layer and by the paucity of S-wave velocity data. In our approach, we extended recent work on accurate depth determination in the South Delaware Basin (Sheng et al., 2022) to (1) construct a general procedure for avoiding location-depth instability due to the Ochoan layer and (2) explore the change in hypocenter depths as a function of Vp/Vs. We have developed a location procedure valid when using close and far station data for avoiding depth bias due to the Ochoan layer. We also examined the sensitivity of hypocentral-depth estimates in the Pecos–Reeves County line area (Figure 1) to variation in Vp/Vs ratio.

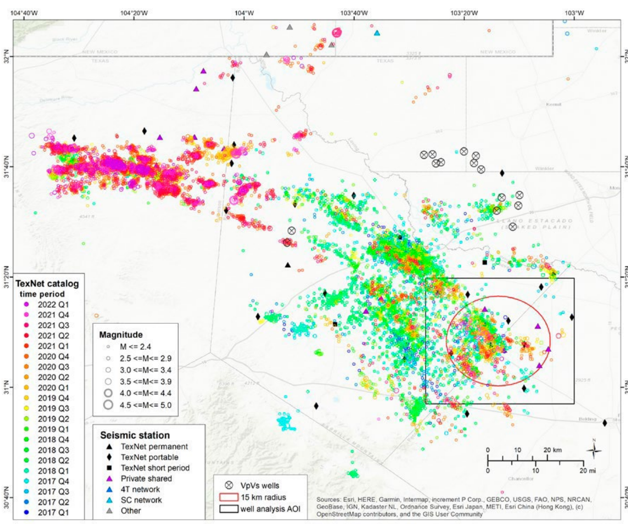

Depth distribution of relocations for Vp/Vs 1.89 (Figure 2) falls around two horizons at about 1.5 and 2.5 km below the surface, mainly in and around the Delaware Mountain Group (DMG) and above the depth of hydraulic-fracturing well laterals. With a lower Vp/Vs of 1.73 and with multi-Vp/Vs, event depths generally increase as the proportion of outlier locations "glued" at the surface decreases markedly. Many events occur in and around the DMG, as with Vp/Vs 1.89, but additionally around 3 to 3.5 km depth in the lower Bone Spring and around the depth of HF well laterals in the upper Wolfcamp, especially for Vp/Vs 1.73. Validity of this modified model for location in the Delaware Basin is supported by general agreement, for Vp/Vs 1.89, between hypocenter depths obtained with this modified model using close and distant stations, and depths obtained by Sheng et al., 2022, with an unmodified well log model and only close stations. We also explored the effect on hypocenter depths with different sets of Vp/Vs ratios applied to the modified model. The proportion of outlier locations "glued" to the surface decreases and event depths generally increase with a decreasing Vp/Vs ratio. For Vp/Vs 1.73, and slightly less so for multi-Vp/Vs, many events occur at the base of the Bone Spring and top of the Wolfcamp Formations around the depth of HF injection activity.

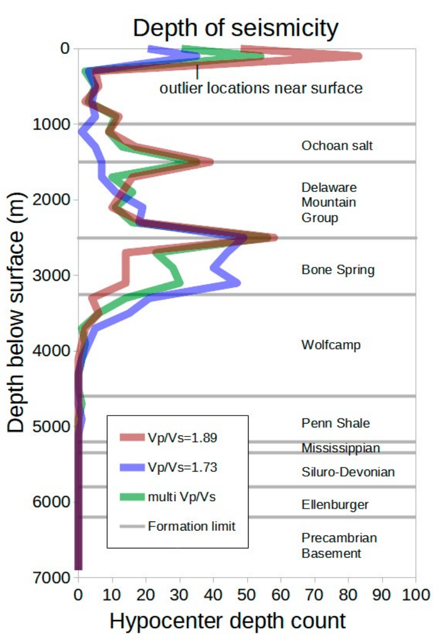

Figure 1: Seismicity in the Delaware Basin from 2017 through 2021. Red circle denotes area where seismicity is analyzed. Rectangular area denotes boundaries of area where injection and hydraulic fracturing wells are presented in Figure 2.

Figure 2. (top) Line histograms of hypocentral depth of relocated seismicity for different Vp/Vs ratios. Approximate depth limits of main geological formations are denoted by horizontal gray lines. Depth is from Earth's surface.

High-resolution and robust microseismic grouped imaging and grouping strategy analysis

G. Huang, X. Chen, O. M. Saad, Y.F. Chen, A. Savvaidis, S. Fomel, and Y. Chen

Geophysical Prospecting, 2022, 70, 980–1002

As an advanced real-time monitoring technique, microseismic source-location imaging provides valuable information during hydraulic fracturing, for example, the development of fracture networks and the effective reservoir reconstruction volume. However, microseismic data always suffer from weak induced energy and susceptibility to noise interference. In the case of a low signal-to-noise ratio, it is extremely challenging to perform robust microseismic imaging. Here, we first introduce several state-of-the-art imaging conditions and two hybrid imaging conditions, which are followed by a detailed analysis of the impact of different grouping strategies. Then, we briefly analyze the sensitivity of different imaging conditions to noise using a one-dimensional signal. Next, several benchmark models, including two-dimensional Marmousi-II and three-dimensional SEG Advanced Modeling, are used as numerical examples for testing the passive-source imaging algorithms. Finally, three-dimensional real microseismic data are used to further investigate the impact of the grouping strategy on the imaging. The numerical examples and field data demonstrate the effectiveness of the proposed grouping strategy for the grouped imaging conditions.

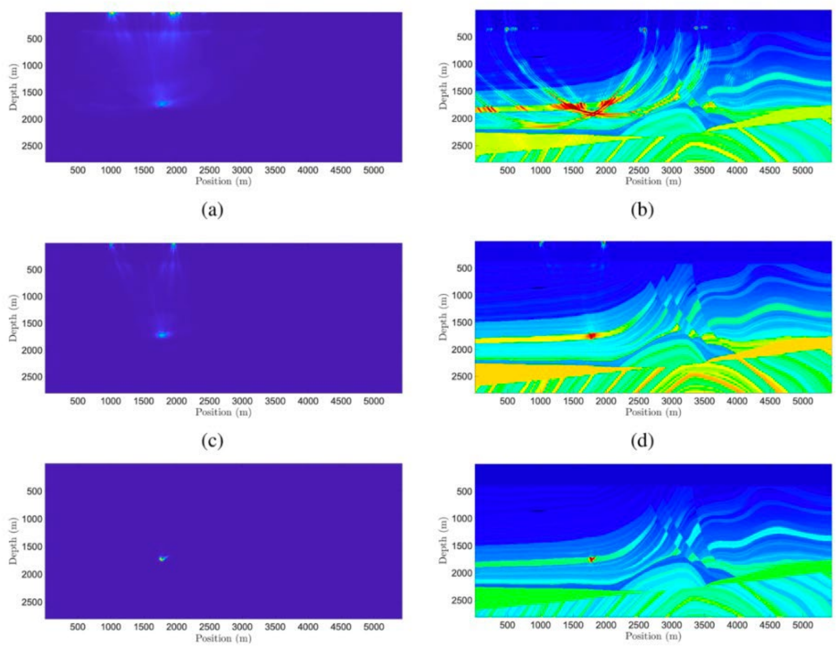

Real-Time Earthquake Detection and Magnitude Estimation Using Vision Transformer

O.M. Saad, Y.F. Chen, A. Savvaidis, S. Fomel, and Y. Chen

Journal of Geophysical Research – Solid Earth, 2022, 127, e2021JB023657

We propose to design two separate vision transformer (ViT) networks: one for picking the P-wave arrival time and the other for predicting the earthquake magnitude using a single station. For real-time application, we pick the P-wave arrival times and consider them as the reference, based on which the non-normalized 30 s (i.e., 1 s before and 29 s after the reference time) three-component seismograms are used to predict the magnitudes of the corresponding earthquakes. The ViT picking network is first trained and tested using the STanford EArthquake Data set (STEAD) and shows robust picking performance, achieving an average picking error of less than 0.2 s compared to the manual picks. Then, the ViT magnitude estimation network is evaluated using several data sets, including those from California, STEAD repository, and Texas. The ViT demonstrates robust magnitude estimation performance in all these test cases as compared with the benchmark methods. For magnitude estimation, the mean absolute error (MAE) and the standard deviation error (σ) for the testing set of the STEAD data set are 0.112 and 0.164 (as compared with 0.141 and 0.219 for the state-of-the-art MagNet method), respectively. The MAE and σ for the California testing set are 0.079 and 0.120 (as compared with 0.089 and 0.138 for the MagNet method), respectively. As a case study, the new ViT networks are applied to the 24-hour continuous seismic data of the TexNet-PB05 station recorded on September 20. The network successfully picks all the events in the TexNet catalog with a small (<=0.42) magnitude error. The ViT network shows promising magnitude prediction results when tested with 4 s long seismograms. This highlights its potential in the earthquake early warning (EEW) system for fast and reliable decisions.

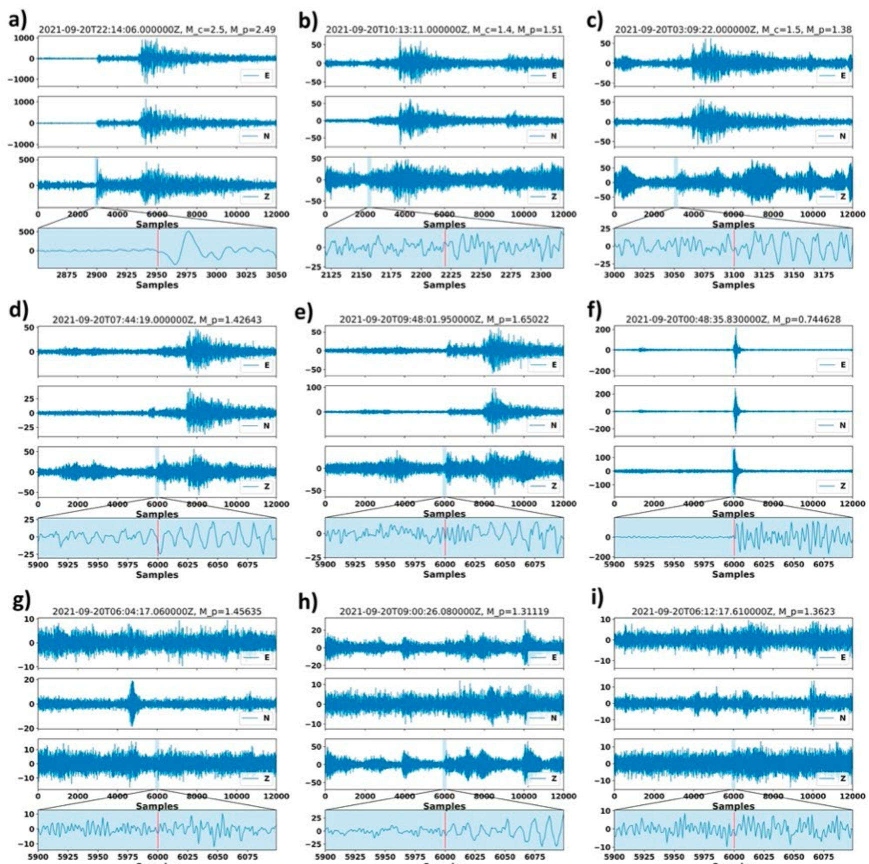

Figure 1. A few examples of the picked events and their predicted magnitude corresponding to the ViT network from one-day continuous seismic data (TexNet). The first row denotes some events in the TexNet catalog. The second row represents some picked events corresponding to the proposed model, which are not listed in the public catalog. The third row shows some false alarms. Mc and Mp denote the catalog and predicted magnitudes, respectively. The vertical line represents the picked P-wave arrival time corresponding to the ViT picking network.

Unsupervised Deep Learning for Single-Channel Earthquake Data Denoising and Its Applications in Event Detection and Fully Automatic Location

O. M. Saad, Y.F. Chen, A. Savvaidis, W. Chen, F. Zhang, and Y. Chen

IEEE Transactions on Geoscience and Remote Sensing, 2022, DOI: 10.1109/TGRS.2022.3209932

We propose to use unsupervised deep learning (DL) and attention networks to mute the unwanted components of the single-channel earthquake data. The proposed algorithm is an unsupervised technique that does not require any prior information about the input data, i.e., no need for the labeled data. The imaginary and real parts of the short-time frequency transform (STFT) are divided into several overlapped patches to be the input of the proposed DL network, while the output target is the absolute value of the STFT. The proposed DL network utilizes a customized loss function to reconstruct the signal mask, where the STFT components related to the seismic noise are muted. An adaptive thresholding technique is utilized to obtain the binary mask, which is multiplied by the real and imaginary parts of the input seismic data, i.e., the binary mask has zero values for the samples corresponding to the unwanted components and ones for the corresponding seismic signal components. Then, inverse STFT is used to reconstruct the denoised signal. The proposed algorithm is evaluated using samples from the STanford EArthquake Data set (STEAD), and the results are compared to the benchmark denoising method, i.e., DeepDenoiser. As a result, the proposed algorithm shows a robust denoising performance and outperforms the DeepDenoiser method by 1.95 dB in terms of signal-to-noise ratio. Its effectiveness and potential are validated through several typical seismological tasks including earthquake event detection and fully automatic earthquake location.

Seismic data denoising can be categorized into two groups, i.e., multichannel and single-channel methods. The former requires a sufficiently dense spatial sampling to take advantage of the spatial coherency of seismic data but could be more effective than the latter. The latter is more flexible to apply regardless of the spatial sampling density but is prone to signal damages due to the lack of spatial constraint. Here, we propose an effective single-channel denoising method that can be widely applied in any earthquake waveforms based on deep learning. Deep learning methods are either supervised, which requires a large number of training labels, or unsupervised, which is free of the tedious label preparation step. The proposed denoising framework is unsupervised, thus is readily applicable in daily seismological monitoring tasks.

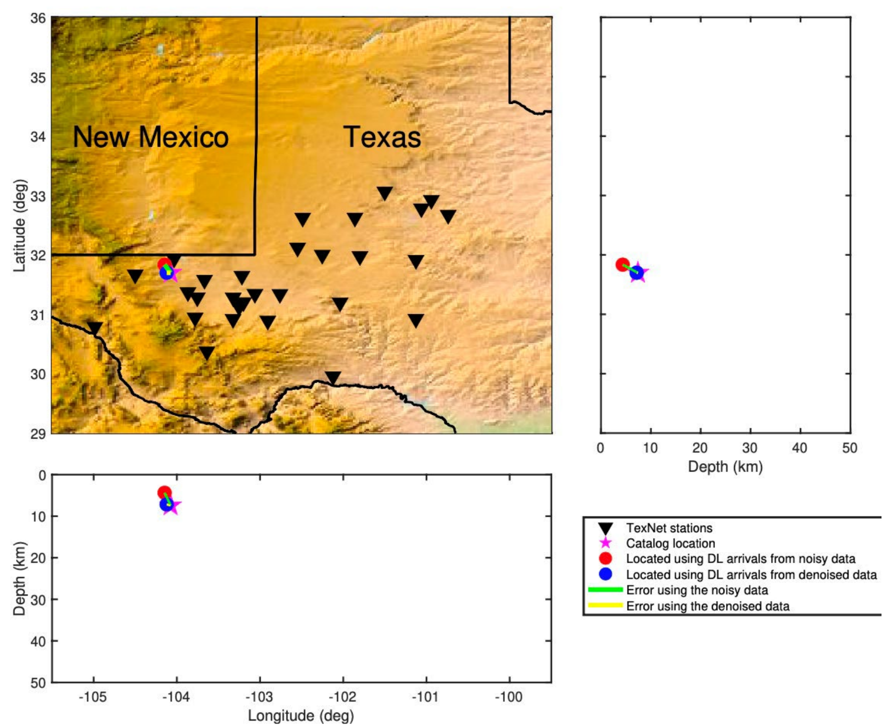

Figure 1. Comparison of the localization results in different cases with the catalog location in the regional scale. The marked 30 stations (black inverted triangles) are the stations used for location using an ML-based method (Chen and others, 2022). Note that the error, especially in depth, of the denoised data has been significantly reduced due to the much more accurate P-wave arrival time picking, since we can barely see the yellow line denoting the error.

Earthquake Forecasting Using Big Data and Artificial Intelligence: A 30-Week Real Case Study in China

O.M. Saad, Y.F. Chen, A. Savvaidis, S. Fomel, X. Jiang, D. Huang, Y.A.S.I. Oboué, S. Yong, X. Wang, X. Zhang, and Y. Chen

Submitted to Seismological Research Letters

Earthquake prediction is one of the most challenging tasks in the field of seismology that aims to save human life and mitigate catastrophic damages. We designed a real-time earthquake prediction framework to forecast earthquakes and tested it in seismogenic regions in southwestern China. The proposed method is based on dimension reduction from massive earthquake waveform data using principal component analysis (PCA) and machine learning using the random forest (RF) method. The input data is the feature provided by the Multicomponent Seismic Monitoring System (AETA), where the data is recorded using two types of sensors per station, i.e., electromagnetic and geo-acoustic sensors. The target is to predict the location and the magnitude of the earthquake that may occur next week, given the data of the current week. The proposed algorithm is trained using the available data from 2016 to 2020 and is evaluated using 30-week real-time data collected during 2021. As a result, the testing accuracy reaches 70 percent, while the precision, recall, and F1-score are 70 percent, 63.63 percent, 93.33 percent, and 75.66 percent, respectively. The mean absolute error (MAE) of the distance and the predicted magnitude using the proposed method compared to the catalog solution are 381 km and 0.49, respectively. This new study sheds light on completely data-driven strategies for detecting earthquake precursors. Combining the findings from this study with physics-based models may have a profound impact on the wide applications of future earthquake prediction practices that could save hundreds of thousands of human lives.

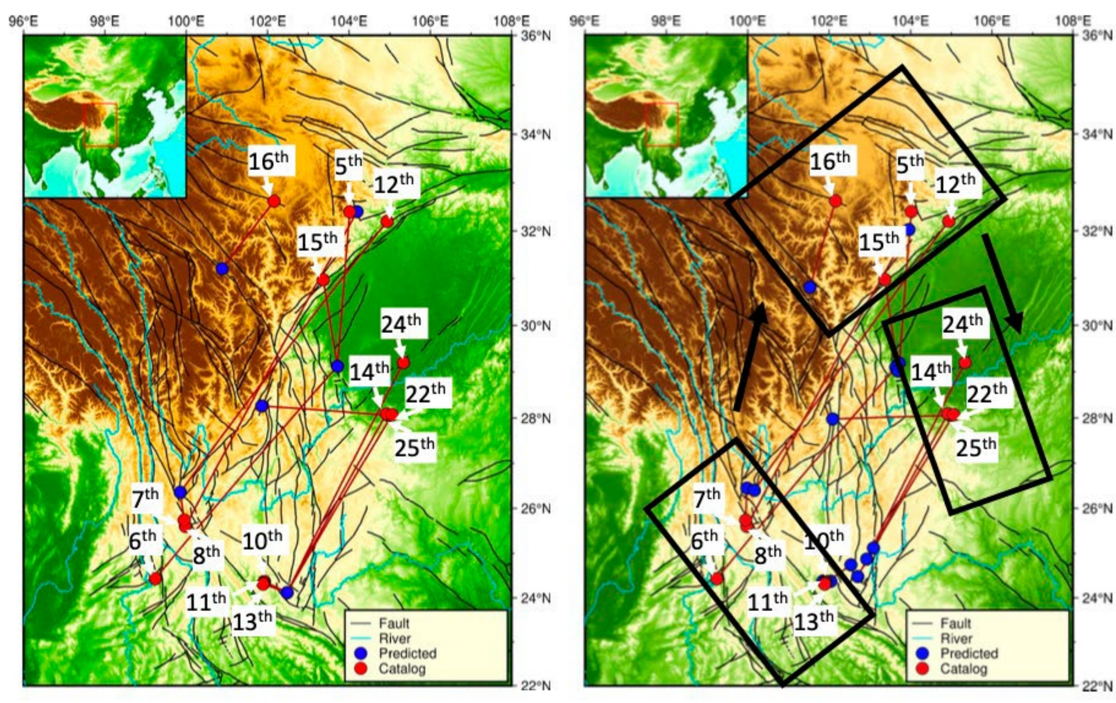

(a) (b)

Figure 1. The predicted location of earthquakes compared to the catalog location. The predicted location is considered to be the centroid of each clustered region (a), while the location accuracy is enhanced considering the earthquake locations in the last month (b). The white labels indicate the week numbers of each catalog earthquake. There is a clear seismicity migration pattern revealed by the labeled catalog events, thus considering earthquakes in the previous weeks could improve the location prediction accuracy in the future weeks.

Earthquake Detection and Phase Picking Using the Compact Convolutional Transformer

O. M. Saad, Y. Chen, D. Siervo, A. Savvaidis, D. Huang, N. Igonin, S. Fomel, and Y. Chen

In submission

We propose applying a compact convolutional transformer (CCT) to pick the P- and S-wave arrival times of the earthquakes (EQCCT). The proposed algorithm consists of two branches, where the output of each branch is the arrival time of the P and S phases, respectively. The input for the model is 60s three-channel seismograms, and the output size is 60s, thus each output label sample corresponds to an input sample. Each branch of the proposed algorithm consists of several blocks, i.e., convolutional block, patching, embedded layer, and transformers. The convolutional block consists of three convolutional layers and one dropout layer with a skip connection between the input and the second convolutional layer. Then, the extracted features from the first block are divided into groups of patches using the patching block. We add an embedded position to each patch using the embedded layer. Afterward, we use the transformer that consists of normalization layers, multihead-attention networks, and multilayer perceptrons (MLP) with two skip connections, i.e., one between the input and the output of the multihead-attention networks and the second between the outputs of the multihead-attention networks and the MLP. The two branches of the EQCCT have the same architecture, with each branch responsible for P- and S-wave arrivals, respectively. We train the proposed EQCCT using an augmented version of the STEAD data set. The augmentation strategy includes adding Gaussian noise, randomly shifting the waveforms, adding a second earthquake to the input window, and dropping one or two channels from the seismogram. We split the augmented STEAD data into 85 percent for training, 5 percent for validation, and 15 percent for testing. As a result, our EQCCT model outperforms both EQTransformer and Phasenet, which are the two most popular deep-learning-based phase-picking methods. We consider the picked phases within 0.2s as a true positive (TP). For P and S picks, the EQQCT has the lowest mean absolute error (MAE) and standard deviation error (σ) compared to the EQTtransformer and Phasenet methods. Besides, our EQCCT method shows the highest precision, recall, and F1 score.

Then, we apply the pretrained model to three independent data sets (not included in the training set), in this case, the Japanese, Texas, and Instance data sets. The proposed method shows promising results in terms of picking accuracy and the missing rate. Figure 1 shows four examples from different data sets. The four examples are from the STEAD, Japan, Instance, and Texas data sets, respectively. As we can notice, the P and S phases are picked accurately using the EQCCT method (solid vertical lines) compared with analysts' picks (dashed vertical lines).

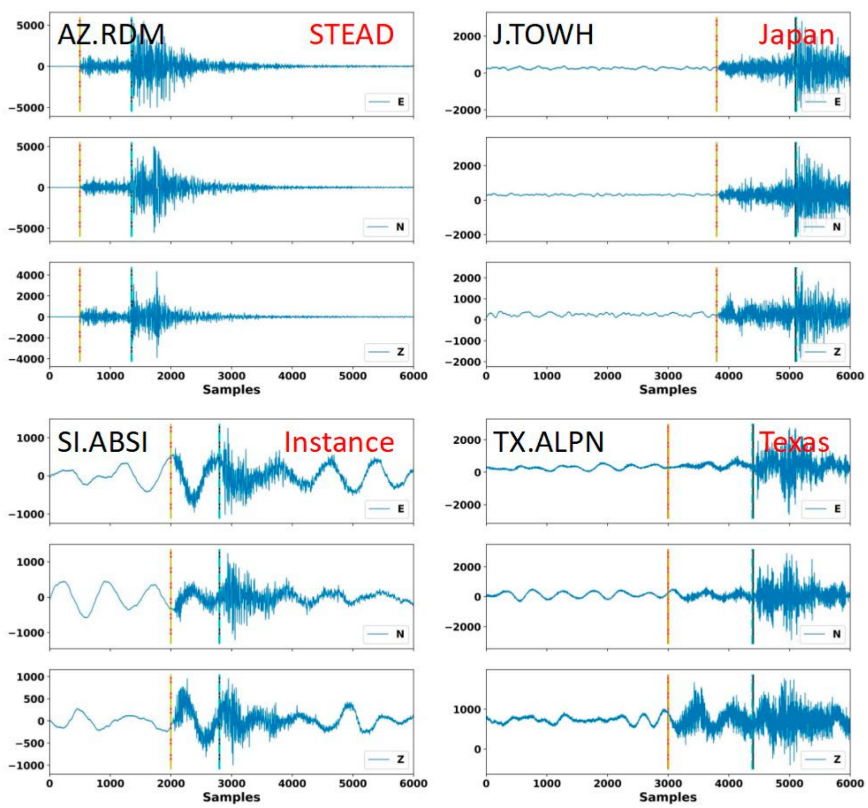

Figure 1. Phase picking results on four different data sets: STEAD, Japan, Instance, and Texas. The solid vertical lines correspond to the EQCCT results, and the dashed vertical lines correspond to analysts' picks.

Machine learning for fast and reliable source-location estimation in earthquake early warning

O. M. Saad, Y.F. Chen, D. Trugman, S. Soliman, L. Samy, A. Savvaidis, M. A. Khamis, A. G. Hafez, S. Fomel, and Y. Chen

IEEE Geoscience and Remote Sensing Letters, 2022, 19, 8025705

We developed a random forest (RF) model for rapid earthquake location with an aim to assist earthquake early warning (EEW) systems in fast decision-making. This system exploits P-wave arrival times at the first five stations recording an earthquake and computes their respective arrival time differences relative to a reference station (i.e., the first recording station). These differential P-wave arrival times and station locations are classified in the RF model to estimate the epicentral location. We train and test the proposed algorithm with an earthquake catalog from Japan. The RF model predicts the earthquake locations with high accuracy, achieving a mean absolute error (MAE) of 2.88 km. As importantly, the proposed RF model can learn from a limited amount of data (i.e., 10 percent of the data set) and far fewer (i.e., three) recording stations and still achieve satisfactory results (MAE < 5 km). The algorithm is accurate, generalizable, and rapidly responding, thereby offering a powerful new tool for fast and reliable source-location prediction in EEW.

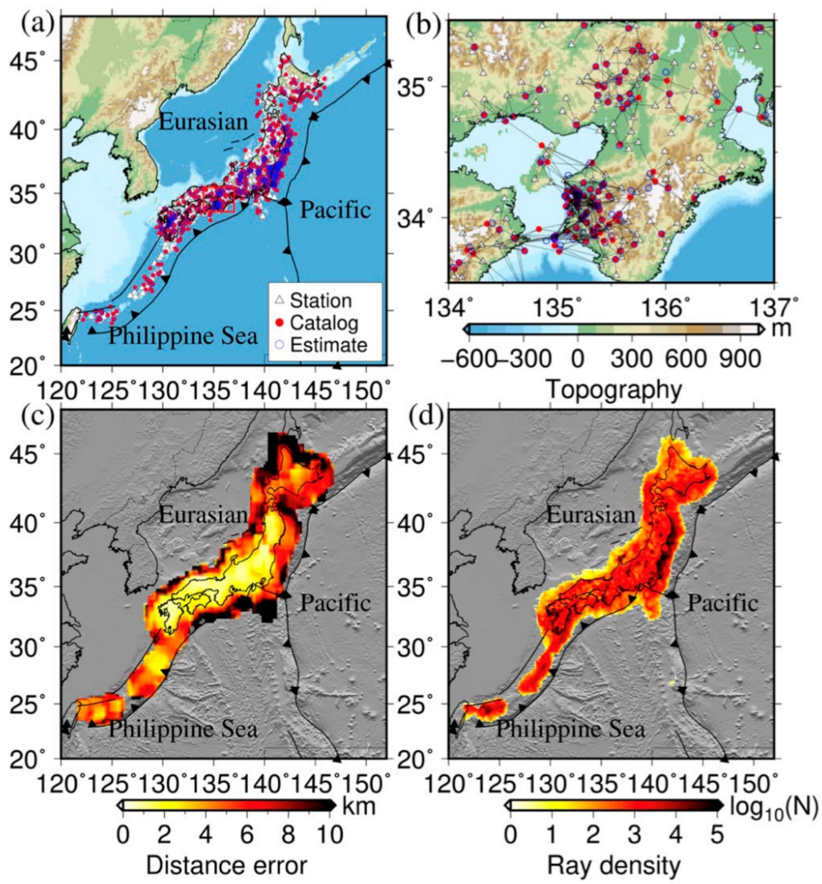

Figure 1. (a) Comparison between predicted (blue circles) and catalog locations (red dots) for 1,000 randomly selected testing events. The white triangles show the Hi-net stations. (b) Zoomed map from (a), with its location highlighted by the red rectangle. The black lines connect a catalog location to the five nearby stations. (c) Spatial distribution of location prediction errors across the study region. (d) Spatial distribution of ray path density.

3D Reconstruction of the Sedimentary and Crustal Structure in the Delaware Basin Using Receiver Functions

Y. Chen, D. Huang, A. Savvaidis, and Y.F. Chen

In submission

The receiver function (RF) method is an effective way to obtain the crustal structure underneath a seismic station by leveraging the P-to-S converted phases in the three component seismograms. While it is mostly easy to obtain the Moho structure, it is more challenging to obtain the structure of the low-velocity sedimentary layer, mainly due to the weak conversion phases when teleseismic waves travel through the sedimentary interface. Here, we propose leveraging an advanced signal-processing method from the exploration seismology community to significantly improve the data quality of the teleseismic RF data to the level that the converted phases related to the sedimentary layers can be clearly recovered. The recovered sedimentary P-to-S converted waves are used to obtain a high-resolution delineation of the sedimentary basin boundary. More importantly, we can compensate for the station shortage when constructing the 3D model and reconstruct the data when no stations are available. The data reconstruction capability enables us to obtain a high-resolution 3D structure of the sedimentary and sub-sedimentary crustal structure. The proposed method is applied to the western Texas broadband seismic recordings and helps obtain a reliable 3D subsurface structure of the Delaware Basin.

In this work, we propose an effective framework to simultaneously deal with the low signal-to-noise ratio (SNR) issue of RFs when estimating the sediment layer thickness and reconstructing the 3D structure of the sediment layers and crusts based on an advanced signal-processing algorithm from the exploration seismology community, known as the damped rank reduction method (DRR). On the one hand, the DRR method can sufficiently remove the strong noise existing in the common receiver RF gathers so that a common H-K stacking method can be stably and reliably applied to obtain the sediment layer thickness. On the other hand, the DRR method can also be used to reconstruct the 3D model of the sediment and crust thickness following the structural pattern.

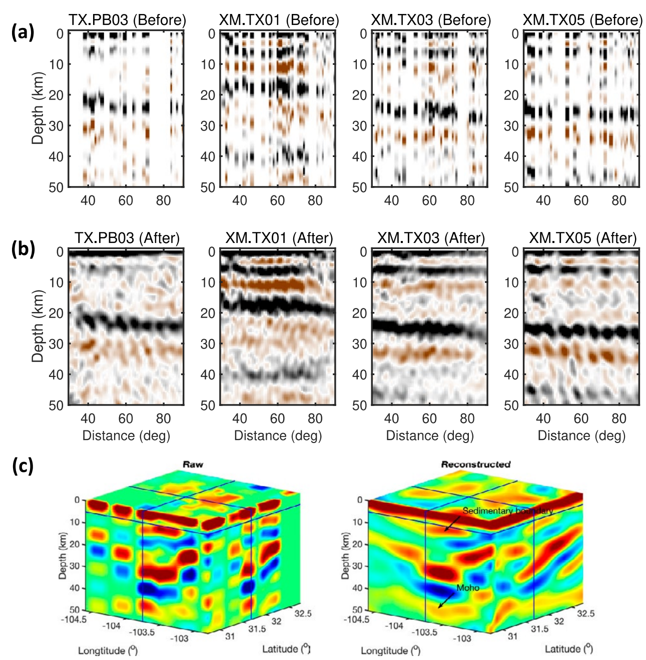

Figure 1. RF comparisons in the depth domain before (a) and after (b) advanced signal processing. The basement thickness is clearly revealed after denoising and reconstruction. (c) 3D sedimentary and crust model before and after the proposed 3D reconstruction method.

RFloc3D: A Machine Learning Method for 3D Real-Time Passive Seismic Source Location Using P- and S-Wave Arrivals

Y. Chen, A. Savvaidis, S. Fomel, O.M. Saad, and Y.F. Chen

Submitted to Geophysics

Passive seismic source location imaging is important to various scientific and engineering research topics spanning from the unconventional reservoir development in exploration seismology to seismic hazard prevention in the earthquake seismology community. The emerging machine learning techniques enable the location of passive seismic sources with unprecedented efficiency and accuracy. Most of the state-of-the-art Machine Learning (ML) methods are based on waveforms, as required by the most popular convolutional neural network (CNN) architecture, which is prone to the sensitivity of velocity models. Here, we present a travel time-based machine learning method, RFloc3D, to locate passive seismic sources from manually or automatically picked P- and S-wave arrivals. The proposed method is similar to traditional travel time-based location methods, where the inverse mapping from arrival times to passive source location is obtained by inverting a nonlinear inverse problem, but differs in leveraging the random forest (RF) method to learn the inverse mapping relation from numerous eikonal-based forward simulations. Details and analyses of the proposed RFloc3D method are illustrated based on a passive seismic monitoring setup. Numerical and real data examples show that the proposed method is capable of real-time location. The inclusion of S-wave arrivals, most importantly the differential time between P- and S-wave arrivals help significantly reduce the depth error (e.g., decreasing the mean average error to a half) of the located sources.

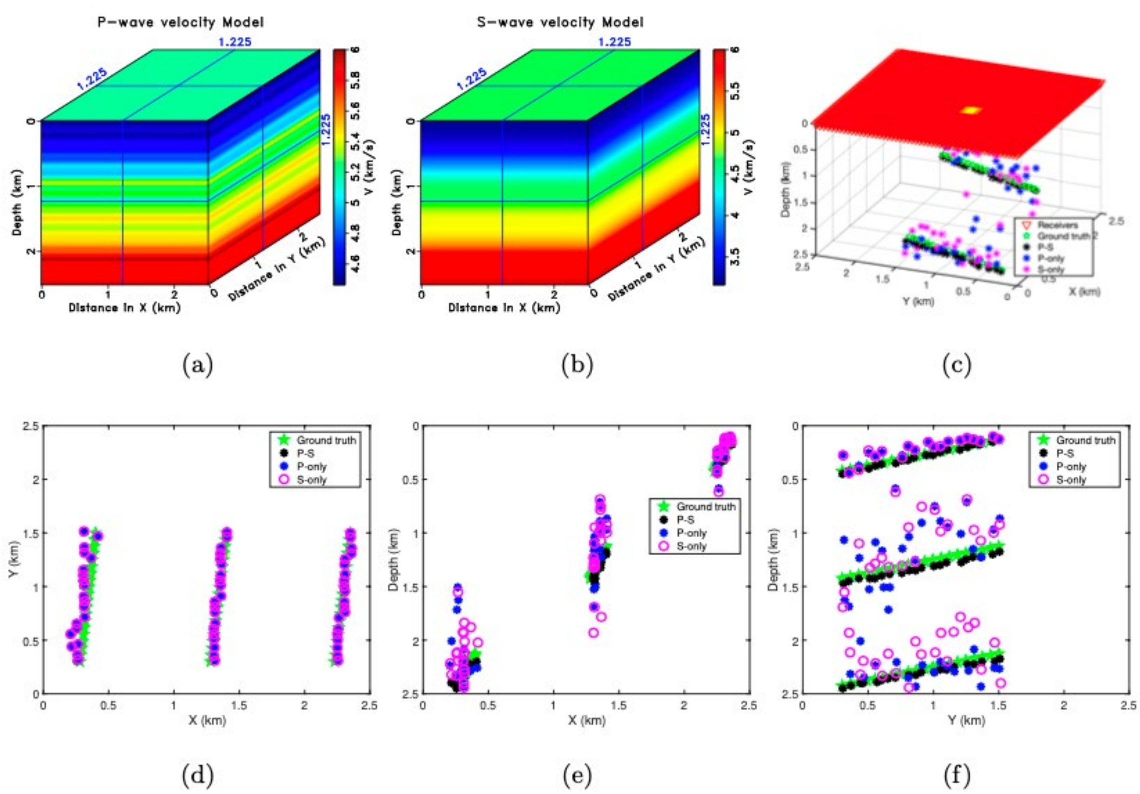

Figure 1. Synthetic location test in the case of three fractures generating seismicity. (a) Practically obtainable 1D P-wave velocity (plotted on a 3D cube). (b) 1D S-wave velocity. The “observed” travel times are calculated from 3D velocity models with mild structural heterogeneity. (c) Location results in different scenarios. Only the nearest 10 stations (with shortest arrival times) are used for location. (d)–(f) 2D comparisons among all scenarios: P-wave-only (P-only), S-wave-only (S-only), P-S-wave-based (P-S). The P-S-wave-based scenario uses P-S-wave arrival times and differential time between P- and S-wave arrivals. It is clear that the P-S case obtains the most accurate location results.

Single-Channel Passive Seismic Denoising Using Dictionary Learning—Applications to Event Detection and Location

Y. Chen, A. Savvaidis, and S. Fomel

Submitted to Geophysics

Passive seismic denoising is mostly performed using a simple bandpass filter, which can be problematic when signal and noise share the same frequency band. More advanced passive seismic denoising methods take advantage of fixed-basis transforms, e.g., the wavelet, to remove noise. We propose a data-driven denoising method that is based on adaptively learning sparse transform. Contrary to the fixed-basis transforms, the proposed method belongs to the adaptive-basis transforms. We learn the 1D features embedded in the passive seismic data from all the available waveform data sets without requiring spatial coherency in a data-driven way. Thus, the new method is flexibly applied in any passive seismic monitoring project because of its data-driven and single-channel nature when implemented. Considering the computationally expensive K-singular value decomposition (KSVD) in the traditional dictionary learning framework, we propose a fast SVD-free dictionary learning method that can be readily applicable to process massive seismic data during passive seismic monitoring. The proposed method is applied to two synthetic data examples and two real passive seismic data sets including a 3-C waveform recorded by TexNet station TX.PH03 to demonstrate its effectiveness in improving the signal-to-noise ratio and its potential in applications like arrival picking and source-location imaging.

It is also found that more available passive seismic waveform data help obtain a better understanding of the key waveform features. The proposed method is a single-channel algorithm, so it does not require a dense spatial sampling of the wavefield, and thus is readily applicable in any passive seismic monitoring project. The proposed method requires negligible human intervention and thus can be conveniently used by analysts for quality control of the waveform data when doing manual or automatic analysis. The proposed method should be applied to process passive seismic data from the same geological region because of the similar source-mechanism features, but it is not strictly limited to this requirement.

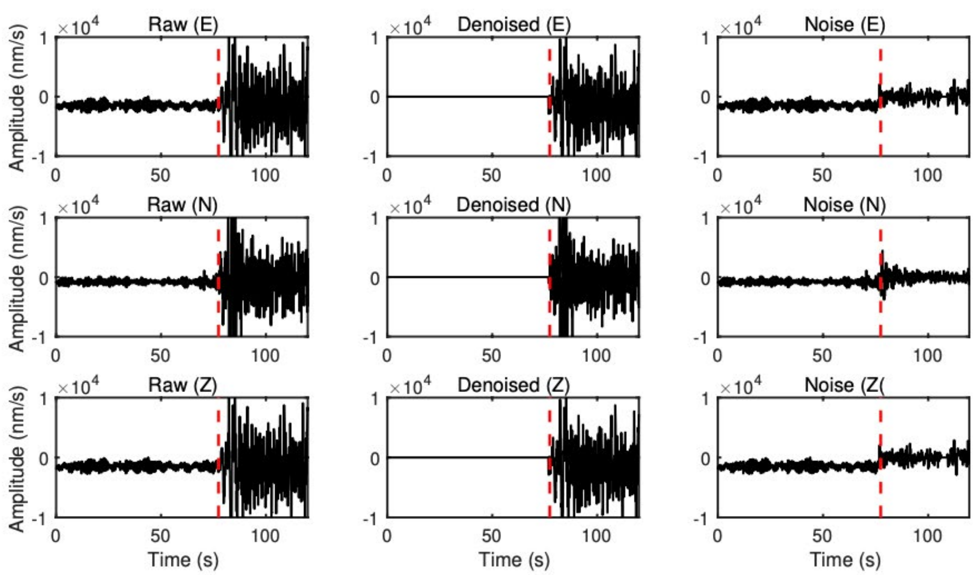

Figure 1. Example of earthquake data denoising of the waveform data of the M4.9 event (texnet2020galz) recorded by station TX.PH03. Left: raw earthquake data. Middle: denoised earthquake data. Right: removed noise. Note that denoising significantly improves the arrival picking accuracy.

Pyseistr: A Python Package for Structural Denoising and Interpolation of Multichannel Seismic Data

Y. Chen, A. Savvaidis, S. Fomel, Y. Chen, O. M. Saad, Y. A. S. I. Oboué , Q. Zhang, and W. Chen

Submitted to Seismological Research Letters

New sensing techniques like nodal geophones and distributed acoustic sensing enable a spatial sampling ratio that has been unprecedentedly high in earthquake seismology. The much higher sampling of seismic wavefields that is close to the level in exploration seismology calls for a unified processing approach for multichannel seismic data, regardless of the research interest, e.g., oil and gas oriented or earthquake-study oriented. Here, we present the first python package for multichannel seismic data that benefits both communities, i.e., exploration and earthquake seismology, called pyseistr. Pyseistr is a python package that is designed to make full use of the structural patterns in multichannel seismic data to facilitate data processing. The pyseistr package currently includes several fundamental functions like slope estimation, structural mean and median filtering, and structural reconstruction of missing data. The pyseistr package (https://github.com/aaspip/pyseistr) is continuously developed to include more functions that benefit both exploration and earthquake communities. There are several key advantages of the pyseistr package listed as follows:

1. It is python-based, which makes it free of licensing-related restrictions, especially when compared with Matlab-based packages.
2. It is almost stand-alone and only depends on the NumPy library, which makes it easy to install and more stable since it is less susceptible to other packages.
3. It fully takes advantage of the structural patterns of the multichannel seismic data, which is a typical characteristic of seismic wavefields.
4. It is being continuously developed. In the current version, we only present the latest functionalities and reproducible examples while more future structure-oriented processing functionalities and more diverse applications in different seismological data sets will be continuously included.

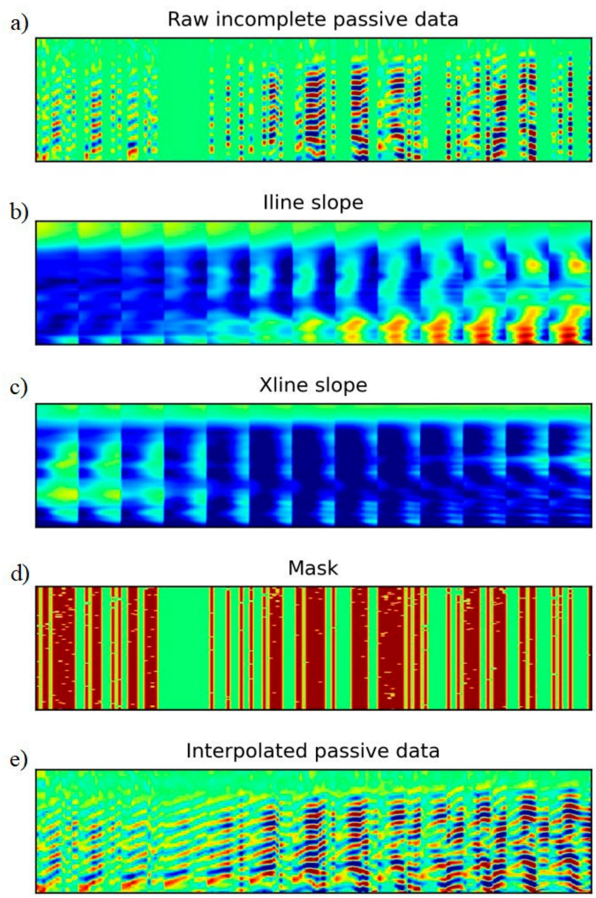

Figure 1. Example of the 3D structure-oriented interpolation on a passive seismic data set. (a) Raw incomplete passive data. (b) Local inline slope estimated using the newly developed algorithm implemented in the pyseistr package. (c) Local xline slope. (d) The mask-sampling matrix. The warm (red) color indicates there is data in this sample. The cool (green) color indicates data is missing for this sample. (e) Interpolated data.

3D Microseismic Monitoring Using Machine Learning

Y. Chen, O.M. Saad, A. Savvaidis, Y.F. Chen, and S. Fomel

Journal of Geophysical Research – Solid Earth, 2022, 127, e2021JB023842

Microseismic source localization is important for inferring the dynamic status of the subsurface stress field during hydraulic fracturing. Traditional deterministic methods for 3D microseismic source localization require either ray tracing or full waveform modeling, thus are computationally expensive. We propose a very efficient (e.g., within 1 s) real-time microseismic source localization method based on machine learning (RFloc3D). First, 3D ray tracing is performed with hypothetical event locations and realistic acquisition geometry to calculate the theoretical travel times. The theoretical travel time differences and the spatial locations of the stations are treated as the input features of the training data set, and the corresponding source locations are used as the labels. The manually or automatically picked arrival time differences between different stations and a reference station after a microseismic event and the actual station locations are fed into the well-trained model for a fast and accurate location prediction. The proposed method is efficient enough to be widely applied for the real-time monitoring of hydraulic fracturing. The machine learning model is analogous to 3D grid search but performs 3D ray tracings before the actual location and needs to be retrained when applied to a new study area. The application of the proposed method to earthquake localization is also straightforward.

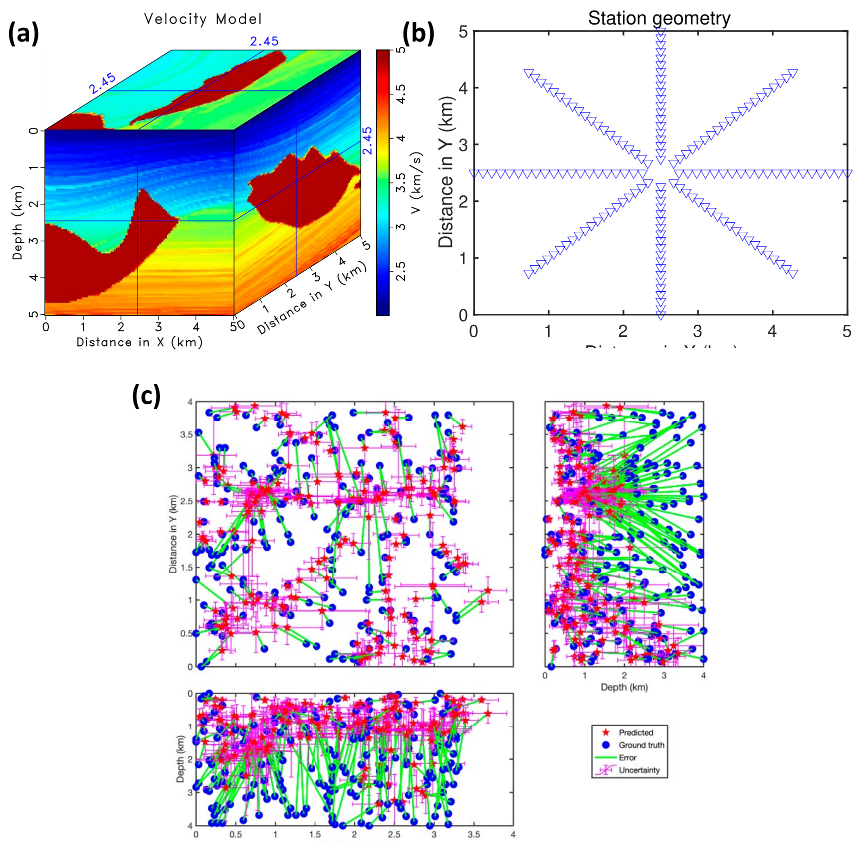

Figure 1. A synthetic test of the new RFloc3D method (a) Velocity model. (b) Acquisition geometry. (c) Uncertainty analysis result. One hundred independent tests are repeated for 200 events to evaluate the uncertainty of the RFloc3D method considering the errors in the velocity model (10 percent of the maximum velocity) and arrival time picking (with five mis-picked samples).

Real-Time Earthquake Location Using Machine Learning-An Application to the M4.9 Mentone Earthquake Sequence

Y. Chen, O. M. Saad, A. Savvaidis, Y.F. Chen, and S. Fomel

In submission

Rapid earthquake location plays an important role in real-time seismic monitoring. Traditional earthquake location methods are either based on travel timetables calculation or solving the full wave equation, thus are generally computationally expensive. Here, we propose an efficient earthquake location method based on machine learning, which allows a fast location in a 3D velocity model within a second. The intensive computation for locating each earthquake is substituted by a pre-location training process, where tens to hundreds of thousands of 3D ray tracings are performed. Once the training process is complete, locating an earthquake is in real-time, given the automatically or manually picked P-arrival times. There are three main steps of the proposed workflow. First, we generate a sufficiently large training data set with numerous 3D ray tracings. Secondly, we apply the random forest (RF) method to map the differential P-arrival times to an earthquake source location. Finally, we apply the trained RF model to recorded differential P-arrival times to predict the location in a real-time way. We applied the proposed method to the M4.9 Mentone earthquake, for which we have a relatively high confidence in the catalog location. We also applied it to the earthquake sequence of the M4.9 event and found that results from the proposed method are comparable to a highly-optimized nonlinear location method (NonLinLoc).

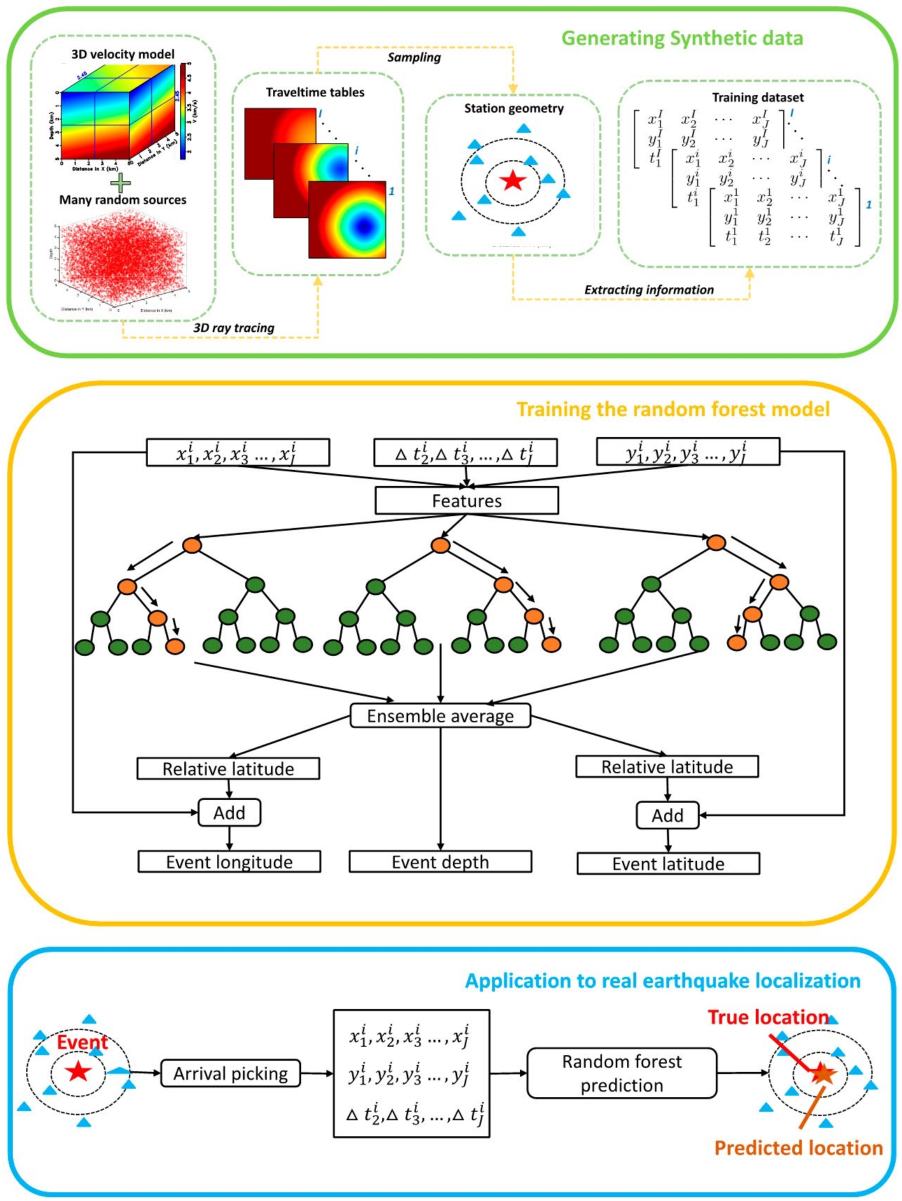

Figure 1. The workflow of the proposed localization method.

Denoising of Distributed Acoustic Sensing Seismic Data Using an Integrated Framework

Y. Chen, A. Savvaidis, S. Fomel, Y.F. Chen, O. M. Saad, H. Wang, Y.A.S.I. Oboue, L. Yang, and W. Chen

Submitted to Seismological Research Letters

Distributed acoustic sensing (DAS) is an emerging technology that offers great potential in the high-resolution multiscale seismic investigation due to its dense spatial coverage and cost-effectiveness. However, DAS data notoriously suffers from the low signal-to-noise ratio (SNR) due to various types of strong noise, e.g., high-frequency noise, high-amplitude erratic noise, or vertical or horizontal noise. Here, we propose a novel denoising framework by cascading several individual denoising methods that are designed for suppressing specific types of noise. Firstly, to suppress the high-frequency noise, we apply a band-pass (BP) filter, which is implemented by recursive infinite impulse response filtering in the time domain. Secondly, to suppress the erratic noise, we apply a structure-oriented median filter from the reflection seismology field. This filter requires the calculation of the local slope of the observed seismic wavefield, which represents the structural pattern of the seismic data. We introduce in detail how we calculate the local slope and the subsequent structural filtering. Finally, to suppress the vertical or horizontal noise, we apply a carefully designed dip filter in the frequency-wave number domain. The overall effect of these cascaded denoising steps is that the DAS data can be dramatically improved in terms of SNR. We introduce in detail the implementation of each step in the proposed denoising framework and analyze their respective contribution towards the final improvement. We demonstrate the effectiveness of the proposed denoising framework through the open-access FORGE geothermal DAS data set and provide the reproducible processing workflows for all the DAS subsets containing the cataloged earthquake and microseismic events. All data sets and fully reproducible codes are available at https://github.com/chenyk1990/dasdenoising.

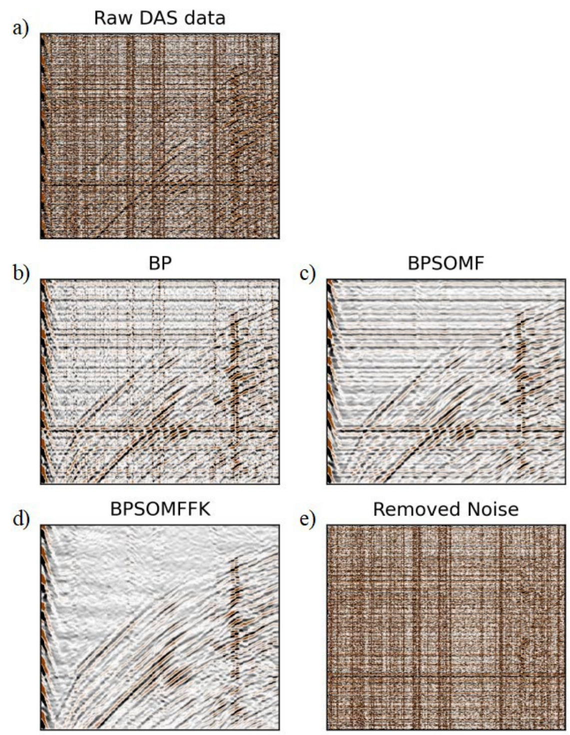

Figure 1. Example of an integrated structure-oriented filtering workflow on a DAS seismic data set. (a) A raw DAS data set from the FORGE project with the file name FORGE_78-32_iDASv3-P11_UTC190426070723.sgy. (b) Filtered data using a BP filter. (c) Filtered data using a cascaded BP and structure-oriented median filter (SOMF) filter. (d) Filtered data using a cascaded BP, SOMF, and frequency-wave number domain-dip (FK) filter. (e) Removed noise.

Seismogenic Characteristics of the Delaware Basin as Constrained by Earthquake Source Mechanisms

D. Huang, E. Horne, F. Kavoura, and A. Savvaidis

Seismological Research Letters, 2022, https://doi.org/10.1785/0220220054

Seismicity in the Delaware Basin appears to be associated with oilfield operations. To better characterize the seismogenic structures revealed by the induced seismicity, in this study we determined source mechanisms for the Delaware Basin of Texas and leveraged the obtained source mechanisms to perform stress inversion for evaluating the region's stress state. Using the seismogenic patterns and seismicity distribution, we identified seven distinctive seismogenic zones. Within each zone, earthquakes form several parallel-trending linear clusters. Most notably, there is an observable change in the seismicity trend on either side of the basin-bisecting Grisham fault zone. Additionally, the hypocentral depth varies greatly across the fault zone: north of the fault zone events are deep and below the basin-basement interface, and south of the fault zone events are shallower. We also see spatial variations of source-mechanism patterns and the direction of the maximum horizontal stress across the Delaware Basin. Most seismic-moment release can be attributed to the basement-rooted tectonic faults in the Culberson-Mentone seismogenic zone.

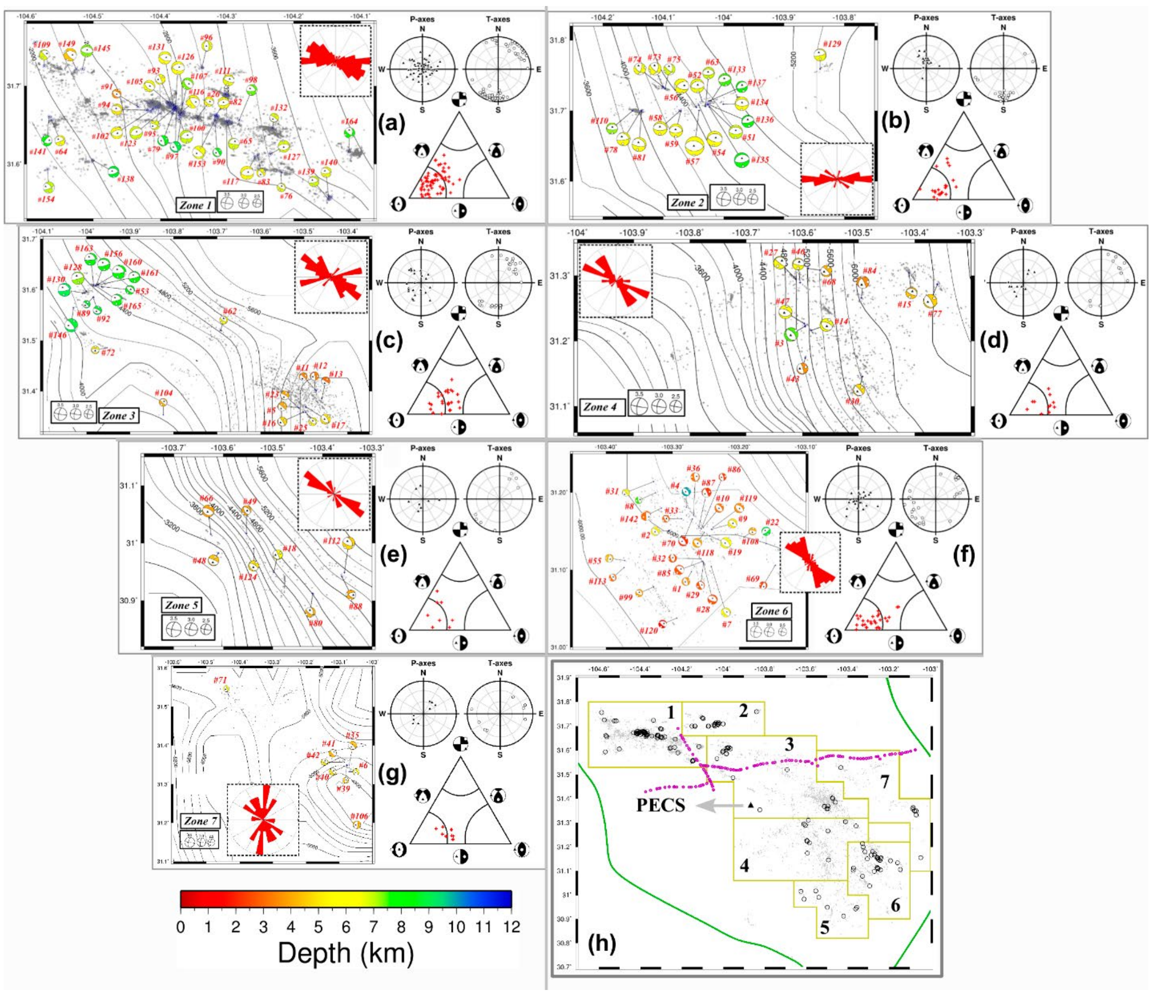

Figure 1. Seismogenic patterns across seven seismogenic zones in our study area. (a)–(g). Beachball diagrams, statistics of nodal planes (i.e., rose diagrams), ternary diagrams (Frohlich and Apperson, 1992), and projections of P- and T- axes from all source mechanisms in each seismic zone combined. Beachballs are color coded by events' focal depths, referring to the color table. Size of each beachball is also scaled by its Mw; see the size reference in each panel. (h) Boundaries of seismogenic zones.

Improving the Catalog of Seismicity in Southeastern New Mexico for Earthquake Hazard Assessment

D. Huang, M. Litherland, and A. Duff

Since 2019 seismicity in the northern Delaware Basin, an area spanning southeastern New Mexico and West Texas, has increased significantly. This increased seismicity is of particular concern because of the location of the Waste Isolation Pilot Plant (WIPP), a nuclear waste disposal facility. WIPP is in the New Mexico part of the Delaware Basin, and it could be impacted by the increasing rate and size of earthquakes in the region. To better understand the hazard posed by induced seismicity and to guide industry and regulatory response, it is essential to have accurate locations for all earthquakes occurring in this region. In this study, TexNet teamed with the New Mexico Tech Seismological Observatory to investigate induced seismicity by using a variety of seismological methods, giving a better understanding of what has been occurring in the basin to date. Results have shown 9 apparent seismogenic zones out of the relocated 805 earthquakes. The overall depth range of seismicity in our study area is 0 to 17 km, and most events are concentrated at 7 to 12 km depths. One major seismogenic zone is distributed in a larger area across the border of Texas and New Mexico, containing most of the observed seismicity. Seismicity in the area across that border has a much wider depth range (0 to16 km depth), whereas a small cluster located in the Central Basin Platform has a narrow depth extent (0 to 5 km depth). A Most of the earthquakes are in the top portion of the crystalline basement, indicating a reactivated basement-rooted fault system. Five source mechanisms are determined for the seismogenic zone across the border of Texas and New Mexico. They all present normal faulting mechanisms, similar to that of the Mentone Earthquake (Mw4.6). Results of stress inversion of the five mechanisms show a vertical principal stress (compressional *S1)* and a horizontal principal axis (extensional *S3*), indicative of an extensional environment.

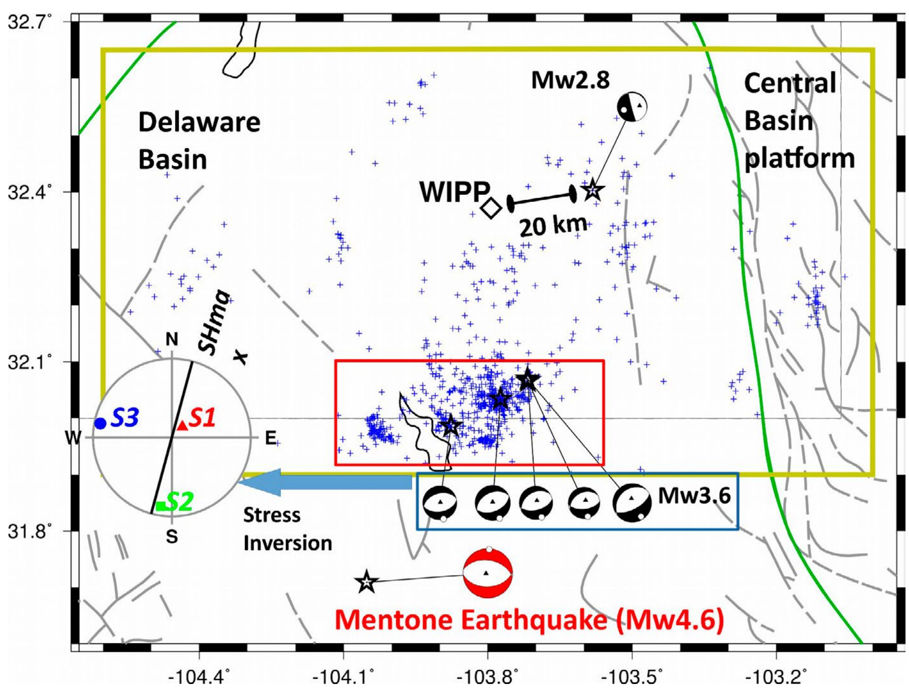

Figure 1. Composite figure showing seismicity, source mechanisms, and the stress state in our study area. Five source mechanisms were determined for seismogenic zone 4. All present normal faulting, which is like that of the largest event recorded since 2017. Stress inversion of the five source mechanisms shows a maximum horizontal stress oriented N5˚E. Further north, one earthquake with Mw2.8 was located 20 km east of the WIPP facility. Its occurrence suggests a basement-rooted fault, where its crustal rheology is brittle, indicating potential to host an earthquake of similar magnitude in the future.

Calibrated Locations of Induced Earthquakes in the Delaware Basin, Reeves County, Texas, 2009–2017

A. Aziz Zanjani, Liliana Binetti, and Heather. R. DeShon

Research in progress

The spatiotemporal association between seismicity and oil and gas production in the Delaware Basin (DB) has been closely monitored since the Texas Seismological Network (TexNet) began in 2017. Initial studies indicate an increase in the seismicity rate beginning in 2009, but earthquake catalogs for pre-2017 events, including the initial TXAR dataset (Frohlich et al., 2020) used here, report epicentral uncertainties on the order of >15 km. Equally poor depth control for pre-2017 catalog complicates the association of seismicity with hydraulic fracturing and both shallow and deep saltwater disposal (SWD) in the DB. Here, we apply a multiple event relocation algorithm (MLOC) to a mixed cluster of post- and pre-2017 earthquakes in Reeves County to constrain the depths of the pre-2017 seismicity. First, we use near-source readings of post-2017 events (the core cluster) for calculating a virtual centroid in space and time (hypocentroid). Short paths in the core cluster (readings at <80 km distance) ensure the minimization of cumulative errors between the true Earth and the theoretical travel-time model. Relocated events in the core cluster have very small relative epicentral errors (<1 km). The hypocentroid errors, as a measure of absolute errors, are 0.4 and 0.5 km in latitude and longitude, respectively; depth uncertainty is <±0.5 km. The station-phase tabulation for the core cluster provides the statistical power to estimate the uncertainties for pre-2017 events by introducing the empirical reading errors (EREs) for each station-phase pair. Pre-2017 events are added with successive estimates of EREs. We relocated a total of 88 events with 49 events from pre-2017. For pre-2017 events, we have introduced 86 additional S-P differential arrival times for single events when one or both parent phases had been flagged out in the calibration. We have also added 498 differential travel times to the pre-2017 catalog from cross-correlation. We have reduced relative epicentral errors to <5 km. Figure 1 shows the final locations of relocated events with relative error ellipses and compares depth histograms before and after relocation. Our results indicate a spatial correlation between post- and pre-2017 DB earthquakes in Reeves County, Texas, with depth estimates consistent with triggering from shallow (1–4 km depth) SWD in the Delaware Basin.

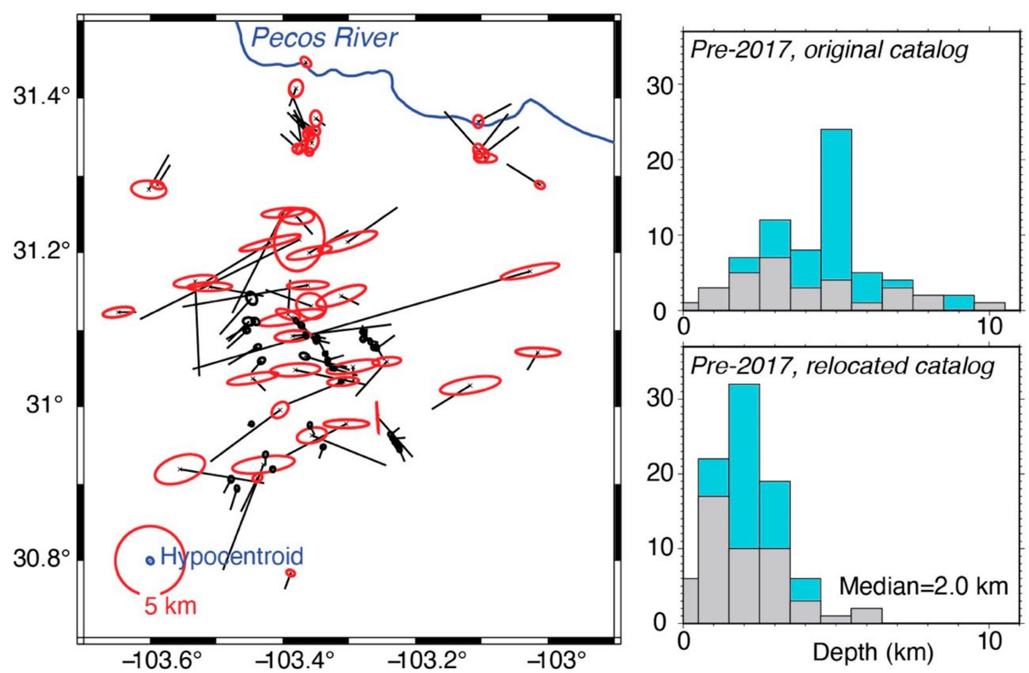

Figure 1. (left) Relocation results with error ellipses for the relocated pre- and post-2017 event cluster. The epicentral locations are represented by black x, and black lines are the displacement of each event from its initial location. Red error ellipses are for the pre-2017 events, and black error ellipses are for the post-2017 core cluster. Blue ellipse is the representation of absolute error and is for the hypocentroid. All errors are less than 5 km in latitude and longitude. Red circle is 5 km and only for reference. (Top right) Histogram of depths before relocation, with the whole cluster in cyan and pre-2017 in gray. Sixteen events in the initial catalog lacked a depth estimation. (Bottom right) Histogram of depths after relocation, with the whole cluster in cyan and pre-2017 in gray.

Stress Variations in the Delaware Basin from Shear-Wave Splitting Analysis

V. Guzman, A. Li., and A. Savvaidis

Seismological Research Letters, 2022, doi: 10.1785/0220220118,

The northwestern Delaware Basin has experienced a sharp increase in seismicity in the past 3 years, including one M5.0 earthquake in March 2020 and one M4.5 earthquake in March 2021. This rise in seismicity has been attributed to wastewater injection and hydraulic fracturing. Investigating variations of stress in the area is critical for better understanding the mechanisms of induced earthquakes. Shear-wave splitting (SWS) in the crust is caused by the preferred alignment of cracks, and the fast polarization orientation could indicate the maximum horizontal stress direction. A temporal variation in fast polarization orientation could signify a change in the fracture system caused by stress or pore pressure increase.

We conducted shear-wave splitting analysis from local earthquakes in the northwestern Delaware Basin to understand the increasing and intensifying seismicity in this area. More than 840 robust SWS parameters, the fast polarization orientation, and the delay time were obtained at 5 TexNet stations by analyzing seismograms of more than 4000 events from 2019 to 2021. The fast orientations from individual events vary in a broad range among all stations, indicating a complex fracture system in the upper crust, even though the averages are consistent with the local fault strikes or the maximum horizontal stress. Fast orientations with large angles from the local stress appeared after the 2020 M5.0 earthquake, evidencing an increase of pore pressure that facilitates slips on less favorable fracture planes by the stress field. Stress change caused by this earthquake could also contribute to the increasing diversity of SWS measurements.

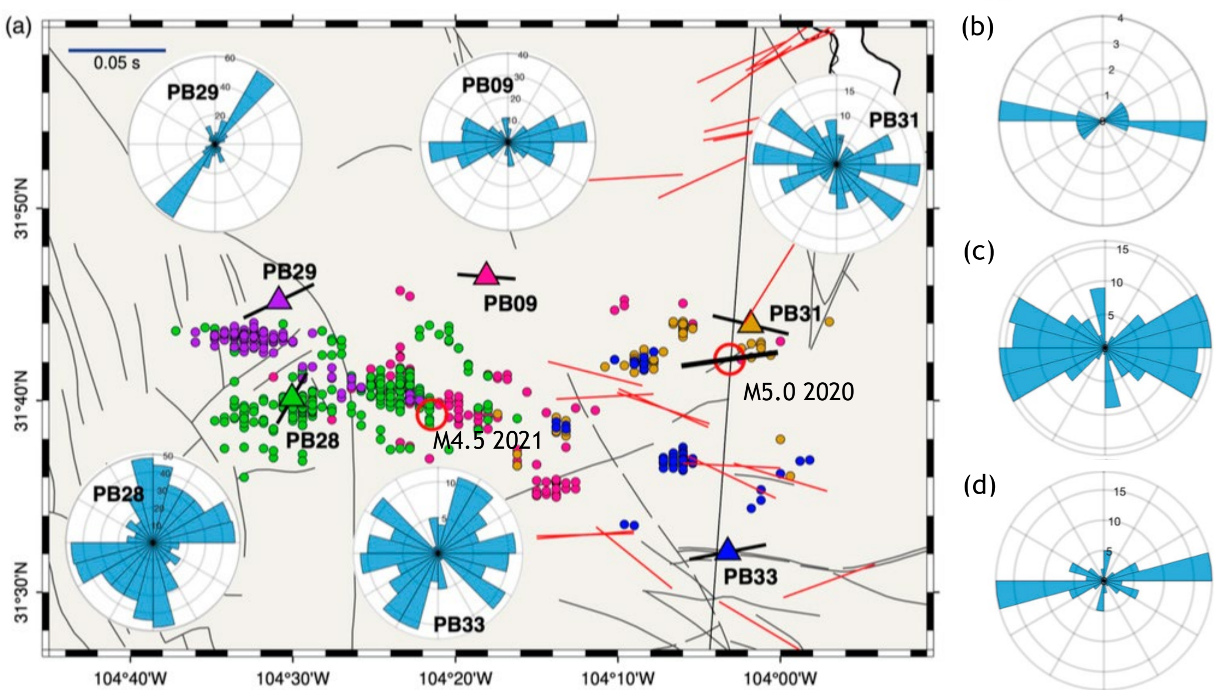

Figure 1. (a) Map showing seismic stations (triangles), event locations (dots), and shear-wave splitting results (black bars at stations and rose diagrams). Events are color-coded by the station. Faults are indicated as gray lines. Red bars indicate the orientations of SHmax. Two red circles show locations of M5.0 and M4.5 earthquakes. The thick black line at the M5.0 earthquake marks the fault strike. (b), (c), and (d) Rose diagrams at PB09 for three periods: before the M5.0 earthquake in March 2020; (b) between March 2020 and the M4.5 earthquake in March 2021; (c) and (d), after March 2021.

Seismogenic Characteristics of the Midland Basin as Constrained by Earthquake Source Mechanisms

D. Huang and A. Savvaidis

Earthquake activities in areas across the Midland Basin have significantly increased since 2019 due to continuous oil and gas industrial activities (Fig. 1). Meanwhile, the induced seismicity has allowed us to discover previously unmapped seismogenic structures. We conducted a study to identify and characterize seismogenic structures in this region: (1) We used the hypoDD algorithm to relocate and delineate seismicity for identifying seismogenic structures, (2) We also performed waveform moment tensor inversion to determine earthquake source mechanisms. Furthermore, the state of stress is determined by stress inversion using the obtained source mechanisms. As a result, eleven distinct seismogenic zones have been identified. All of them commonly present linear patterns with various orientations. Combining seismicity geometry and earthquake rupture patterns has demonstrated that the Midland Basin is an extensional tectonic regime, its seismicity was accommodated by a series of strike-slip and few normal faults. The two types of basement-rooted faults coexist within the basin and form a specific structural pattern, in which a basement-rooted rift structure is shown to transect the Midland Basin (fig. 2).

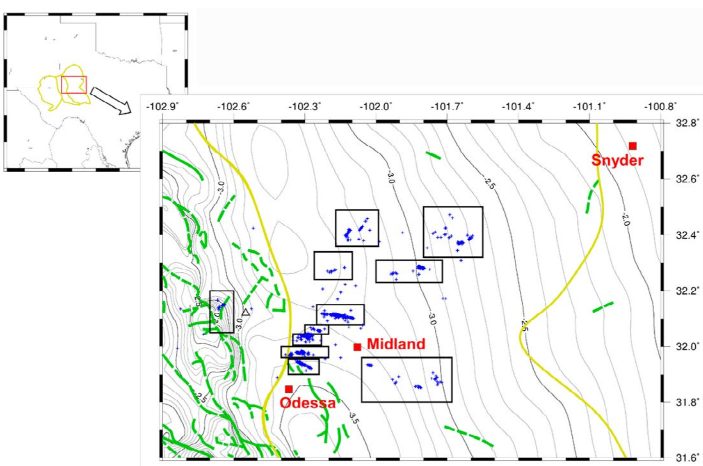

Figure 1. Tectonic map of the study area. Blue crosses denote the relocated seismicity. The contour lines represent the topography of basin-basement interface. Green lines locate the surface traces of tectonic faults (Ewing, 1991).

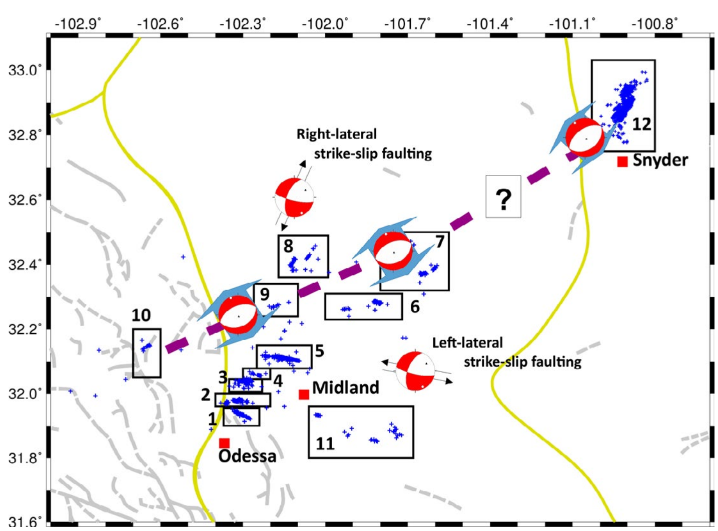

Figure 2. Interpreted seismotectonic map. Along with the Snyder seismic zone, an apparent rift structure is present and transecting the Midland Basin. On two sides of the rift, lateral extensions are accommodated by left-lateral strike-slip motions (to the south) and right-lateral strike-slip motions (to the north).

Site Amplifications from Earthquake Data and V_{S30} in the Fort Worth Basin

S-J. Jeong, B. W. Stump, and H. R. DeShon

Seismological Research Letters, 2022, 93(3): 1787-1799. https://doi.org/10.1785/0220210140

After the development of unconventional oil and gas production in the Fort Worth Basin, Texas, a rapid increase in basin-wide seismicity began in 2008 that grew to include earthquakes affecting a substantial portion of the Dallas–Fort Worth metropolitan area. To assess and mitigate the seismic hazard, which in this region is impacted by the thickness of the sedimentary basin and accompanying soft soil layer, we estimate site effects at 22 seismic stations deployed to record these earthquakes (fig. 1). Site responses are derived using two different datasets and approaches: (1) a modified generalized inversion technique (GIT) based on the *S*-wave Fourier amplitude spectra from earthquakes; and (2) application of the quarter-wavelength approximation (QWA) using estimates of average shear-wave velocities in the upper 30 m, known as V_{S30} (fig. 2). We find that site amplification estimates based on the two techniques are roughly consistent with one another (median of the amplification ratio = 0.92) over frequencies where a quarter-wavelength corresponds to ~30 m depth. The site amplification factors from the two approaches are found on average to be about 3 at the quarter-wavelength frequency (QWF). These site amplification estimates are not well correlated with geologic characteristics including rock type and geologic age. Finally, QWA values at six sites do not match GIT site amplification at the QWF (outside of ± median absolute deviations boundary), which we attribute to a combination of the underlying assumptions of the QWA, uncertainty in V_{S30} estimates, and unmodeled site response complexity.

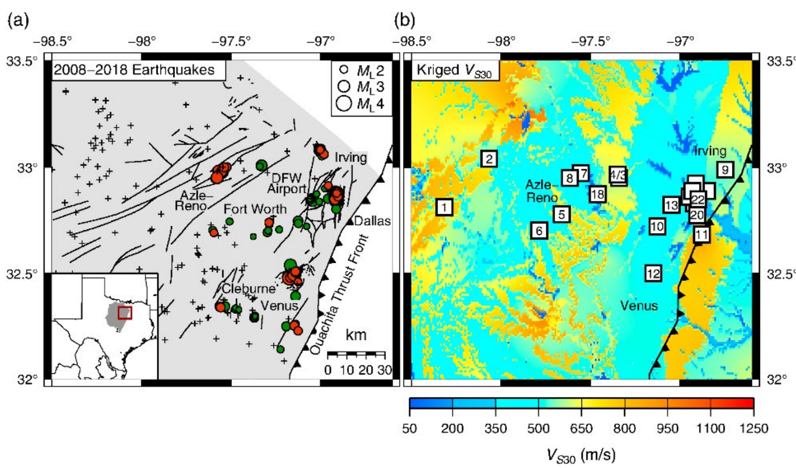

Figure 1. Map illustrating (a) the earthquakes (circles) from the North Texas Earthquake Study catalog in the Fort Worth Basin, Texas (Quinones et al., 2019) and (b) the V_{S30} values that integrate field measurements and geologic proxy predictions (Li et al., 2020). The V_{S30} map is interpolated using the Kriging method (Li et al., 2020). In (a), events in red are used in this study. Regional faults (solid black lines) and the Ouachita thrust front intersection with the Ellenburger Formation (saw-toothed line) are taken from Horne et al. (2020). Cross symbols denote wastewater injection wells. The inset displays the distribution of the Barnett Shale (gray area). (b) Sites used in this study are illustrated as squares with numbers. Sites 14, 15, 16, 17, 19, and 21 are not noted due to their proximity to 22.

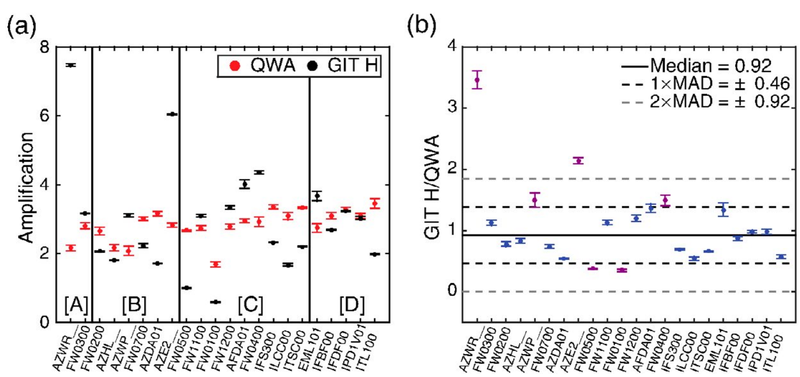

Figure 2: (a). Site amplification factors with error bars at the QWF from QWA (red) and GIT H (black) for 22 sites. Vertical lines and capital letters divide the 22 sites into geologic ages. (b). Ratio between GIT H and QWA amplification estimates at the QWF at 22 sites. Median (black line) and ± 1×median absolute deviations (MAD) (black dashed lines) are given relative to ± 2×MAD (gray dashed line). The outliers over ± 1×MAD are illustrated in purple.

Capturing and Unraveling Complex Triggering in the Permian Basin by Comparing Earthquakes in the Delaware and Midland Basins

J. Rosenblit and H. R. DeShon

Research in progress

We seek to unravel the complex interactions between saltwater disposal and hydrofracking-induced earthquakes in the Permian Basin by application and development of state-of-the-art event location methods. The Permian Basin, including the Delaware and Midland sub-basins, is a large and geologically complicated area, making it challenging to calculate earthquake depths precisely; thus, there is a demand for novel approaches to solve this complex problem. Here we report on progress toward a location technique that takes advantage of the full waveform through use of converted phases to accurately constrain event depths. We are developing the technique using events in the Midland Basin. Previously, focal depths in the Midland Basin have been determined using region-specific velocity models developed by TexNet, but uncertainties in depth remain high. Significant seismic wavespeed contrasts in sedimentary basins, however, can lead to S-energy converting to P-energy, and vice versa, and these so-called converted phases can be used to uniquely determine event depth. Waveforms analyzed for the Midland Basin show measurable S-to-P converted phases (fig. 1); particle motion plots confirm that the converted phases are near vertically incident P-waves at the station. The time difference between the S-wave and sP converted phases provides initial travel time data at earthquake locations and also reflects local velocity beneath the station. We are now systematically identifying converted phase travel times for use in earthquake location. Measurable sP converted phases results from moving suddenly from fast to slow velocity, which in the Midland Basin can occur at the top of the Salado Formation salt at ~0.5 km depth or top of Ellenburger Formation limestone at ~3.5 km depth. Synthetic seismograms will be used to confirm the theoretical characteristics of converted phases in the Midland Basin.

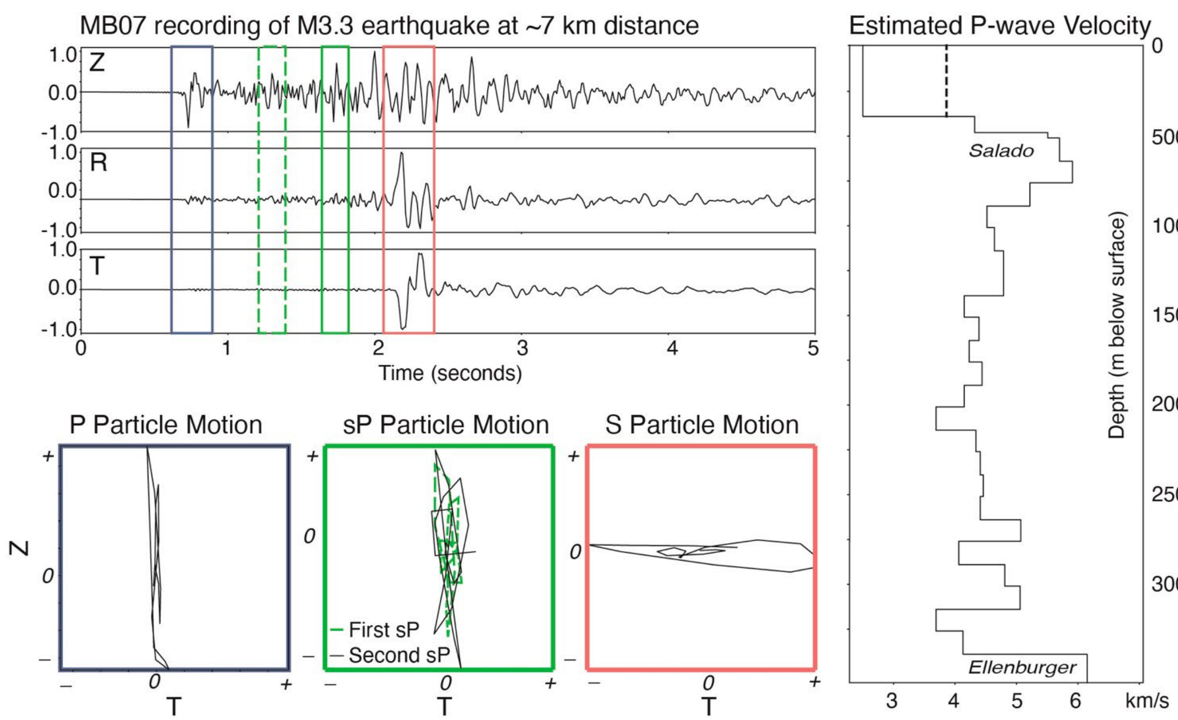

Figure 1. (Top left) Recording of a M3.3 earthquake near Midland by station MB07, located between Midland and Odessa. The P-wave (blue window), sP conversions (green windows) and S-wave (red window) are shown. The recordings have been rotated so that P-energy is maximized on the Vertical (Z), and S-energy is maximized on the Radial (R) and Transverse (T) components. Waveforms are normalized in amplitude. (Bottom left) Particle motion plots to confirm the P vs S motion. As expected, the P-wave shows +/- motion in Z but not T, and the S-wave +/- motion is in T and not Z. The converted phases are near vertically incident P-waves but due to the time separation from the P-wave, the phase spent significant time moving slowly as an S-wave within the basin. (right) A working hypothesis is that the timing of the two converted phases reflects conversion from the top of Ellenburger (dashed green) and from top of salt (solid black).

Stress Drop Variations of Induced Earthquakes near Dallas-Fort Worth Airport

S-J. Jeong, B. W. Stump, and H. R. DeShon

The Seismic Record, 2022, 2 (2): 68-77. https://doi.org/10.1785/0320220003

We estimate stress drops for injection-induced earthquakes near Dallas-Fort Worth Airport in the Fort Worth Basin (FWB), Texas, to investigate source properties in response to fluid injection. Stress drops at the Airport sequence show three unique characteristics compared to those estimated for other earthquake sequences in the FWB: (1) stress drops have lower mean and median values; (2) stress drops increase with moment magnitude; and (3) stress drops increase in size over the first 1.5 km in radial distance from the injection point. The low stress drop Airport events occurred shortly after the initiation of injection near a fault within hundreds of meters of the well. Pore pressure perturbations in the Airport area are 1 order of magnitude lower than those from the other sequences, suggesting that absolute pore pressure changes may not be the main factors in stress drop variations. We suggest that the low stress drop events may be related to transition from aseismic slip to seismic rupture previously observed in laboratory and field experiments.

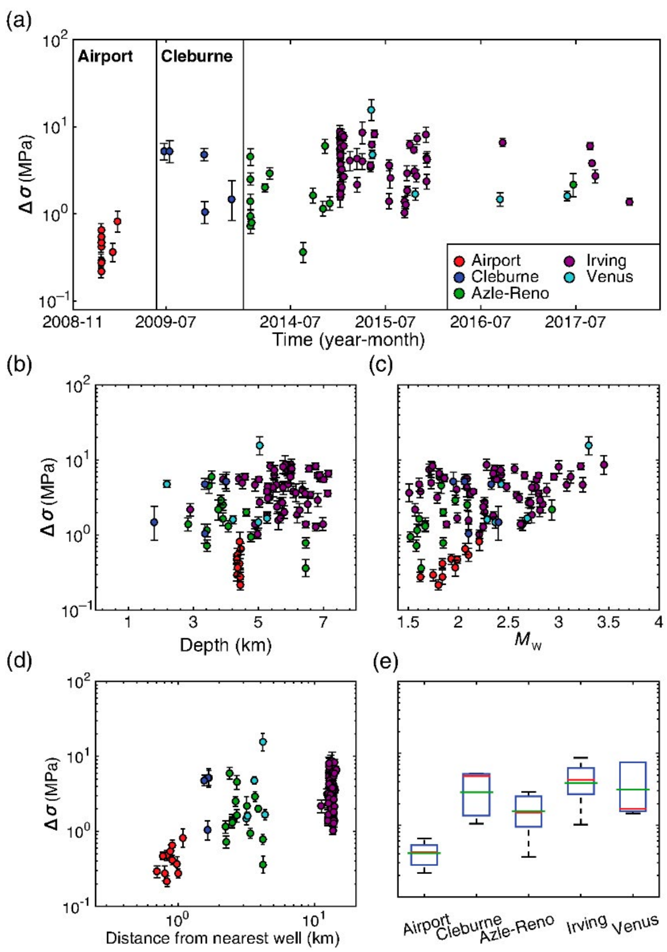

Figure 1. Stress drop estimates plotted against (a) time, (b) event depth, (c) moment magnitude Mw, (d) distances from the nearest injection points, and (e) box plots. (a–d) Error bars represent the 95% confidence intervals for the stress drop estimates. Colors indicate individual sequences following Figure 1 and are described in the legend in (a). In (a), note the time breaks after both the Airport and Cleburne sequences. (c, d) The Airport earthquakes display an increase in stress drop with magnitude and range, whereas stress drops from the other sequences do not correlate with moment magnitude or distance. Note that the Irving-Dallas sequence locates at >10 km from the nearest well in (d). In (e), each box plot includes the mean (green lines) and median (red lines) values with the 25th and 75th percentiles at the bottom and top boundaries of each blue box, respectively. The whiskers extend to one times the interquartile range. For Cleburne and Venus, stress drops show significant differences between mean and median values due to the small sample sizes. The median values in real numbers are 0.42, 4.80, 1.50, 4.26, and 1.68 MPa for Airport, Cleburne, Azle-Reno, Irving-Dallas, and Venus, respectively. The mean values are 0.41, 2.89, 1.58, 3.87, and 3.13 MPa for each earthquake sequence. *Reproduced with permission from Jeong et al. (2022).*

Potential Causes and Consequences of the Dallas-Irving Earthquake Sequence, Fort Worth Basin, Texas

L. Quinones and H. R. DeShon

To be submitted to The Seismic Record, 2023

Earthquake sequences within the Fort Worth Basin (FWB) in Texas have been linked to direct pore-fluid pressure increases caused by fluid injection activities from wells located near the now-active faults in the basin. However, the Dallas–Irving earthquake sequence (fig. 1) has no nearby (<15 km distance) fluid injection wells to its source fault and so lacks the influence that would be producing a direct pore-fluid-pressure effect. Here, we examine the potential that basin-wide stress changes associated with basin-wide fluid injection activities could be the main stress change inducing slip on the source fault of the Dallas–Irving sequence. We present a thorough examination of the seismic history of the Dallas–Irving sequence using observed, relocated, and template-matched earthquake catalogs. We then compare the seismic history of the sequence against the temporal changes in basin wide pore fluid pressure and poroelastic stress changes associated with injection activities using a coupled geomechanical model of the FWB. Overall, we observe that while injection associated stress changes at the Dallas–Irving sequence site are of small magnitude, the stress changes did reach the source fault of the sequence prior to the onset of seismicity. We thus conclude that the Dallas–Irving sequence is a fluid-injection-induced sequence.

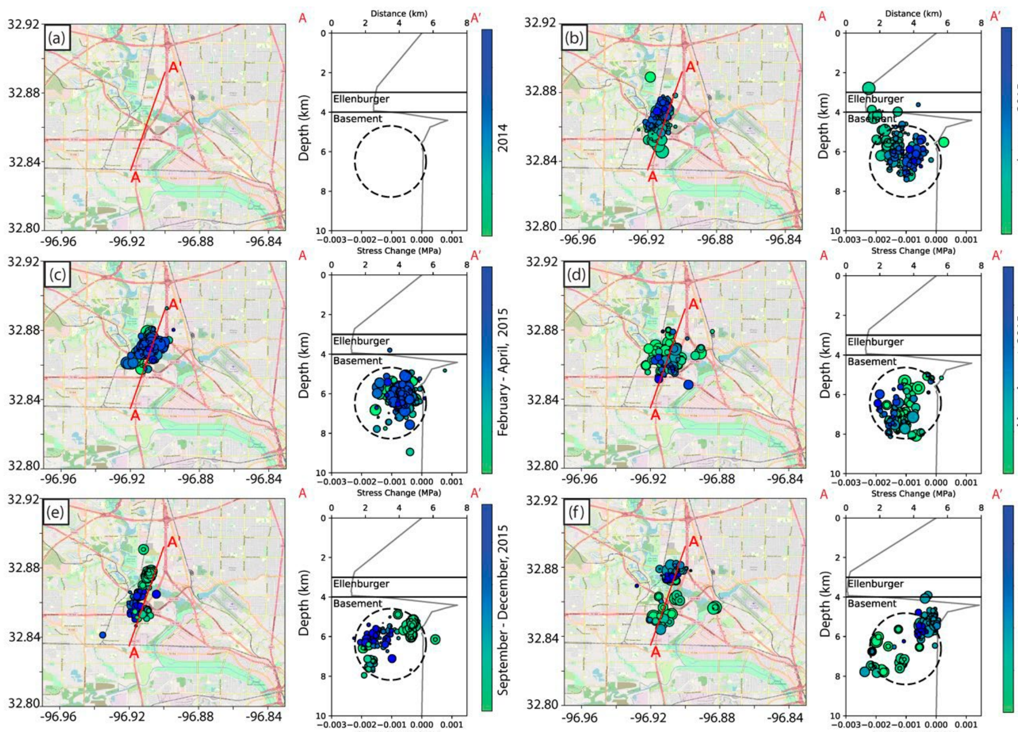

Figure 1. Time sequence of the Dallas–Irving earthquake sequence in map view (left) and along the A-A′ cross section (right). Earthquakes are scaled by magnitude and colored by time; note that the time duration in each panel changes as earthquake rates change. Although there are known Dallas–Irving earthquakes in 2014 (based on template matching), the events were not well recorded and do not appear in the double-difference high- resolution earthquake catalog shown here. Earthquakes in January 2015 have larger depth uncertainties and are likely not in the Ellenburger. The top of the Ellenburger Formation and crystalline basement are shown. The gray line in each cross section shows modeled stress change with depth derived from a coupled pore pressure diffusion and poroelastic geomechanical model of the Fort Worth Basin, 2005–2021.The black dashed circle is provided to guide the eye to see earthquake migration within time along the causative NE-striking normal fault.

Structural Characteristics of Shallow Faults in the Delaware Basin

E. A. Horne, P. H. Hennings, K. M. Smye, S. Staniewicz, J. Chen, and A. Savvaidis

Journal of Interpretation – 2022, https://dx.doi.org/10.1190/int-2022-0005.1

The Delaware Basin of Texas and New Mexico is undergoing elevated levels of seismicity. More than 130 earthquakes with moment magnitudes of at least 3.0 were recorded between 2017 and2021, occurring in both spatiotemporally isolated and diffuse clusters. Many of these events have been linked to oilfield operations such as hydraulic fracturing and wastewater disposal at multiple subsurface levels. However, the identification and characterization of earthquake-hosting faults has remained elusive. Two distinct levels of faulting appear in the central region of the basin, where most earthquakes were measured (fig. 1). These fault systems include a contractional, basement-rooted fault system and a shallow, extensional fault system. Shallow faults trend parallel to, and rotate along with, the azimuth of SHMAX, are vertically decoupled from the basement-rooted faults, accommodate dominantly dip-slip motion, and are the product of more recent processes including regional exhumation and anthropogenic influences. The shallow fault system is composed of NW-SE- striking, high-angle, parallel trending faults that delineate a series of elongate, narrow, extensional graben. Although most apparent in 3D seismic reflection data, these narrow, elongate graben features are also observed from Interferometric Synthetic Aperture Radar (InSAR) surface deformation measurements and can be delineated using well-located earthquakes. In contrast to the basin-compartmentalizing, basement-rooted fault system, shallow faults do not display any shear movement indicators, and have small throw given their length, producing an anomalous mean throw-to-length ratio of 1:1000. These characteristics indicate that these features are more segmented than can be mapped using conventional subsurface data. Much of the recent seismic events in the south-central Delaware Basin are associated with these faults. InSAR surface-deformation observations show that these faults may also be slipping aseismically.

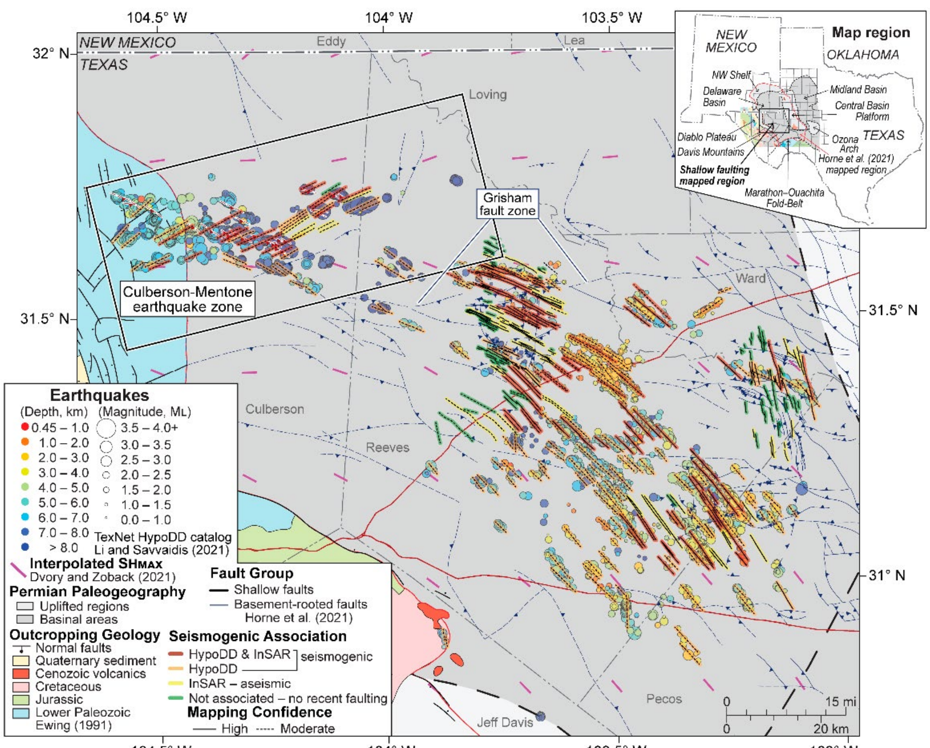

Figure 1. Map of the central Delaware Basin showing newly mapped shallow fault interpretations and basement-rooted fault traces from Horne et al. (2021). Shallow faults are colored according to seismogenic association. Shallow faults that are proximal to earthquakes are outlined in orange. Seismogenic faults that are also associated with InSAR surface deformation features are outlined in dark red. Fault segments that are associated only with InSAR observations are outlined in yellow. Segments that are not associated with recent seismicity or surface deformation are highlighted in green. Earthquake relative relocations are from Li and Savvaidis (2021), and hypocentral locations are sized by magnitude and colored by depth of relocated event.

Structural Characterization and Rupture-Hazard Assessment of Faults in the Midland Basin, West Texas

E. A. Horne, P. H. Hennings, K. M. Smye, A. Z. Calle, A. P. Morris, D. Huang, and A. Savvaidis

In Preparation

The Midland Basin has had an increase in both rate and magnitude of seismicity: 60 ≥3.0 Mw events have occurred since 2019. These events are of anthropogenic origin, as Saltwater Disposal (SWD) into deep and shallow formations have increased fourfold from 2015 through 2021. To understand the causal factors of earthquakes in the region and assess the evolving hazard, we present a new regional fault interpretation and a fault-slip hazard assessment in the form of Fault Slip Potential (FSP). Our results show a total of more than 5,000 km of fault length mapped across the Midland Basin (fig.1). Faults are characterized according to morphology (length, orientation, structural style), as well as according to mapping confidence (high and moderate), as there are distinct variabilities in the quality, density, and aerial extent of data. Faults mapped at all scales and data resolutions have been simplified to capture the kinematic evolution of the region. These framework faults are classified by scale of deformation, which include 1st order (major fault blocks); 2nd order (intra-block fault zones); and 3rd order (local, minor faults). Deformation is expressed by two fault styles: high-angle (~65 ±10˚) reverse, and near-vertical (~80 ±10˚) strike-slip faults. High-angle reverse faults trend NNW-SSE and NNE-SSW and are cross-cut by WNW-ESE and WSW-ENE trending strike-slip faults. The 1st order high-angle reverse faults that trend NNW-SSE define the margin of the Central Basin Platform and accommodate the greatest structural relief. This relief diminishes basinward. Local (2nd order), fault-bounded uplifts and fault propagation folds are cross-cut by WNW-ESE trending, left-lateral and WSW-ENE trending, right-lateral strike-slip fault zones (2nd and 3rd order). Notably, the vergence directions of these contractile faults and fault-propagation folds change polarity across these strike-slip fault zones, and many show continued movement along these E-W systems. Our observations suggest that these E-W faults are likely the product of pre-Paleozoic tectonism, and they were reactivated during the diachronous Paleozoic orogenies. These faults have played a significant role in the initiation and evolution of the structural architecture of the greater Permian Basin. Under present-day stress conditions, DFSP and PFSP results show that these WNW-ESE and WSW-ENE oriented faults are also extremely sensitive to reactivation under modest increases in pore pressure.

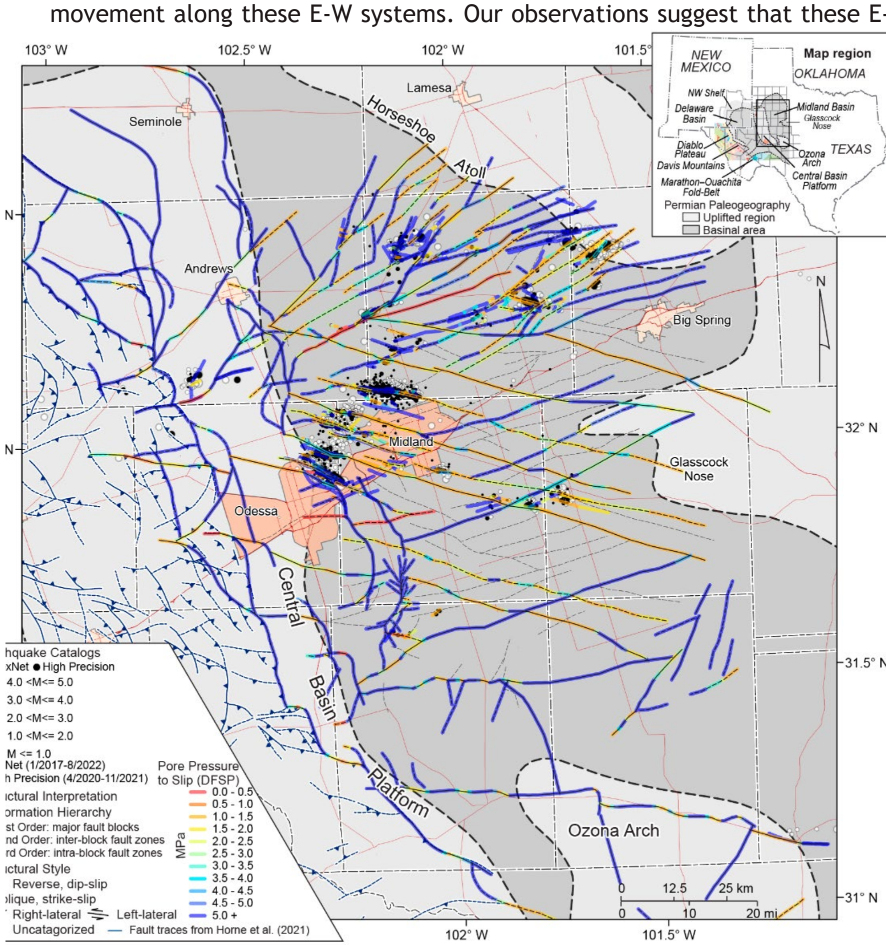

Figure 1. Regional framework fault map of the Midland Basin. Faults are colored according to DFSP results, warm colors indicting lower pore pressure perturbation needed to induce slip under present day stress conditions.

Structure and Characteristics of the Basement in the Fort Worth Basin

E. A. Horne, K. M. Smye, and P. H. Hennings

Bureau of Economic Geology Report of Investigations No. 286, 2022, https://dx.doi.org/10.23867/RI0286C7

The Fort Worth Basin of Texas (fig. 1) has experienced over 125 Mw ≥2.5 earthquakes since 2006. These earthquakes are attributed to increased pore fluid pressure from wastewater injection and from cross-fault pore pressure imbalance caused by injection and production. Understanding the structural and compositional characteristics of basement rocks that may control aspects of earthquake-prone faults is vital to quantifying known hazards. Here we provide a synthesis of recent work completed to characterize the structure of the crystalline basement. We also characterize the suite of lithologies and document compositional changes of the uppermost crystalline basement and basement-sediment interface through stratigraphic and petrophysical analyses of logged basement-penetrating wells. The geologic history, composition, and structural architecture of the Fort Worth Basin are not unique; therefore, the characteristics of the basement and variables that have impacts on seismic hazard can be applied more broadly. Our results show that the crystalline basement in the Fort Worth Basin is dominantly granitic in composition and that basement rocks are frequently found to be altered. Evidence of prolonged subaerial exposure is observed at the basement—sediment interface in the form of increased porosity and the presence of hematite. Paleotopographic variation of the basement surface is evidenced by the presence of granite wash that is more than 60 m (200 ft) thick in some paleolows. Strata overlying basement in the Fort Worth Basin vary from west to east, with siliciclastic lithologies proximal to the Cambrian shoreline in the west, transitioning basinward to carbonate lithologies in the structurally deepest part of the basin to the east. The crystalline basement and overlying lower Paleozoic strata are deformed by northeast-trending normal faults, which create a series of elongate horst and graben structures. Deformation ranges from isolated faults to linked and crosscutting relay systems, with segments ranging in length from 0.5 to 80 km (~0.3 to 50 mi). Faults that have recently become seismogenic are generally less than 10 km (~6.2 mi) long and exhibit more than 50 m (~164 ft) of dip-slip, vertical displacement.

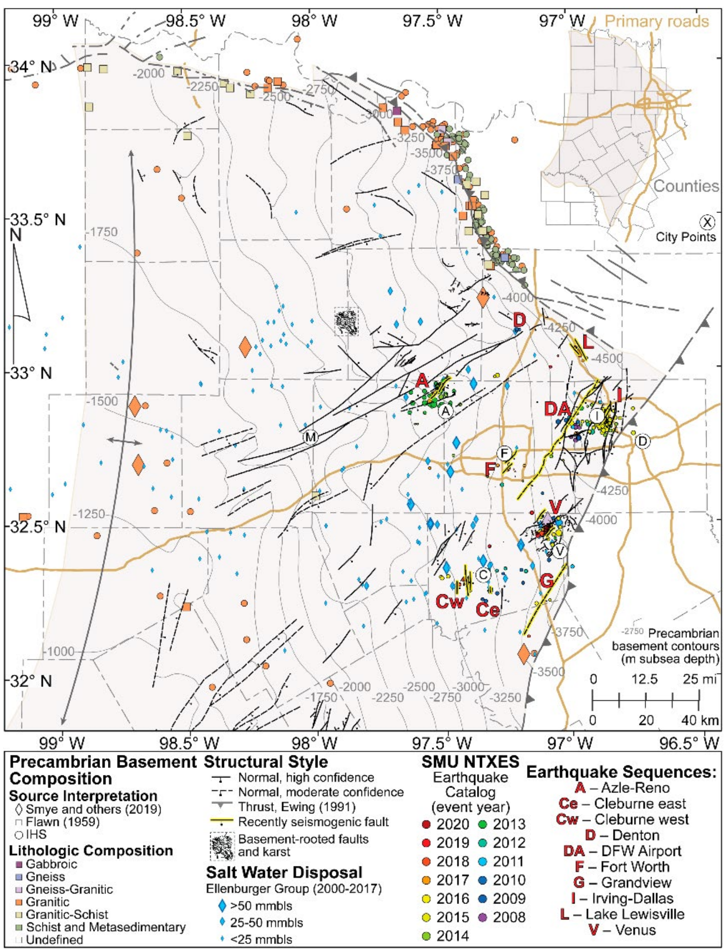

Figure 1. Detailed map of the northeastern Fort Worth Basin showing saltwater disposal wells, the entire record of seismicity from the Southern Methodist University North Texas Earthquake Study (DeShon and others, 2018), the earthquake sequences studied by Hennings and others (2021), traces of basement-rooted faults from Horne and others (2020), and Precambrian basement lithologies as defined by Flawn (1959), Smye and others (2019), IHS (2009), and this study. The approximate traces of main tectonic features, including the Muenster Arch and Ouachita thrust front, are highlighted in gray.

Lithology and Reservoir Properties of the Delaware Mountain Group of the Delaware Basin and Implications for Saltwater Disposal and Induced Seismicity

K. Smye, D. A. Banerji, R. Eastwood, G. McDaid, and P. Hennings

Journal of Sedimentary Research – 2021, https://doi.org/10.2110/jsr.2020.134

Deepwater siliciclastic deposits of the Delaware Mountain Group (DMG) in the Delaware Basin (DB) are the primary interval for disposal of hydraulic fracturing flowback and produced water from unconventional oil production. Understanding the storage capacity of the DMG is critical in mitigating potential risks such as induced seismicity, water encroachment on production, and drilling hazards, particularly with likely development scenarios and expected volumes of produced water. Here we present a basin-wide geologic characterization of the DMG of the Delaware Basin. The stratigraphic architecture, lithology, and fluid-flow properties—including porosity, permeability, amalgamation ratios, and pore volumes—are interpreted and mapped (figs.1, 2). Lithologies are predicted using gamma-ray and resistivity-log responses calibrated to basinal DMG cores and outcrop models. Sandstones exhibit the highest porosity and permeability, and sand depocenters migrate clockwise and prograde basinward throughout Guadalupian time. Permeability is highest at the top of the Cherry and Bell Canyon formations of the DMG, reaching tens to hundreds of millidarcies in porous sandstones. Porous and permeable sandstones are fully amalgamated at the bed scale, but at the channel scale, most sandstones are separated by low-permeability siltstones or carbonates where net sandstone is less than 30%. This geologic characterization can be used to assess the regional storage capacity of the DMG and as input for dynamic fluid-flow models to address pore-pressure evolution, zonal containment, and induced seismicity.

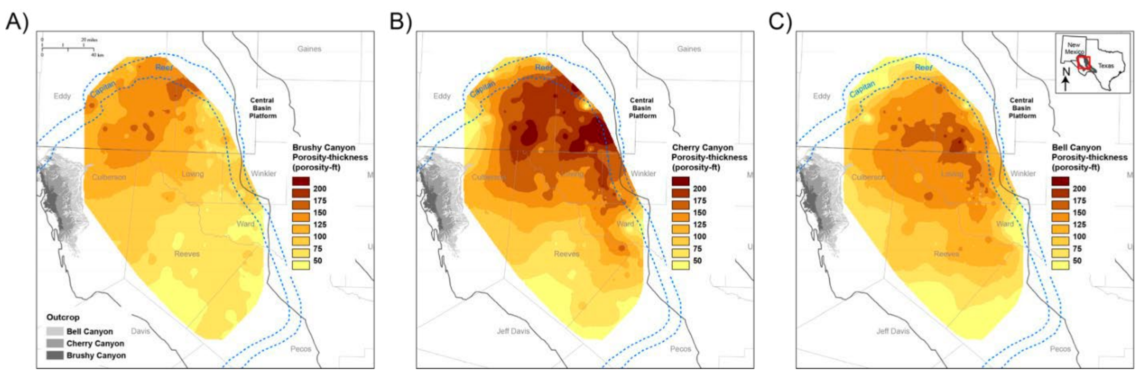

Figure 1. Delaware Mountain Group porosity-thickness maps combining stratigraphic-thickness interpretations with model-derived porosity values for A) Brushy Canyon, B) Cherry Canyon, and C) Bell Canyon.

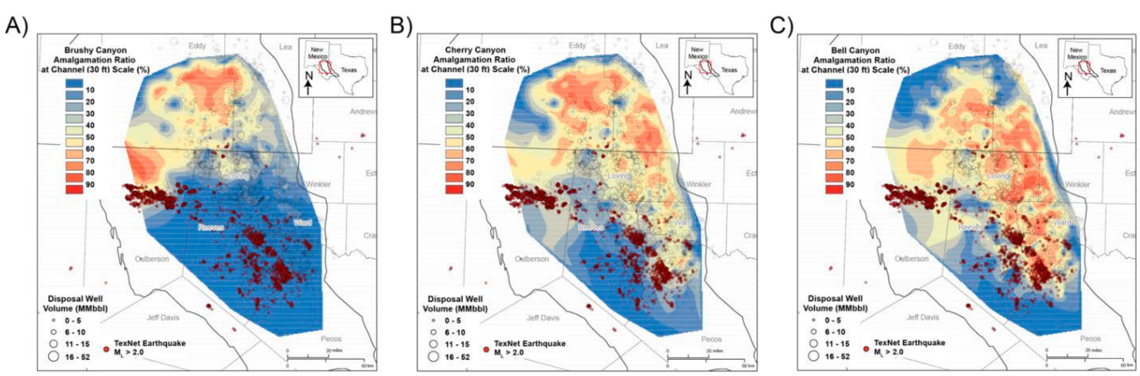

Figure 2. Delaware Mountain Group amalgamation ratios at the channel (30 ft) scale for A) Brushy Canyon, B) Cherry Canyon, and C) Bell Canyon shown with TexNet earthquakes M_L>2.0 since 1/1/17 and cumulative saltwater disposal volumes for all DMG disposal wells.

Role of Deep Fluid Injection in Induced Seismicity in the Delaware Basin, West Texas and Southeast New Mexico

K. M. Smye, J. Ge, A. Morris, E. A. Horne, A. Calle, R. L. Eastwood, J.-P. Nicot, and P. Hennings

Submitted to *Geochemistry, Geophysics, Geosystems*

Rates of seismicity in the Delaware Basin of West Texas and southeast New Mexico increased from 10 earthquakes per year of local magnitude 3.0 and above in 2017 to more than 160 in 2021, coincident with an increase in unconventional oil and gas activity. The largest magnitude events occur on basement-rooted faults that extend into the pre-Permian sedimentary section that has been targeted for deep injection of more than 3 billion barrels of oilfield wastewater. Deep injection has been shown to be the causal agent for much of this seismicity, and here we demonstrate the link between injection geology, pore pressure evolution, fault stability, and induced seismicity. Subsurface geologic characterization shows that the layers targeted for injection are predominately dolomitized platform carbonates with low matrix porosity and fracture-enhanced permeability, with inherent heterogeneity in flow properties. A comprehensive, three-dimensional geological model, populated with reservoir properties, is used as the basis for fluid-flow modeling, with global calibration supplemented by dynamic injectivity data. Pore pressure changes with deep injection are as much as 3.5 MPa (500 psi) from 1983 to early 2022 (fig. 1), increasing the native pore pressure state by asmuch as 10% locally. Earthquakes occurring at distances of as much as 30 km (20 mi) from deep injection have experienced small (<0.1 MPa) pore-pressure increases, indicating that the faults hosting these earthquakes are highly sensitive to changes in effective stress, and they probably have less frictional stability than is generally assumed. Our results serve as a critical first step in understanding the stress changes acting to induce earthquakes in one of the most seismically active and geologically complex basins in the United States.

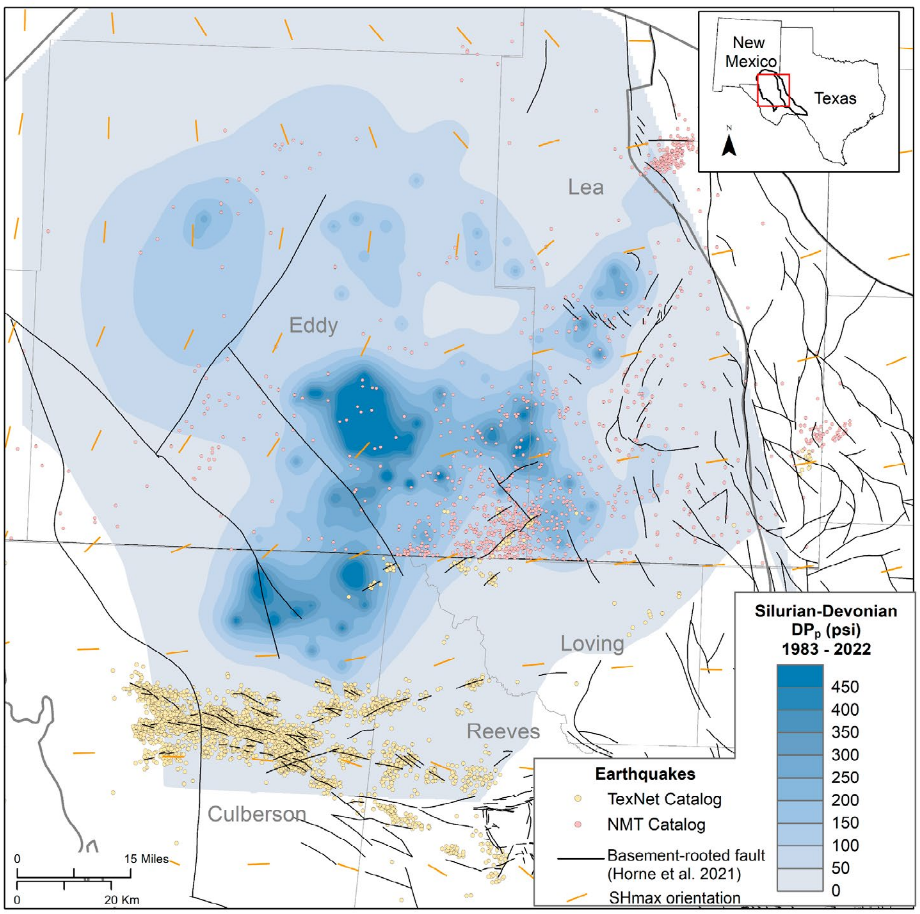

Figure 1. Modeled change in pore pressure (ΔPp), 1983–Jan. 2022, in upper Ordovician, Silurian, and Devonian injection strata, shown with TexNet and NMT catalogued earthquakes, basement-rooted faults *(*modified from Horne et al., 2021), and S_{Hmax} azimuth (Dvory and Zoback, 2021).

Variations in Vertical Stress in the Permian Basin Region

K. M. Smye, P. H. Hennings, and E. A. Horne

AAPG Bulletin – 2021, https://doi.org/10.1306/10092019189

Constraining the magnitude of vertical stress (Sv), or overburden pressure, is key in determining a region's stress state and has implications for reservoir geomechanics and the potential for induced seismicity. Of the principal stress orientations (Sv, minimum horizontal stress [Shmin], and maximum horizontal stress [SHmax]), Sv is the most straightforward to constrain using wire-line log data. The magnitude of Sv varies because of lithology and burial history, potentially causing local perturbations in the in-situ stress field. Previous studies of the state of stress in the Permian Basin use a constant Sv, relying on determination of SHmax and Shmin, and yield an interpretation that the faulting regime transitions from normal faulting in the west to normal to strike-slip faulting in the east. Here, we present an interpretation of the spatial and depth variability in Sv trends in the Permian Basin (Fig. 1) based on density log integration. Where density measurements are absent, values are calculated from compressional velocity logs using a transform that is fit to local data. Notable variations include higher Sv gradient on carbonate platforms and shelves, where high-density carbonates are thicker and are found at shallower depths than in the basins. Within the basins, the magnitude of Sv gradient is as low as 1.06 psi/ft at depth. This work shows the potential for regional interpretations of Sv to gain insight into the effect of variations in Sv on state of stress.

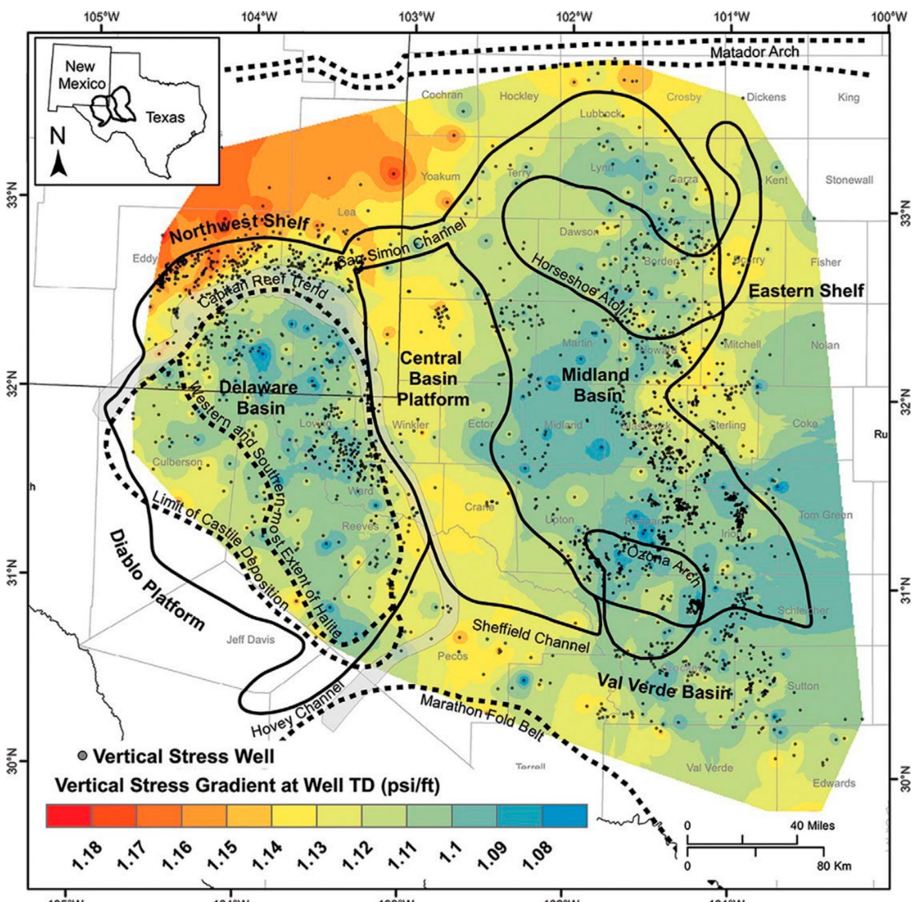

Figure 1. Vertical stress gradient (psi/ft) at well total depth (TD) for 2476 wells. Castile and halite deposition extent from Anderson (1981).

Using InSAR to Understand Regional Anthropogenic Uplift, Subsidence, Faulting and Earthquakes in the Delaware Basin, West Texas and Southeast New Mexico

P. H. Hennings, S. Staniewicz, K. Smye, J. Chen, E. A. Horne, J.-P. Nicot, J. Ge, R. Reedy, and B. Scanlon

Submitted to Nature Communications Earth & Environment

Advances in InSAR remote sensing have greatly improved our ability to monitor land-surface changes in response to subsurface fluid movement. Here we show the impact of fluid withdrawal from oil production and injection of wastewater on land-surface subsidence and uplift in the entirety of Delaware Basin in West Texas and New Mexico (fig. 1). This basin is the largest producer of oil globally, totaling 4 billion barrels from 2015 through 2021. This production has necessitated disposal by injection of 14 billion barrels of coproduced wastewater. The associated and accelerating changes in land-surface elevation reflect significant geomechanical sensitivity, including shale compaction, reservoir pressurization and inflation, faults deflecting the ground surface, and induced earthquakes of multiple causes. The subsidence region comprises ~16,000 km^2 with a maximum lowering of 18 cm (332 million m^3), whereas the uplifted region comprises 18,000 km^2 (maximum uplift: 7 cm, 155 million m^3). Subsidence correlates linearly with fluid volume produced, whereas injection causes complex patterns of uplift spreading laterally and complexly. Our data and results can directly assist in managing sustainable development of the Delaware Basin, especially the vitally important injection resource. and in mitigating negative consequences of development.

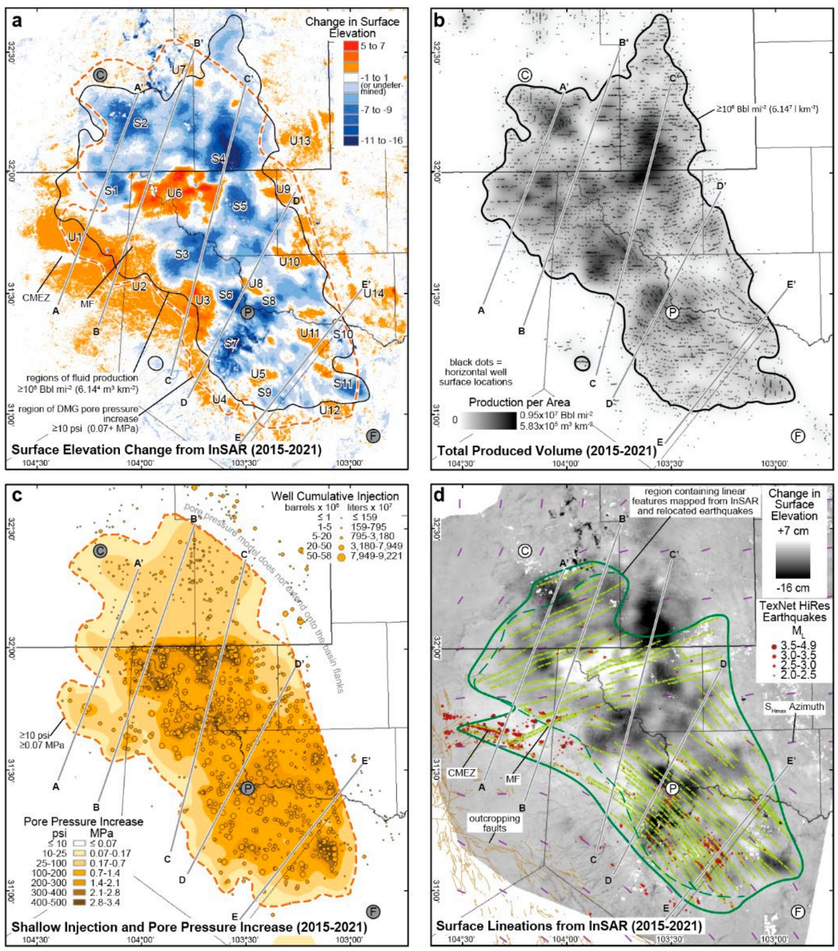

Figure 1. Maps of the 2015—2021 temporal window. **a.** Vertical ground-surface displacement. The region of minimum fluid production is from **b,** and the region of minimum pore pressure increase is from **c**. Regions designated S1–S10 are specific subsidence regions, and U1–U14 are specific uplifted regions. b. Total fluid production from shale strata. Variable color contour shows interpolated production per unit area. Two contours of total production are indicated. **c.** Pore pressure increase in the Delaware Mountain Group (DMG) from shallow injection with cumulative volume injection per well shown. **d.** Distribution of linear features as interpreted from the InSAR data and relocated earthquakes. Some of these linear features are faults as mapped, and some are interpreted here to indicate possible zones of faulting in the subsurface. The azimuth of S_{Hmax} is indicated. The region of linear features is enclosed by the dark-green line.

Stability of the Fault Systems that Host Induced Earthquakes in the Delaware Basin of West Texas and Southeast New Mexico

P. H. Hennings, N. Dvory, E. A. Horne, P. Li, A. Savvaidis, and M. Zoback

The Seismic Record – 2021, https://doi.org/10.1785/0320210020

The Delaware Basin of West Texas and southeast New Mexico has had elevated earthquake rates linked spatiotemporally to unconventional petroleum operations. Limited knowledge of subsurface faults, the in situ geomechanical state, and the exact way in which petroleum operations have affected pore pressure (Pp) and stress state at depth makes causative assessment difficult, and the actions required for mitigation are uncertain. To advance both goals, we integrate comprehensive regional fault interpretations, deterministic fault-slip potential (DFSP), and multiple earthquake catalogs to assess specifically how faults of two systems—deeper basement-rooted (BR) and shallow normal (SN)—can be made to slip as Pp is elevated. In their natural state, the overall population faults in both systems have relatively stable deterministic fault-slip potential, which explains the low earthquake rate prior to human inducement. Basement-rooted faults with naturally unstable DFSP and associated earthquake sequences are few, but they include the Culberson–Mentone earthquake zone, which is near areas of wastewater injection into strata above basement. As a system, the shallow-normal faults in southcentral Delaware Basin are uniformly susceptible to slip with small increases in Pp. Many earthquake sequences have occurred along these shallow faults in association with elevated Pp from shallow wastewater injection and hydraulic fracturing. Our new maps and methods can be used to better plan and regulate petroleum operations to avoid fault rupture.

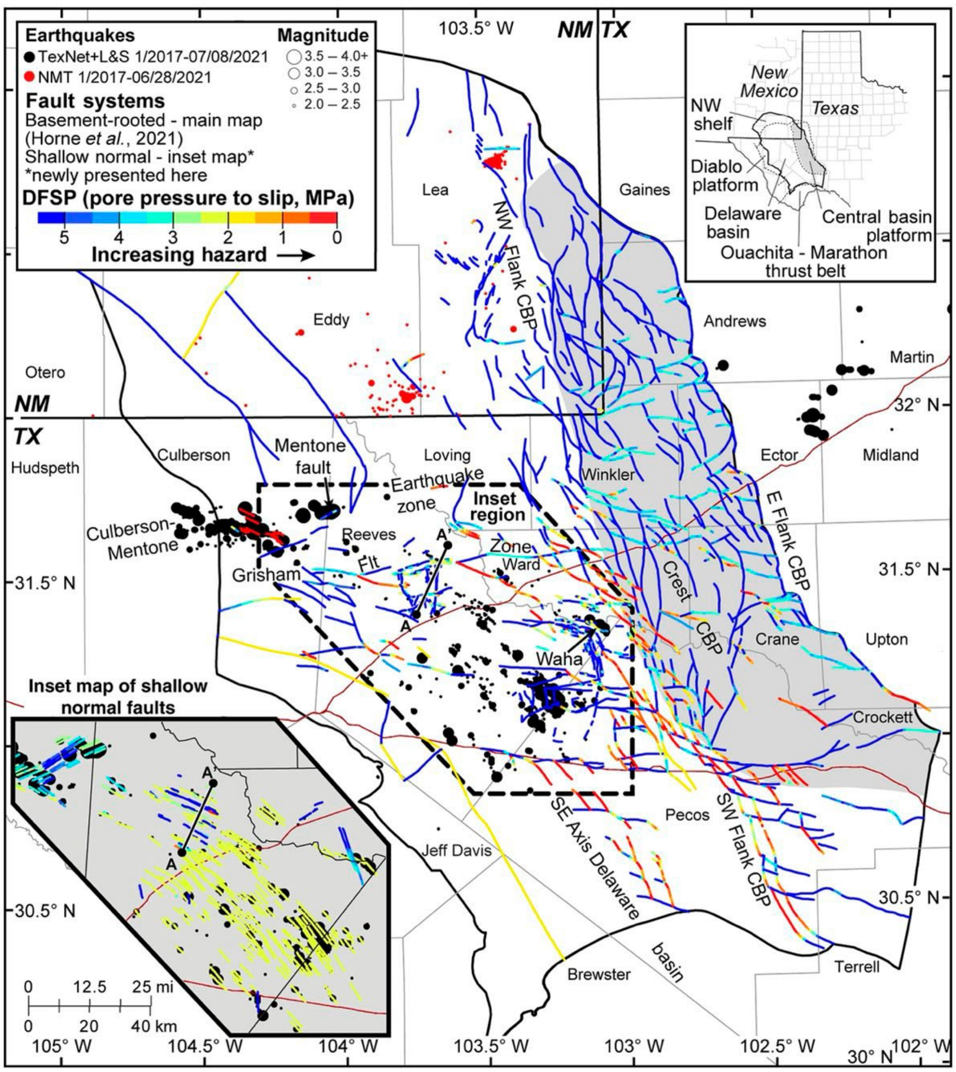

Figure 1. Map of DFSP, showing basement-rooted faults (main map) and f shallow normal faults (inset map). Both maps use the same scale.

Stability of Basement-Rooted Faults in the Delaware Basin of Texas and New Mexico, USA

A. P. Morris, P. H. Hennings, E. A. Horne, and K. M. Smye

Journal of Structural Geology - 2021, https://doi.org/10.1016/j.jsg.2021.104360

Since 2009 the Delaware Basin of Texas and New Mexico has experienced increased seismicity related to oilfield operations. Available near-present-day principal stress orientations, relative magnitudes, and vertical stress estimates are integrated to characterize 20 stress domains in the Delaware Basin. Data density, variability, and quality inform classification of most likely, less likely, and least likely stress tensor fields. A new interpretation of 3D basement-rooted faults in the Delaware Basin is analyzed for stability using most-likely stress tensors. Fault stability is expressed in terms of slip tendency (Ts) and critical pore pressure (ΔPfc; fig. 1). Individual faults are compared in terms of their stability and potential seismic capability, and stress scenarios can be compared for their effects on fault stability. Faults range from stable to critical under the conditions investigated, revealing that 8% of the total mapped fault area may become critically stressed by small pore-pressure increases (1 MPa, 145 psi) above ambient. Comparison of stability measures with focal mechanisms of recent pore-pressure-induced seismicity indicates that Ts and ΔPfc have predictive value. This work provides critical information for earthquake hazard research and mitigation studies of the Delaware Basin.

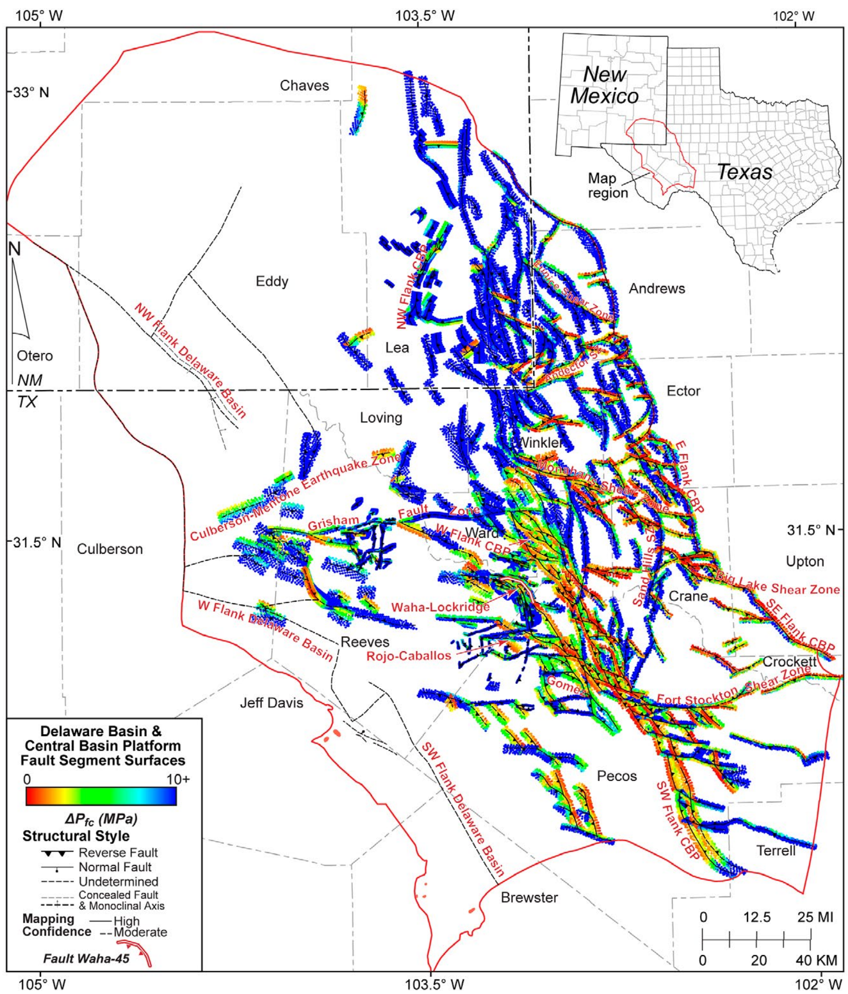

Figure 1. Fault stability represented as ΔPfc under the most likely stress state in each stress domain within the Delaware Basin. Low values of ΔP_{fc} imply lower stability.

Low Pressure Buildup with Large Disposal Volumes of Oil Field Water: A Flow Model of the Ellenburger Group, Fort Worth Basin, Northcentral Texas

R.S. Gao, J.-P. Nicot, P.H. Hennings, P. La Pointe, K.M. Smye, E.A. Horne, and R. Dommisse

AAPG Bulletin, 2021, https://doi.org/10.1306/03252120159

Produced water generated by hydrocarbon production from the Mississippian Barnett Shale in the Fort Worth Basin has been injected into geologically complex carbonates of the Ordovician Ellenburger Group (EBG) for 20 years. The basin experienced anomalous seismicity in the crystalline basement induced by the associated pore pressure increase. A comprehensive hydrogeologic flow model of the EBG covering ~30 counties provides estimates of pore pressure evolution through space and time that can be used for understanding the seismic events and for management of the disposal resource. A salient aspect of the model is the thorough treatment of faults and fractures. They form important features of these structurally complex formations, and their permeability was estimated through a discrete fracture network modeling approach. A total of 127 saltwater disposal wells injected a cumulative volume of 2.23 billion bbl (354 × 106 m^3) from ~2003 to 2018. Overall, the EBG is very resilient to large injection volumes with small pore pressure increases up to 1.4 MPa (200 psi). Several high-permeability faults act as pressure distribution and attenuation features, distributing pressure increases vertically and preventing it from extending to the next fault compartment. However, pressure diffusion away from injection centers is controlled by the fractured rock matrix. In addition, the overlying Barnett Shale modulates pressure increases when in direct contact with the EBG because it acts as a compressible cushion, but the impact of gas production does not seem to be as significant. Water withdrawal from the EBG through gas production wells, which has been observed, also contributes to limiting the pressure increases.

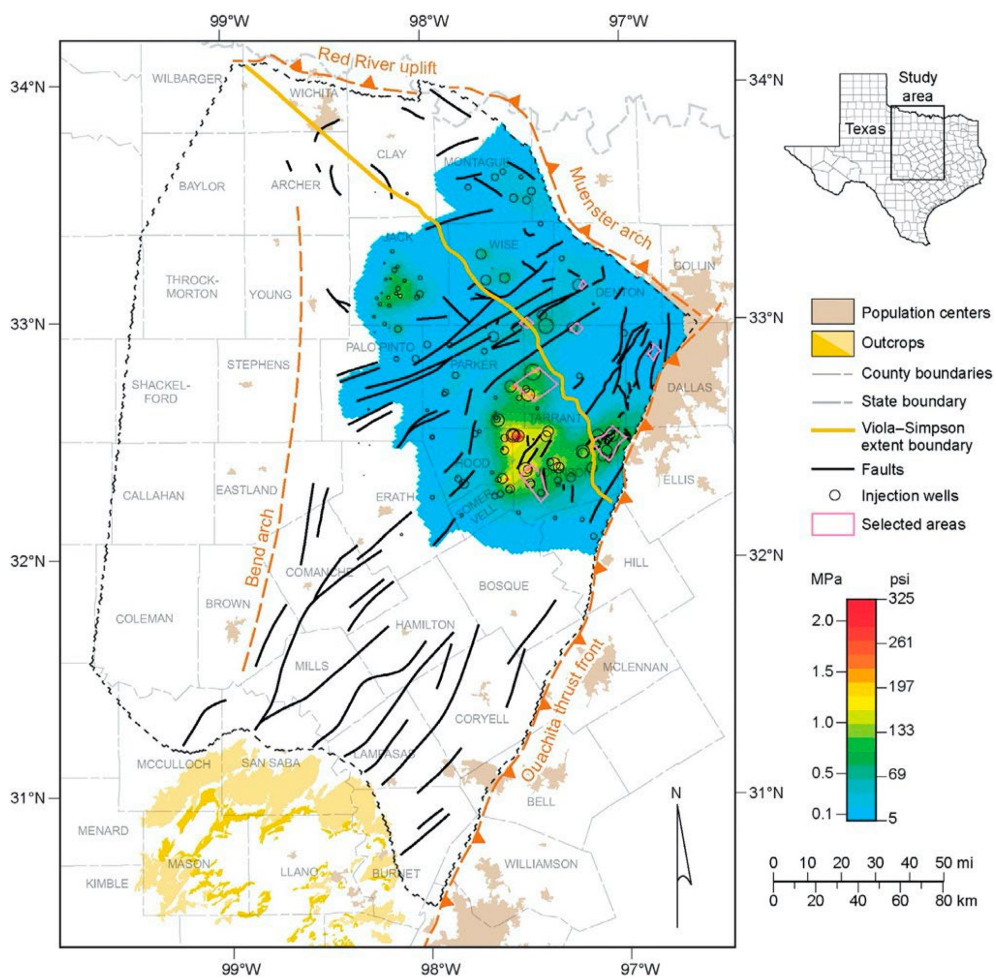

Figure 1. Map of pressure increase in the basal sediment layer. Cumulative injection volumes at the well locations are shown by variable-size circles (nonlinear scale). Cumulative injection volumes range from 84 million bbl to 37,000 bbl (median is 10.7 million bbl and average is 17.6 million bbl). The pressure increases are collocated with injection well cluster locations.

Pore-Pressure Threshold and Fault-Slip Potential of Induced Earthquakes in the Dallas-Fort Worth Area, North-Central Texas

P. H. Hennings, J.-P. Nicot, R. S. Gao, H. R. DeShon, J.-E. Lund Snee, A. P. Morris, M. R. Brudzinski, E. A. Horne, and C. Breton

Geophysical Research Letters – 2021, https://doi.org/10.1029/2021GL093564

Earthquakes were induced in the Fort Worth Basin from 2008 through 2020 by increase in pore pressure from injection of oilfield wastewater in saltwater disposal wells (SWD). In this region and elsewhere, a missing link in understanding the mechanics of causation has been a lack of comprehensive models of pore pressure evolution (ΔP_p) from SWD. We integrate detailed earthquake catalogs, ΔP_p, and probabilistic fault slip potential (FSP) and find that faults near large-scale SWD operations became unstable early, when ΔP_p reached ~0.31 MPa and FSP reached 0.24. Faults farther from SWD became unstable later, when FSP reached 0.17 and at much smaller ΔP_p. Earthquake sequences reactivated with mean ΔP_p of ~0.05 MPa. The response of faults shows strong variability, with many remaining stable at higher ΔP_p and few that became seismogenic at smaller changes. As ΔP_p spread regionally, an ever-increasing number of faults were impacted, and the most sensitive became unstable.

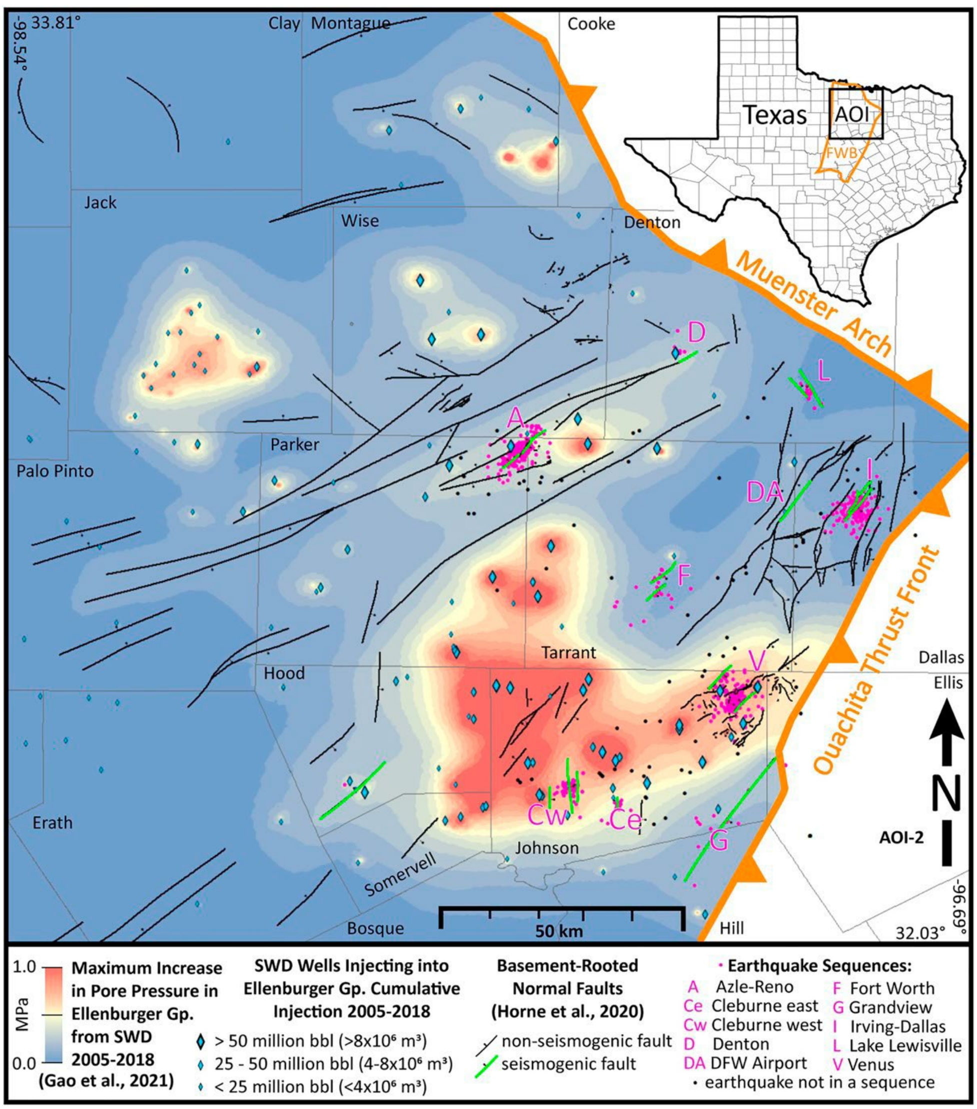

Figure 1. Map of the area of interest (AOI) in the Fort Worth Basin showing saltwater disposal wells and cumulative injected volumes, the entire record of seismicity from SMU NTXES, the earthquake sequences that we study here, traces of basement-rooted faults from Horne et al. (2020), and the distribution of the maximum ΔPp at the basement-sediment interface from the Gao et al. (2021) hydrogeologic model.

Understanding Anthropogenic Fault Rupture in the Eagle Ford Region, south-central Texas

C. McKeighan, P. Hennings, E.A. Horne, K. Smye, A. Morris

Bulletin of the Seismological Society of American – 2022, https://doi.org/10.1785/0120220074

There is a well-known occurrence of felt seismicity and smaller seismic events in many areas where hydraulic fracturing (HF) operations occur. The Eagle Ford shale play of south-central Texas experienced an increase in the rate of felt seismicity from 2014-2019, temporally coincident with petroleum development in the region. By mid-2019, the rate of seismicity decreased alongside a reduction in the rate of well completions, thus prompting this investigation of the relationship between HF operations and geologic conditions that contribute to induced earthquake hazards. The goals of this work included mapping and conducting a geomechanical characterization of faults that delineate seismogenic regions of the Eagle Ford to understand the conditions that lead to inducing fault rupture. An integrated regional dataset composed of published data, wells, earthquakes, and interpretations from operators provided input for a 3D structural framework. Earthquake relocation analyses helped constrain the distribution of earthquakes that correlate to interpreted faults and enable identification of those that have been seismogenic. In-situ stress state of faults was analyzed to determine fault sensitivity in situ. A spatiotemporal analysis of HF operations and earthquakes further revealed induced-earthquake clusters that are linked to specific faults. We show how seismogenic and aseismogenic fault systems relate to earthquakes by determining which faults are more sensitive and which faults have been seismogenic. Faulting is dominated by NE-SW striking normal faults with 21% having hosted induced earthquakes since 2017. Faults in the Eagle Ford region have a geologically quasi-stable in situ stress state. Using a conservative scheme, we directly associate 45% of earthquake ruptures to HF to build our analysis dataset. Of those events, 70% are located within 1 km of a mapped fault. Stress conditions on seismogenic faults show a wide range of sensitivity to rupture. This suggests that all faults close to HF operations should be considered as candidates likely to rupture.

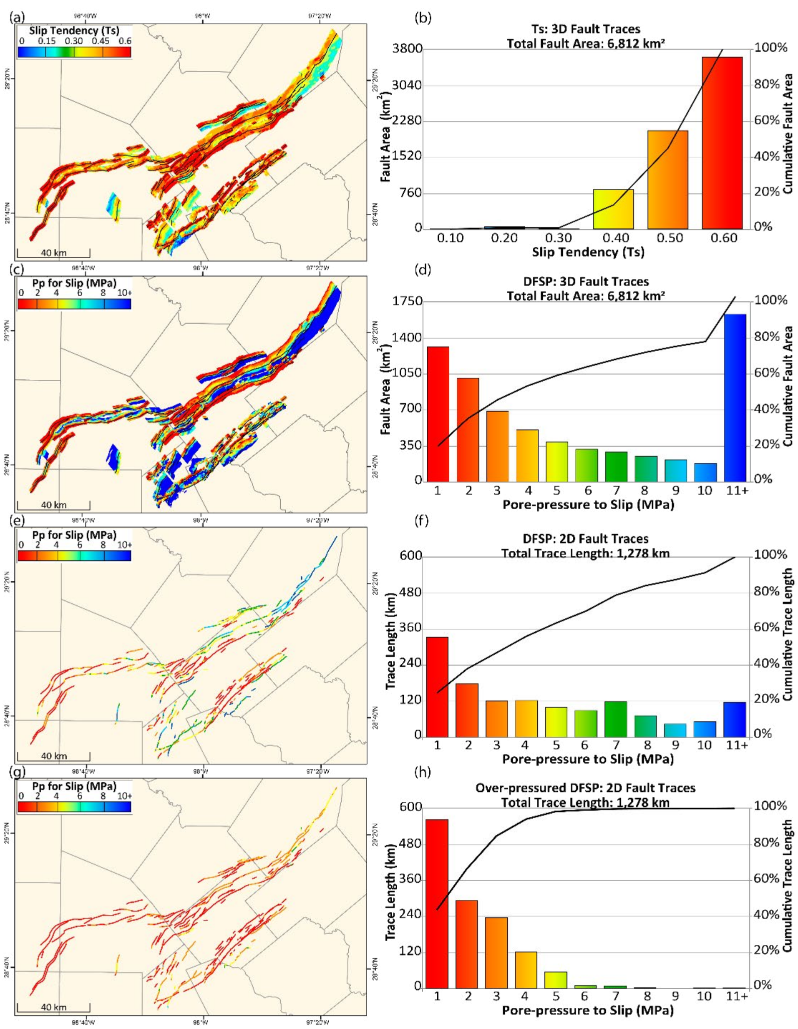

Figure 1. Maps and data distribution for slip tendency (Ts) and DFSP stress analysis on 2D and 3D faults. (a) slip tendency on 3D faults (b) slip tendency (Ts) ranges from 0-0.6. (c) DFSP results for Pp to slip in MPa for 3D fault surfaces, (d) distribution of DFSP results for Pp to slip (MPa) on 3D fault surfaces (e) DFSP analysis using a normal-pressured condition (0.011 MPa/m) representative the Buda Fm. for Pp to slip in MPa for 2D fault surfaces (f) distribution of normally-pressured DFSP results for Pp to slip (MPa) on 2D fault surfaces (g) DFSP analysis using an over-pressured condition (0.019 MPa/m) representative of the Eagle Ford Fm. for Pp to slip in MPa for 2D fault traces (h) distribution of over-pressured DFSP results for Pp to slip (MPa) on 2D fault traces.

Earthquake Statistics across Texas and Prevalence of Runaway Rupture

N. Igonin, C. Bolton, and A. Savvaidis

There are statistically significant differences in seismicity due to various kinds of injection and the geomechanical properties of the basin where the seismicity is occurring. To understand a particular region's sensitivity to injection, these differences need to be quantified and compared on a large scale, which can then be used to build a framework to describe the range of basin response to injection. For example, the Barnett Shale in Texas has been extensively hydraulically fractured, and yet the seismicity is negligible (Schultz and others, 2020). In contrast, the Eagle Ford and Delaware basins have seismicity associated with hydraulic fracturing and wastewater injection (Grigoratos and others, 2022).

We will link several different measures together to determine if there are any relationships between spatiotemporal changes with changes in seismicity. These measures include *b*-values over space and time per fault segment, aftershock productivity, and exceedance probability (Langenbruch and others, 2020). One of the measures we are looking for is runaway rupture, which occurs when there is an earthquake that is larger than it should be based on the previous events recorded and can be identified based on a low exceedance probability (e.g., <10%). Magnitude frequency distributions can also be used to obtain the stress drop regime and seismogenic index, which can be used to infer fault roughness (Shapiro and Dinske, 2021).

In order to carry out this analysis, a comprehensive catalog is required. The TexNet public catalog was supplemented with all available published catalogs (e.g., Frohlich and others, 2014, 2020; Walter and others, 2016, 2018; Skoumal and Trugman, 2021, etc.). Then, a clustering analysis using the Python package scikit-learn was used to group events on individual faults. Figure 1 shows an example of a cluster from Snyder in map view. The time series, magnitude frequency distribution, and exceedance probability are also shown. By comparing the various event statistics for each well-resolved fault strand in each basin, we aim to probe the seismogenic properties of each basin. The long-term goal of this project is to be able to describe how and why different basins have different degrees of induced seismicity risk and exhibit different seismogenic responses.

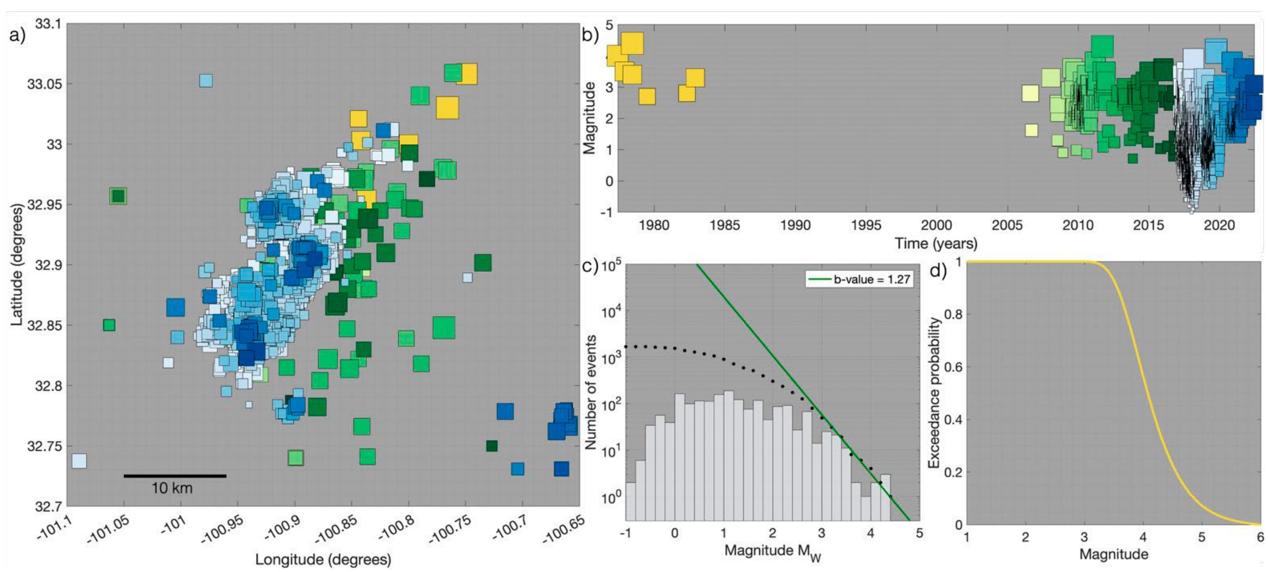

Figure 1. Preliminary analysis for a seismicity cluster close to Snyder, Texas. a) Map view, with the events colored in time; b) Time series of the seismicity; c) Magnitude frequency distribution for all of the events; d) Exceedance probability of the largest event based on all the previous events.

Workflow of Seismicity Causal Analysis

A. Savvaidis and I. Grigoratos

Since 2017 the Texas Seismological Network has been recording ground motion in Texas and providing seismicity information. The earthquake catalog and Oil and Gas (O&G) operations data are the primary datasets that help us understand the causal factors of seismicity in the state. In our analysis, we investigated three types of causal factors: (1) hydraulic stimulation, (2) shallow produced water injection, and (3) deep produced water injection.

In our paper Savvaidis et al. (2020; BSSA; https://doi.org/10.1785/0120200087), we showed that hydraulic stimulation can be identified as a causal factor of seismicity by statistical analyses of seismicity due to high clustering characteristics of seismicity and occurrence of earthquakes during and shortly after the hydraulic-stimulation process. In the case of produced-water injection, although statistical methods can be used to identify causal linkages between seismicity and injection, accurate depth estimates of seismicity are important in verifying every result.

In such cases, one O&G operation should be employed, and, currently, only physics-based approaches are able to provide information useful in complex cases in which more than one O&G operation is applied. In the recent work of Grigoratos et al. (2022; SRL; https://doi.org/10.1785/0220210320), we demonstrated that such methods could provide reliable assessment of induced-seismicity causal analysis while rich datasets are used.

Through our analysis, we managed to create a workflow (Figure 1) that can be useful according to availability of data, complexity of O&G operations, and area of interest (i.e., one well or an area with a group of wells). Although this workflow has been applied successfully in different areas (e.g., Oklahoma, Texas) we think that accurate hypocentral-depth estimation (Savvaidis et al., 2022; https://doi.org/10.1190/image2022-3751081.1) can be an additional parameter that can validate any statistical, physics-based, or geomechanical-model assessment of causal linkage of seismicity with O&G operations and should be included in induced-seismicity assessment.

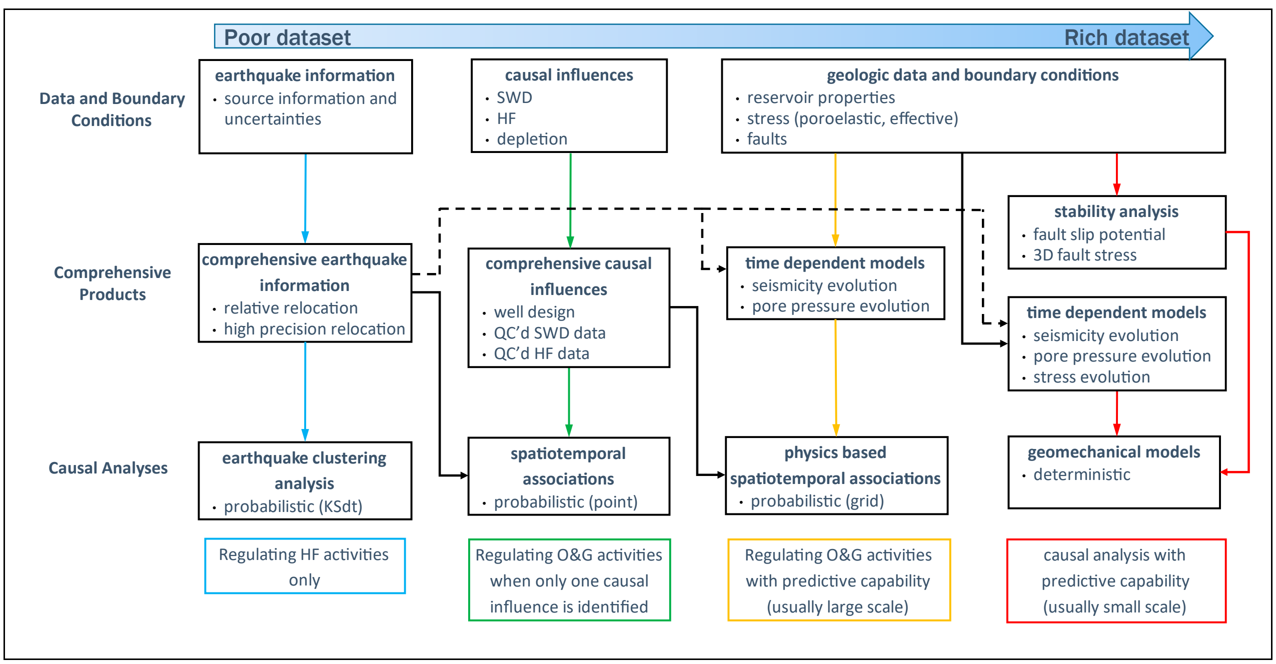

Figure 1. Workflow of seismicity causal analysis.

A Regional Ground Motion Model for Earthquake Shaking in Texas

M. Li, E. Rathje, and others

Regional ground motion models (GMM) predict the expected levels of earthquake ground shaking as a function of magnitude, distance, and site condition. These models are important for understanding the potential impacts of earthquakes on the built environment. To develop a GMM model for Texas, a database was created of recorded motions from earthquakes between January 2005 and February 2022 with reported magnitudes greater than 3.5. The database includes 10,461 motions recorded at 403 seismic stations from 343 separate earthquakes from Texas, Oklahoma, and Kansas. Each motion was associated with the moment magnitude of the event (M_w), the closest distance to the fault rupture (R_{rup}), and the average shear wave velocity over the top 30 m of the site (Vs30). Many of the recordings come directly from TexNet seismic recording stations, and the assignment of Vs30 took advantage of statewide Vs30 characterization that was supported by TexNet in the past.

The recorded data were used to develop an empirical model that predicts ground shaking as a function of M_w, R_{rup}, and Vs30. The developed model is an improvement over the NGA-East model for Central and Eastern North America, which tends to overpredict ground shaking as compared to the recordings in Texas (Figure 1), and predicts larger ground shaking at small R_{rup} than the previously developed Texas model by Zalachoris and Rathje (2019). Additionally, the developed model more accurately describes the influence of site conditions on ground shaking. Figure 2 shows the pseudo spectral acceleration (PSA) response spectrum predicted by the GMM for a M_w = 5 event at a distance of R_{rup} = 10 km and two values of Vs30. Hard rock sites with Vs30 close to 3000 m/s show more intense shaking at short periods (T < 0.08 s), while soft rock sites with Vs30 around 760 m/s show more intense shaking at longer periods. The different frequency contents for these motions will directly influence the potential for damage in structures with different natural periods.

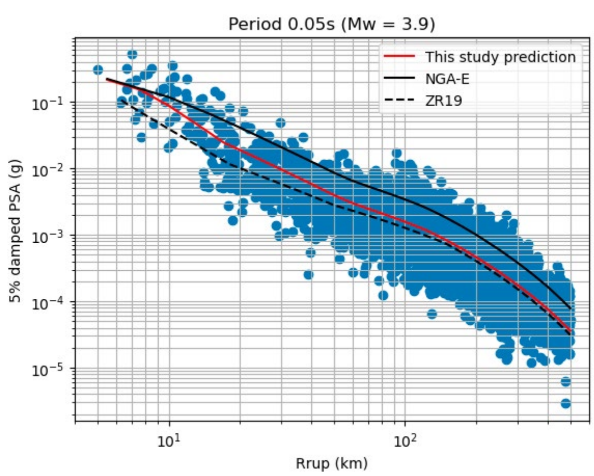

Figure 1. Recorded ground motions as a function of distance (R_{rup}) as compared with new and existing ground motion models.

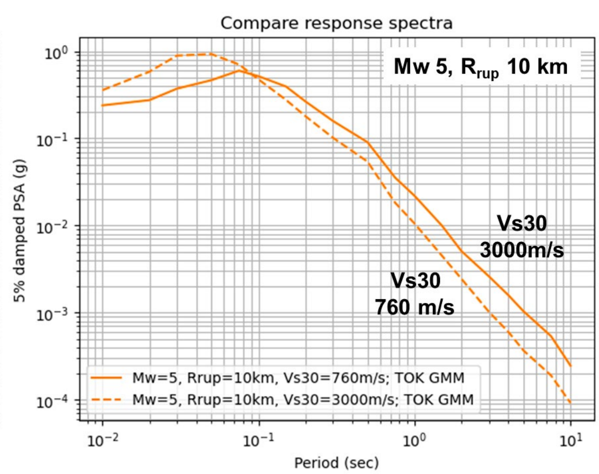

Figure 2. Predictions of acceleration response spectra for a M_w = 5 event at a distance of R_{rup} = 10 km and Vs30 of 3,000 and 760 m/s.